UNIVERSITY OF SOUTH AFRICA

THESIS

Submitted for the degree of

MASTER'S IN PHYSICS

FACULTY OF SCIENCE

ENHANCED THERMAL CONDUCTIVITY OF Ag-H₂O NANOFLUID BY PULSED LASER ABLATION IN LIQUID(PLAL)

CANDIDATE: MR. SNENKOSI WELCOME DLAMINI

PROMOTERS:

- Prof. S. M. Dhlamini (UNISA, dhlamms@unisa.ac.za)
- Dr. C. Ndlangamandla (UZULU, NdlangamandlaC@unizulu.ac.za)
- Prof.M. M. Maaza (iThemba LABS-NRF-UNISA, Maazam@unisa.ac.za/Maaza@tlabs.ac.za)

Declaration

I, Snenkosi Welcome Dlamini, hereby certify that this master's thesis, titled "ENHANCED THERMAL CONDUCTIVITY OF Ag-H_2O NANOFLUID BY PULSED LASER ABLATION IN LIQUID" represents the culmination of my extensive research towards the completion of my master's degree in the field of Physics at UNISA. I certify that the material offered here is original and reflects my intellectual capacity, independence of thinking, and meticulous efforts.

I believe and know the following to be true:

This thesis's material has not been submitted in its entirety or in part for the granting of any other degree or certificate. It is an original, unpublished work of intellectual research. Every source of information and inspiration used in the creation of this thesis has been appropriately recognized and cited. The authors of any direct quotations, paraphrases, or information taken from other publications are properly acknowledged in accordance with accepted academic citation and reference guidelines. I have expressed my gratitude for the assistance, advice, and support I received from others while doing this research. Any academic, technical, or financial support from directors, professors, research associates, or organizations has been appropriately acknowledged.

Signed: _____   Date: _____

Abstract

In this study, we present a straightforward, one-step pulsed laser ablation in liquid (PLAL) method for creating a surfactant-free nanofluid with silver nanoparticles suspended in water (AgNPs-H_2O). The ND-YAG laser of 1064 nm wavelength is used to ablate a pure silver (Ag) target's surface in a deionized water base fluid under standard conditions. Six AgNPs-H_2O nanofluids were synthesized, with concentrations corresponding to varied ablation periods (t_a = 2.5; 5; 10; 15; 20; and 25 min). The synthesized nanofluid was characterised for morphology, composition, optical properties, stability tests, thermal properties, and surface tension. The nanoparticles in the water organised into an aggregate network of spherical nanoparticles, with sizes averaging between 21 and 37 nm. Apart for carbon from coating during SEM and EDS examinations, no contaminants are detected from a basic study in the fluid that is produced. AgNPs are dispersed throughout our water host fluid, as evidenced by a plasmonic peak in the UV-vis spectrum at 400 nm. Unfortunately, these nanofluids are not stable with time, at higher concentration of AgNPs in water, they settle under gravitation. That is why we lose some plasmonic peaks at high concentration (t_a = 10; 15; 20; and 25 min) and only at low concentration (t_a = 2.5 and 5 min) where AgNPs are stable even after 5 months.). The thermal characteristics of the generated samples were evaluated using thermal conductivity measurements, which were carried out at various nanoparticle concentrations and at temperatures ranging from 25 °C to 45 °C. The results showed that the thermal rise of Ag-water nanofluid was larger than that of pure water. When temperature rises, nanofluids become more thermally conductive. The thermal conductivity improvement was found to be around 19.45% at a temperature of 45°C and a nanoparticle volume percent of ta = 5 min. This results from the instability of AgNP at higher concentrations. Also, we assessed the contact angle, which unmistakably demonstrates that it is concentration dependant. So, even at low concentrations, the presence of silver nanoparticles will have an impact on the flow of the silver-water nanofluid. Also, it is demonstrated that a tube's surface will influence fluid flow, demonstrating the importance of careful design.

Acknowledgements

Contents

List of abbreviations

Ag	Silver
H_2O	Water
AgNPs	Silver nanoparticles
PLAL	Pulsed Laser Ablation in Liquid
Laser	Light Amplification by Stimulated Emission of Radiation
Ag-H_2O	Silver water nanofluid
NPs	Nanoparticles
HTF	Heat Transfer Fluid
Nd-YAG	Neodymium-doped Yttrium Aluminium Garnet; Nd: $Y_3Al_5O_{12}$
IC	Integrated circuit
UV-Vis	Ultraviolet –visible spectrophotometry
SEM	Scanning electron microscopy
EDS	Energy dispersive X-ray spectroscopy
T_h	High temperature in the inner cylinder
T_c	Outer cylinder at a cool temperature
LHP	Loop Heat Pipe

List of symbols

K	Thermal conductivity
Q	Heat flow
H	Heat transfer coefficient
A	Area
ΔT	Differential that causes the heat flow
ω	Kinematic viscosity
μ	Dynamic viscosity
ρ	Density of the heat transfer fluid.
Re	Reynolds number
u	Flow speed
L	Pipe diameter
Pr	Prandtl number
α	Thermal diffusivity
C_p	Specific heat
$\emptyset$	Particle volume fraction
m	Nanoparticle shape parameter
ψ	Sphericity
D	Diffusion constant

k_B	Boltzmann constant
d	Particle diameter
τ_D	Characteristic time scale for covering a route equal to particle diameter
D_T	Thermal diffusivity
P	Porosity
$V(void\ space)$	Volumes of void space
$V(total)$	Total volume
E	Transmitted irradiance
E_0	Incident irradiance
α	Target attenuation coefficient
z	Absorber thickness in the same units of length as α
I_0	Incident light
I_A	Absorbed light
I_T	Transmitted light
I_R	Reflected light
A	Absorbance
ε	Molar absorption coefficient
l	Path length
c	Concentration
T	Transmittance
$R(\%)$	Percentage of reflection

$n_1 \& n_2$ Materials' refractive indices

l_α Distance travelled by a beam into a material

l_t Thermal penetration depth during the ablation during a pulse,

F_{th} Threshold fluency

H_v Heat of vaporisation

C_e Electron volumetric heat capacity

C Lattice volumetric heat capacity

T_e Electron temperature

T Lattice temperature

k_e Electron Thermal conductivity

Γ_{e-p} Electron-Lattice temperature coefficient

$\eta(\%)$ Thermal enhancement

Subscripts

p Particle

f Fluid

nf Nano fluid

np Nano particle

bf Base fluid

List of figures

List of Tables

CHAPTER 1

1.1 Introduction: Nanoscience and nanotechnology

The study of particles with distinctive physical and chemical characteristics between 1 and 100 nm in size is referred to as nanoscience [1]. It is another universe beneath the reality we see, with much yet to be discovered. Nanotechnology has a large-scale application of nanoscale materials and nanoscience principles to have a societal impact [2]. Nanotechnology takes advantage of the unique properties that nanoscale surfaces have, managing and enhancing them [3]. It is a branch of contemporary science that is quickly developing. In 1959, Richard Feynman made a future-looking statement when he observed, "There is enough room at the bottom." He asserted that the key to future technological advancement was to reduce to the nanoscale. [4]. Drexler published a paper on molecular nanotechnology in 1981, two decades after Feynman's lecture, since then nanotechnology grew [5]. As science and technology advance, so does the demand for exceptional functionality of devices with outstanding reliability, precise operation, and stable performance. Scholars gathered to work on the thermodynamic efficiency of thermal systems [6].

1.2 Nano electronics and cooling challenge

Overheating in electronic devices requires cooling [7, 8]. Cooling is essential for the optimization of the operation of any electronics, especially in nanoelectronics currently and the upcoming nanoelectronics revolution. According to Al-Mubarak [7], as electronic gadgets are becoming smaller, overheating is unavoidable. Manufacturers of electronics components must pack transistors into even tiny spaces in order to meet the growing demand for smaller devices, and this crowded engineering design makes it more susceptible to overheating because it has less thermal flow [7]. The quest for improved coolants in nanoelectronics is continuous, given our society's fast-rising reliance on information and communications technology (ICT). According to Moore's law, a microprocessor chip's transistor count doubles roughly every two years, which typically increases chip performance [9]. The peak power output and heat flux from high-performance computer processors were anticipated to reach around 360 W and 190 W/cm^2 by 2020, respectively [10, 11]. Electrical components, including circuits, transistors, diodes, resistors, and capacitors among others, are engineered to endure specific heat thresholds [7]. Electronic parts produce heat while they are functioning leading to overheating, which could potentially harm an electrical component. Figure 1.1 shows the effect of overheating on

electronics devices.
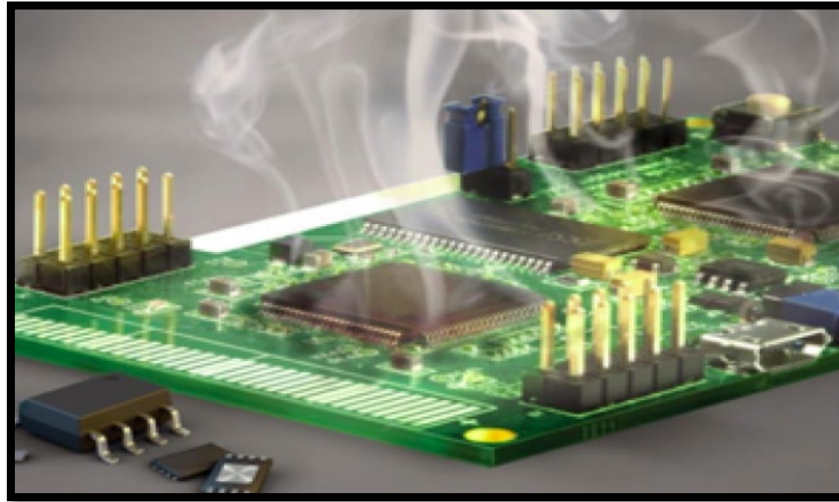
Figure 1.1 Effect of overheating on electronics

1.2.1 Electronics that are overheated might suffer from several drawbacks, including:

Reduced Performance: The performance of electronic gadgets might suffer when they get too hot. This can show up as higher mistakes or crashes, slower processing rates, and slower reaction times.

Reduced longevity: Excessive heat can harm an electrical device's internal components and reduce its longevity. Repairs or replacements may be required as a result, which could be expensive.

Damage to the batteries in electrical devices due to overheating can result in shorter battery life and poorer performance.

Extreme situations of overheating may provide safety issues, including the possibility of a fire or explosion (see Figure 1.1).

Data Distortion or Losses: Thermal overload can also result in data damage or loss, especially in storage devices like hard drives or solid-state drives.

Electronic gadgets shouldn't be exposed to extreme heat to avoid these harmful impacts. This can be accomplished by storing them in well-ventilated spaces, minimizing exposure to harsh light or heat sources, and making sure they aren't used continuously for long periods of time. Additionally, routine upkeep and cleaning can aid in preventing the buildup of dust or debris, both of which can cause overheating.

1.3 Nanofluids

Coolants used so far which are water, ethylene glycol, and mineral oil, among others, have low thermal conductivity while that of metals and their oxides is very high (see Figure 1.2). A material's capacity to conduct heat is referred to as thermal conductivity. Metals typically transmit heat more efficiently than base fluids. This implies that base fluids do not conduct heat as well as metals do. Maxwell proposed the use of small solid particles with high thermal conductivity in fluids to improve thermal conductivity [12].
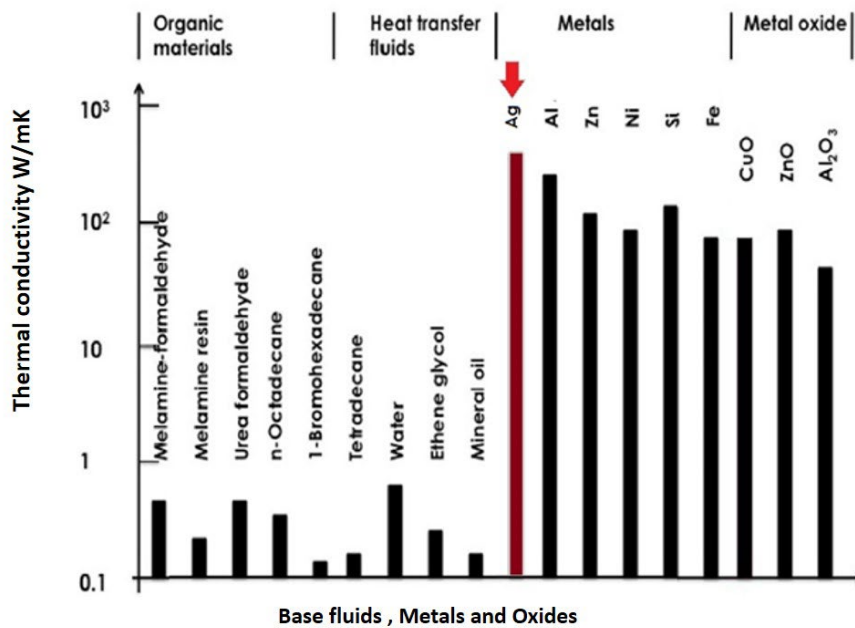
Figure 1.2 A figure showing thermal conductivities of bases fluids and metals and their oxides.

The study was aimed at suspending micro- or millimeter-sized solid particles in liquids [13]. Addition of tiny particles to a base fluid increased the effective thermal conductivities of the base fluid [13, 14]. His plan worked, albeit with some noticeable drawbacks. There were technical difficulties that such particles could lead to, for example, rapid settlement periods, micro channel closure, surface abrasion, pipeline erosion, and increased pressure drops [15] which is against the properties of a good heat transfer fluid (HTF). Ahuja also investigated the thermal performance of tiny particles with outstanding thermal conductivity in a base fluid. Even though Ahuja was able to increase thermal conductivity in his system by using minuscule Polystyrene particles, channel obstruction because of the accumulation of particles became a major problem [16, 17]. This was a concern to the scientific community and the threat had to

3

be addressed using new methods. Nanoparticles were suspended into a base fluid instead of micro or millimeter size solid particles. A new class of fluid called a "nanofluid" is formed of colloidal nanoparticle suspension (which ranges in size from 1 to 100 nm) that has been engineered in a base fluid [18]. The thermal conductivity (k) enhancement of nanofluids, paved the way for additional research in this area [19]. Nanotechnology application in thermal engineering was suggested by Choi of the United States' Argonne National Laboratory [20]. According to the study, compared to pure liquid, scattering highly conductive nanoparticles into a liquid substantially enhances the suspension's thermal conductivity. Since then, nanofluids have become well-known as a cutting-edge class of thermal transfer fluids, and they are still a popular study area [21].The groundbreaking idea of incorporating solid particles into coolants to enhance thermal conductivity is credited with the birth of nanofluids [22]. Nanofluids have increased heat transfer fluid efficiency in recent years, thanks to advances in nanoscience and nanotechnology [23-29]. Thus, nanoparticles are usually used with high thermal conductivity made of metal or metal oxide materials [30-32].

1.4   Synthesis of nanoparticles

Nanomaterials are materials that have at least a single dimension that falls inside the range of the nanoscale, often between 1-100 nanometers. Different physical and chemical processes are used to create nanomaterials, and the method used relies on the target nanomaterial's characteristics and potential uses (see Figure 1.3). Two general strategies for creating nanoparticles are bottom-up and top-down methods.

In bottom-up processes, individual atoms or molecules are assembled into nanoparticles. These procedures usually include the utilisation of chemical processes, where the molecules that serve as precursors are combined in a laboratory setting and the conditions for the reaction are then changed to encourage the creation of nanoparticles. Precipitation, hydrothermal synthesis, and sol-gel synthesis are a few typical bottom-up techniques.

Top-down techniques, on the other hand, require breaking down large materials into tiny nanoparticles. These techniques frequently make use of physical techniques like milling, etching, or lithography. Up until it reaches the required size, the bulk material is physically handled or treated to remove material from the surface. The use of ball mills, laser ablation, and electron beam lithography are a few typical top-down techniques.
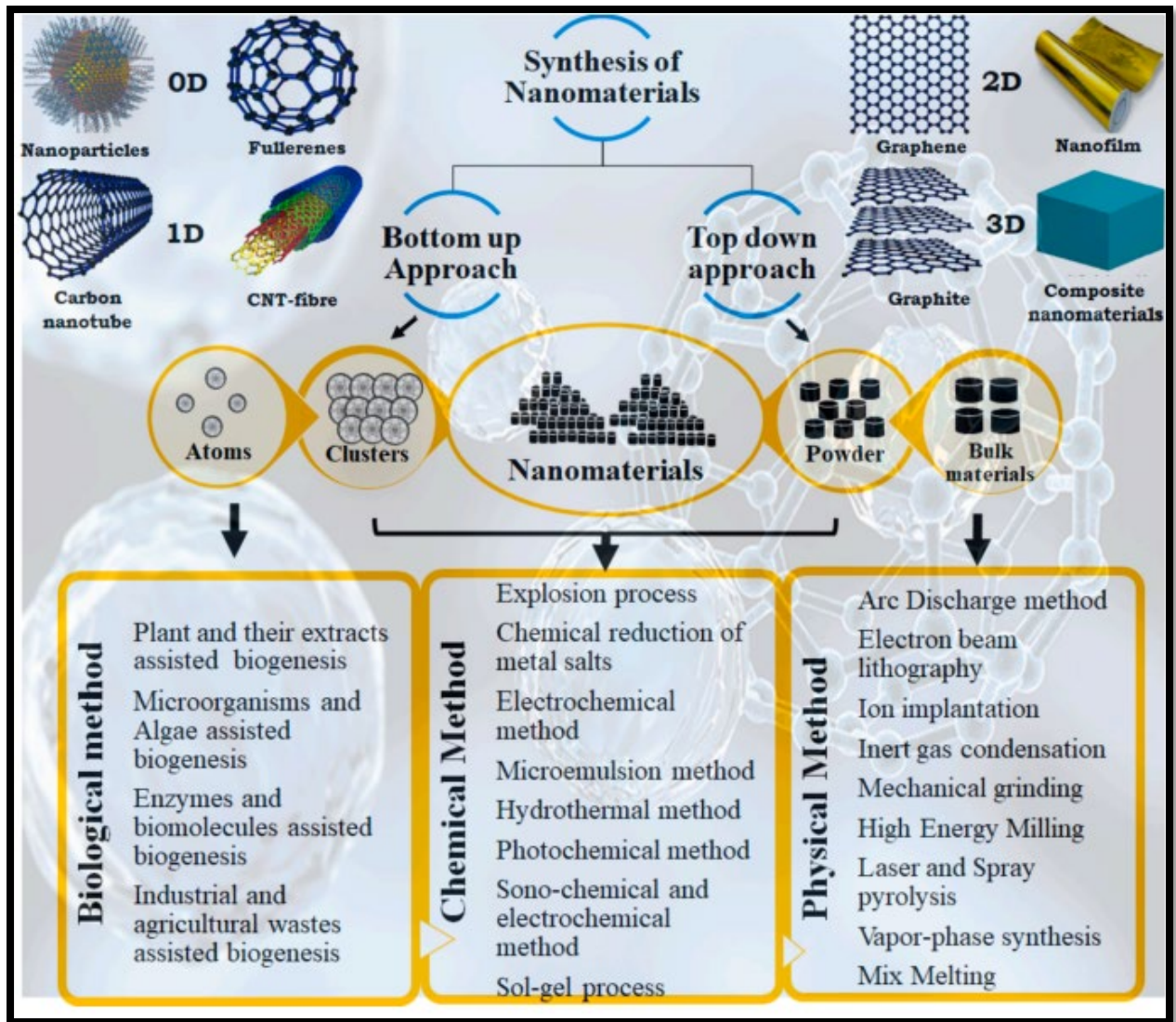
Figure 1.3: Dimensional categorization of nanoparticles and diverse techniques for synthesising nanoparticles [33].

The synthesis of nanofluids entails dispersing nanoparticles into a base fluid, such as water, ethylene glycol or mineral oil, to create a stable and homogeneous mixture (see Figure 1.4). Many experiments, including the initial explorations of nanofluids, used a two-step technique in which the production of nanoparticles as a dry powder was followed by their dispersion into a fluid. The one-step process, in contrast, requires the direct production of nanoparticles in the heat transfer fluid. A lot of research has been done on silver nanoparticles (AgNPs) because of their distinctive optical, electrical, and antibacterial characteristics. Several techniques, including chemical reduction, electrochemical deposition, and green synthesis, have been used to create them. However, the production of AgNPs via pulsed laser ablation is thought to be a safe, effective, and green process.
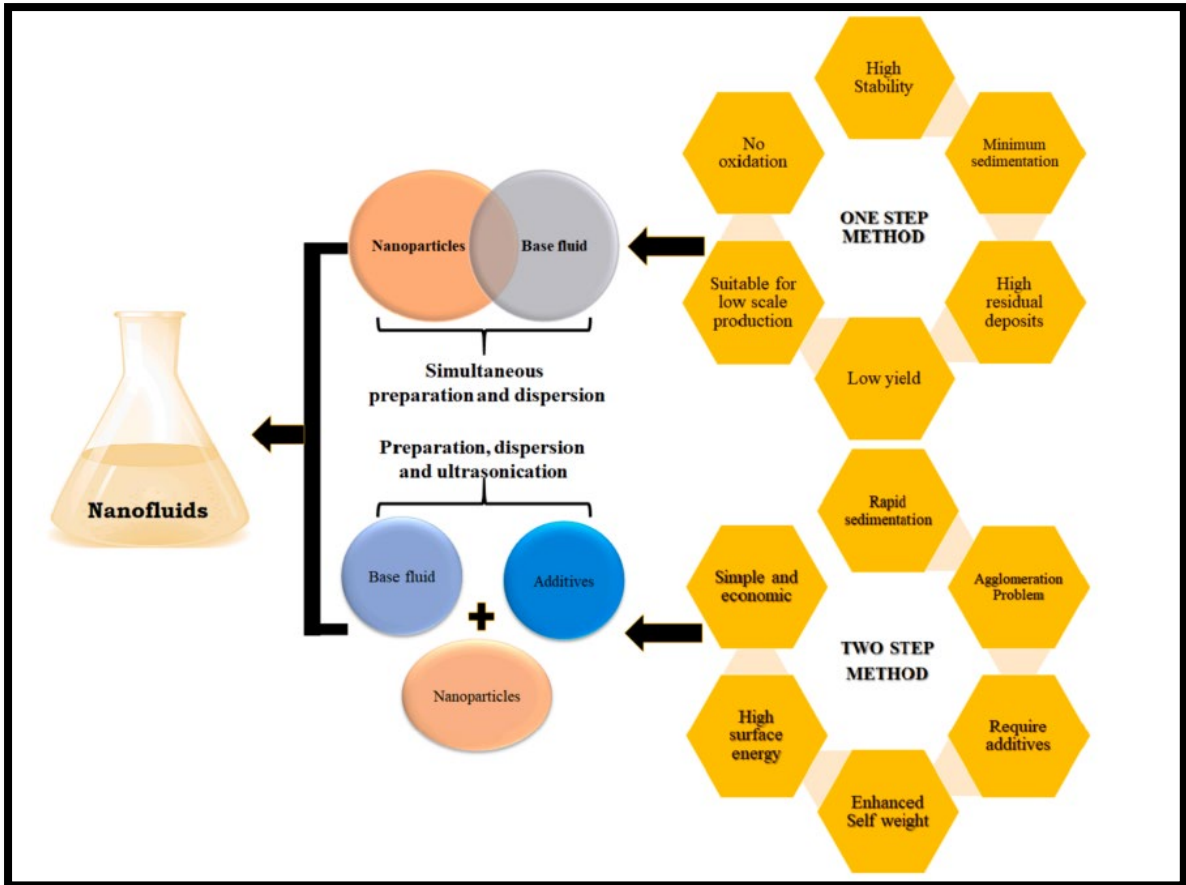
Figure 1.4: Synthesis of nanofluids [33].

1.4.1 Single step method

This method avoids the requirement for separate dispersion, transit, and freeze-drying preservation by simultaneously synthesizing and distributing nanoparticles throughout the base fluid. Fluid stability is improved, and nanoparticle aggregation is successfully reduced. [34]. With the use of a ground-breaking one-step method created by Argonne, metallic source materials' direct nanoscale vapor dispersion into fluids with low vapor pressure is now possible. By successfully overcoming the van der Waals interactions between nanoparticles and doing away with the requirement for dispersants, this novel method produces stable suspensions [35]. The one-step physical method is costly and unable to produce nanofluids on a large scale. The fundamental benefit of a one-step procedure is that the nanoparticles are more uniformly sized and pure. Additionally, the one-step technique has significant drawbacks [36]. The primary factor is the presence of residual reactants in the nanofluids because of unstable reactions or

6

stabilization. Furthermore, this method only works with base fluids with low vapor pressures. [37].

1.4.2 Two step method

The two-step procedure' key benefit is that nanoparticles can be created separately using a commercial technique that enables their mass-market and low-cost manufacture [38, 39]. Compared to metallic nanoparticles, this method works well with oxide nanoparticles. Agglomeration of nanoparticles is the two-step method's main issue. Studies revealed that after a few hours of ultrasonic treatment, particles significantly aggregated both before and after being dispersed in a host fluid. Nanoparticles are often purchased as powders, which scientists blend with the original fluid. These nanofluids do, however, frequently display instability, which can be lessened by modifying the pH and adding surfactants. As a second option, some scholars choose to buy fully manufactured and sold nanoparticles that are commercially accessible. However, these nanofluids include contaminants and nanoparticles whose sizes deviate from those recommended by the seller [40].

1.5 Basic HTF classifications and working temperatures.

Several categories can be used to classify heat transfer fluids. In general, there are four classifications for beat transfer fluids. These include fluids with a very low temperature, fluids with a low temperature, fluids with a medium temperature, and fluids with a high temperature (see Figure 1.5).

| ULTRA - LOW TEMPERATURE FLUIDS THE LOWEST OPERATING TEMPERATURE BELOW -50 °C | LOW TEMPERATURE FLUIDS THE LOWEST OPERATING TEMPERATURE FROM -50 °C TO 0 °C | High TEMPERATURE FLUIDS THE LOWEST OPERATING TEMPERATURE FROM 200 °C TO 400 °C | ULTRA - HIGH TEMPERATURE FLUIDS THE LOWEST OPERATING TEMPERATURE ABOVE 400 °C |
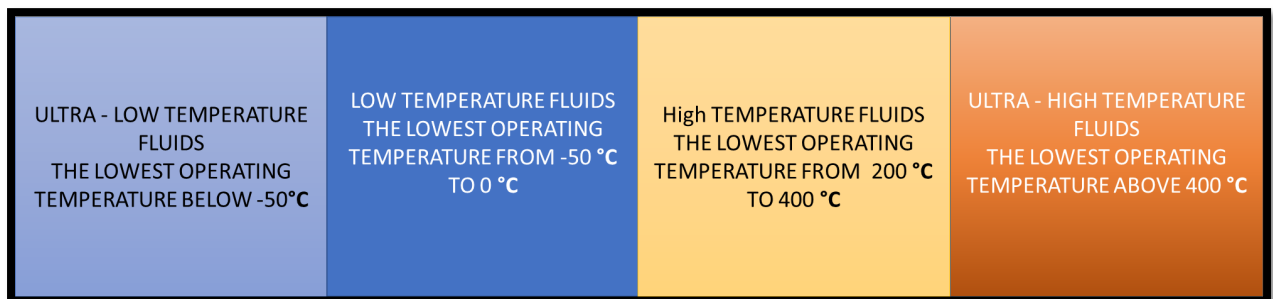
Figure 1.5: Basic HTF classifications and working temperatures [41-44].

1.6 Why Nanofluids

Nanofluids are often used for a variety of applications aimed at providing improved energy sources and applications [45]. With their large specific surface area and increased surface area for heat transmission between fluids and particles, this new family of fluids demonstrates exceptional features. Brownian motion is the dominant kind of particle motion. [46, 47], This leads to stable dispersion [48]. Less pumping power is required compared to pure liquid to intensify heat transmission by the same amount. [48]. Less particle clogging than typical slurries, allowing for system downsizing [49]. Thermal conductivity and surface hydrophilicity can be adjusted by altering particle concentrations to suit diverse applications. The cooling system used for each type of a device requires a different cooling method. It is critical to choose the best coolant for each equipment. Depending on the cooling system and electrical equipment being used, the type of coolant required may differ. Utilizing nanofluids with greater critical heat flux could facilitate the efficient cooling systems of ever smaller and more potent electronic devices, allow for power increases in commercial nuclear plants, and allow for the creation of more tiny heat exchangers for the petrochemical industry, among other things.

1.7 Aim

The purpose of this research is to explore the creation of silver-water nanofluid using pulsed laser ablation in liquids (PLAL) and its use as a coolant for nanoelectronics. To fully comprehend the characteristics and functionality of the nanofluid, the study intends to investigate the interaction between nanoparticle formation, shape, stability, thermal conductivity, and contact angle. The study intends to contribute to the creation of a cutting-edge cooling system that can successfully disperse heat from nano electronics, enhancing their performance and dependability.

1.8 Research Objectives

The aim will be achieved by these objectives:

1. To synthesize an AgNPs-H_2O nanofluid, by pulsed laser ablation in liquids (PLAL) approach, to better understand how silver nanoparticles form and scatter in water.

2. examining the distribution of silver nanoparticles as well as the morphology and composition of the produced nanofluid,

3. Investigating the stability of the AgNPs-H2O nanofluid over time and at various concentrations to understand the impact of concentration on aggregation and sedimentation function.

4. By measuring the thermal conductivity of the AgNPs-H2O nanofluid and contrasting it with that of pure water, one may evaluate the improvement in thermal conductivity of AgNPs-H2O.

5. By determining the contact angle of the AgNPs-H2O nanofluid on various surfaces and examining its wetting behavior.

1.9   Significance of the study

In the context of increased heat dissipation, better thermal management, energy efficiency, developments in nanofluid technology, and useful applications in electrical engineering, the study on silver-water nanofluid for heat transfer applications is important. The findings have significance for several sectors depending on effective heat transfer and thermal management practices and help to build more efficient and environmentally friendly cooling systems. Overall, the importance of this work resides in its potential to further knowledge of the synthesis, stability, thermal conductivity, and contact angle of silver-water nanofluids, as well as its implications for the creation of better cooling systems for nano electronics. The results may open the door for more study and advancements in the area, which would ultimately improve the functionality and dependability of electronic equipment in a variety of applications.

1.10 Research scope and limits

The aim of this study is to synthesize AgNPs-H$_2$O Nanofluids for heat transfer, with particular attention paid to the synthesis of the silver nanoparticles, the stability and morphology of the nanofluid, the measurement of its thermal conductivity, and the contact angle as a function of concentration. To evaluate the nanofluid's potential as a coolant for nano electronics, the study attempts to give a thorough knowledge of its characteristics and behavior.

It's crucial to recognize the limits of this study, though. First off, the analysis is only focused

on a single synthesis approach that uses pulsed laser ablation in liquid; as a result, the findings might not be readily transferable to other synthesis methods. Additionally, the study excludes other varieties of nanofluids or other base fluids in favor of concentrating on the behavior and characteristics of the silver-water nanofluid.

The study's conclusions are also based on experimental data acquired under well controlled laboratory circumstances, therefore their relevance to actual situations may differ. In actual cooling systems, factors like flow dynamics, pressure, and temperature gradients are not completely considered in this study. Therefore, more investigation and testing are required to confirm the findings in practical settings.

The study also notes that the nanofluid's stability is constrained, particularly at high concentrations when particle settling might take place over time. Additional research is needed to determine the nanofluid's long-term performance and stability in diverse operating situations and settings.

Finally, although the work sheds light on the nanofluid's thermal enhancement, the precise mechanisms and interactions that led to the observed increase in thermal conductivity are not fully studied. To fully comprehend the underlying physical and chemical mechanisms involved in the thermal increase of the nanofluid, more investigation is required.

Despite these drawbacks, this study provides a useful framework for further investigation into the fabrication of nanofluids and their use in heat transfer systems. The results serve as a foundation for additional research on nanofluid formulation optimization, stability enhancement techniques, and the creation of cutting-edge cooling solutions for nano devices.

1.10 CHAPTERS DIVISION

CHAPTER1

The inquiry into the creation of silver-water nanofluid for use in heat transfer applications is introduced in Chapter 1. The chapter opens by emphasizing the necessity for efficient coolants in nanoelectronics and by outlining the primary goal of the study, which is to investigate the production properties of the nanofluid. Along with the precise objectives to be met, the

importance of this study in developing cooling technology is emphasized. The chapter also explores the study's limitations and scope, which offers a clear foundation for the next chapters.

CHAPTER 2

The use of highly conductive metals and their oxides to increase the thermal conductivity of base fluids is supported by a thorough literature analysis that is covered in Chapter 2. It is explored how the size and form of nanoparticles affect heat conductivity, and it is also explained how nanofluids may be used in a variety of scientific fields. The chapter also examines the literature that has already been published on the stability and wettability of nanofluids, offering insight on key issues in the subject.

CHAPTER 3

The laser ablation method (PLAL) and its use in the production of nanofluids are the main topics of Chapter 3. It gives a comprehensive explanation of laser theory and how it interacts with matter, with special emphasis on how laser parameters affect the production of nanofluids. This chapter lays the groundwork for the upcoming experimental chapters by explaining how PLAL functions.

CHAPTER 4

In Chapter 4, the PLAL synthesis of AgNPs-H2O nanofluid is described in full, along with a thorough discussion of the design of the experiment and the parameters used. This chapter establishes the foundation for the succeeding analyses and acts as a manual for duplicating the synthesis process.

CHAPTER 5

Using scanning electron microscopy (SEM) and energy-dispersive X-ray spectroscopy (EDS), Chapter 5 concentrates on the morphology and composition investigation of the silver-water nanofluid. The findings are given, providing important new understandings of the nanofluid's size distribution, shape, and surface characteristics. A fuller knowledge of the physical properties of the created nanofluid is provided by this investigation.

CHAPTER6

Using UV-Vis spectroscopy, Chapter 6 examines the optical characteristics of the silver-water nanofluid. To understand the long-term behaviour of the nanofluid's optical characteristics, the stability of the plasmonic peak in the nanofluid is investigated over a period of 5 months. Important details on the stability and dependability of the nanofluid for prospective applications are provided in this chapter.

CHAPTER 7

In Chapter 7, the investigation of the silver-water nanofluid's thermal conductivity is covered in depth. It examines how thermal conductivity and stability are related, showing the effect of a nanofluid's properties on heat transmission. This chapter provides insights into the possibilities for the nanofluid to be used in effective heat transfer applications by thoroughly investigating its thermal behaviour.

CHAPTER 8

Beginning with pure copper and moving on to copper sulphide, Chapter 8 concentrates on the measuring of contact angles on various substrates. This research adds to our full understanding of the nanofluid's interaction with various surfaces by offering important information on the wetting behaviour and interfacial characteristics.

CHAPTER 9

The study is finally ended in Chapter 9 with a thorough analysis of the data, insightful conclusions, and recommendations for future research. The main ideas from the previous chapters are summarized in this chapter, which also provides insightful information on the consequences and prospective uses of the silver-water nanofluid in heat transfer systems.

CHAPTER 2 : LITERATURE REVIEW

2.1 Introduction

This section collects the most recent nanofluids recommendations. Researchers have contributed to this field, which cannot be adequately addressed in a single study. Cooling may be achieved in two ways: either by using novel devices such as fins, microchannels, integrated cooling, or by improving fluid heat transfer [50]. Nanoparticles have distinct and special properties when compared to bulk materials of similar proportions, including magnetic, chemical, thermal, electrical, and optical properties [18, 51]. Research on nanofluids around the world have revealed that nanofluids have demonstrated that nanofluids outperform basic fluids in terms of thermal performance [52]. Other distinguishing properties of nanofluid thermal conductivity have been discovered, including excellent temperature-dependent thermal conductivity [53] and strong size-dependent thermal conductivity [54]. Nanofluids are thermally enhanced differently depending on the nanoparticle concentration [55-57]. Since the word "nanofluids" was coined, the amount of research on them has multiplied [58].

.

2.2 Silver nanoparticles

The most common manufactured nanomaterial found in consumer items is silver nanoparticles (AgNPs), whose primary utility is due to the metal's inherent antibacterial characteristics. Previously, colloidal silver was marketed under names such as "Argyrol" in 1902 (or "Silver Algaeden") [59]. The natural solubility of silver and the larger surface area of nanoparticles (NPs) combine to make silver commercially appealing to industry since it uses considerably less of it, at a cheaper cost, to produce the same antibacterial effect [60-62]. For flexible electronics applications that demand compliant electrodes, the electronics industry is investigating the use of colloidal silver inks for printing circuit components [63-66]. Silver is regarded as an asset and has a large assortment of commercial applications. Ancient people valued silver highly because of its various qualities. First, it is a metal with a thermal conductivity of 429 W/mK (see Table 2-1). It is common, ductile, luminous, corrosion-resistant, malleable, shiny, conductive, and antimicrobial. In addition to being utilized as money, silver was also employed in electrical connections, photography, jewelry, and decorations [67].

Table 2-1Thermal properties of Materials.

Material	Melting point	Thermal conductivity (W/m. k)	Linear coefficient of thermal expansion (($\times 10^{-6}$)($°C$)$^{-1}$
Metals			
Copper	1083	238	17
Silver	961	427	24
Steel	1535	79.5	11

Although they were unaware of it, silver nanoparticles were created in a process when silver was combined with other elements in the past by craftsmen to make crafts. The various colors they created in their crafts demonstrated this. Nowadays, silver nanoparticles are used in a broad variety of fields, including energy research, healthcare, the space industry, and light-emitting devices [68]. Due to its characteristics, silver has a broad variety of uses. We can mention consumer goods, electronics, computers, cosmetics, water, and environmental disinfectants to name a few [69].

2.3 Justification for the Use of Water as a Base Fluid for Silver Nanofluids in Heat Transfer

For heat transmission, water is usually used as the base fluid because of its many advantages. This formal and advanced level rationale evaluates the benefits of using water as a base fluid while also addressing its disadvantages, coming to the conclusion that water can be a good option depending on the particular application and operating conditions.

2.3.1 Accessibility and Environmentally Friendly:

Water stands out as a superior basic fluid due to its accessibility, availability, and ecological friendliness [70, 71]. Water is an economical and accessible base fluid that may be used in a variety of heat transfer applications, unlike other base fluids like ethylene glycol and oil [72].

A greener approach to heat transfer operations is also made possible by its eco-friendliness, which is in line with sustainability objectives [73, 74].

2.3.2   High Specific Heat Capacity:

Water has a remarkable specific heat capacity of 4.18 kJ/kg.K, which enables it to absorb and retain a significant amount of heat per unit mass [75]. This property encourages effective heat transfer and aids in preserving temperature stability within the nanofluid. Water is a good choice since it has a higher heat capacity per mass than other fluids, which improves the nanofluid's overall thermal performance.

2.3.3   High Boiling Point:

At atmospheric pressure, water has an extraordinarily high boiling point of 100°C [76]. For purposes that demand hot temperatures, including industrial processes and power plants, this trait is very helpful. Water's capacity to function at high temperatures without vaporisation guarantees that the nanofluid maintains a stable liquid state, enabling constant and dependable heat transfer performance.

2.3.4   Flexibility in Nanoparticle Mixing:

To produce stable nanofluids, water mixes well with a variety of nanoparticles, including metallic, oxide, carbon, and ceramic particles [77, 78]. Due to their versatility, nanofluids may be customised to have better thermal properties, which improves heat transfer efficiency. It is possible to modify the nanofluid to fulfil certain needs for heat transmission by combining water with different nanoparticles.

2.4   The disadvantages of utilising water as a base fluid for nanofluids in heat transfer must be considered, though:

2.4.1   Low Thermal Conductivity:

Water has a comparatively low thermal conductivity of 0.6 W/mK when compared to other fluids [79]. As a result, the efficiency of heat transfer inside the nanofluid is hampered.

2.4.2   Freezing point

Water has a high freezing point of 0°C, which may restrict its usage in cold conditions heat transfer operations without the addition of antifreeze compounds [80]. When utilising water as a basic fluid, the requirement for additives to avoid freezing adds extra costs and considerations. Alternative base fluids with lower freezing points could be more suited in certain circumstances.

2.4.3   Corrosion Risk:

Metal surfaces and components exposed to nanofluids may corrode as a result of the high pH and dissolved oxygen content of water [81]. Precautions like the use of corrosion inhibitors or surface treatments are required to be taken in order to mitigate this possible issue. These extra steps raise the difficulty and expense of using water as a foundation fluid for nanofluids.

In conclusion, when the benefits exceed the negatives and the application and operating conditions are appropriate, water can be a useful base fluid for silver nanofluids in heat transfer. It is a versatile option due to its accessibility, cost, high specific heat capacity, and simplicity of nanoparticle mixing. However, based on the demands of the heat transmission system, the constraints of low thermal conductivity, high freezing point, and corrosion risk should be carefully examined and addressed.

2.5   Heat transfer fluid (HTF)

Heat transfer is a common occurrence in daily life and technical systems and is required for device cooling (see Figure 2.1).
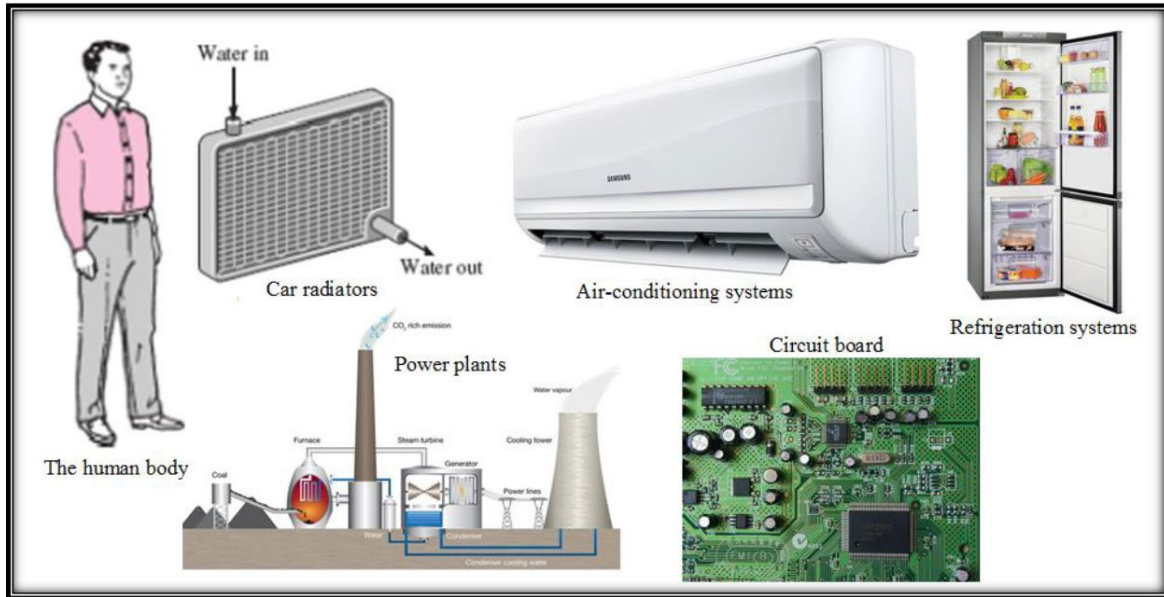
Figure 2.1: A heat transfer diagram of our daily lives electronics and industry

Three methods—convention, conduction, and radiation—can be used to transmit heat (as shown in Figure 2.2). These three mechanisms are used to transfer thermal energy to the heat transfer fluid (HTF). The function of a heat transfer fluid is to gather, transmit, and exchange heat from a heated surface to a cold surface. Heat is gathered, moved, and traded to assure electronic cooling in the case of electronic devices.

2.6   Characteristics of a heat transfer fluid

According to Czaplicka et al. [82], The HTFs must have excellent thermal conductivity coefficients and specific heat capacities within the selected temperature range [83]. They should also exhibit good thermal and thermo-oxidative stability, be non-toxic, and be compatible with building materials used in heating systems. HTFs must be resistant to accumulation of debris on system walls [82]. Additionally, it is crucial to have a pour point that is set for the conditions the system may be subjected to, as well as the proper viscosity for the operating temperature range. Another crucial factor is the fluid's life charge (see Figure 2.2).
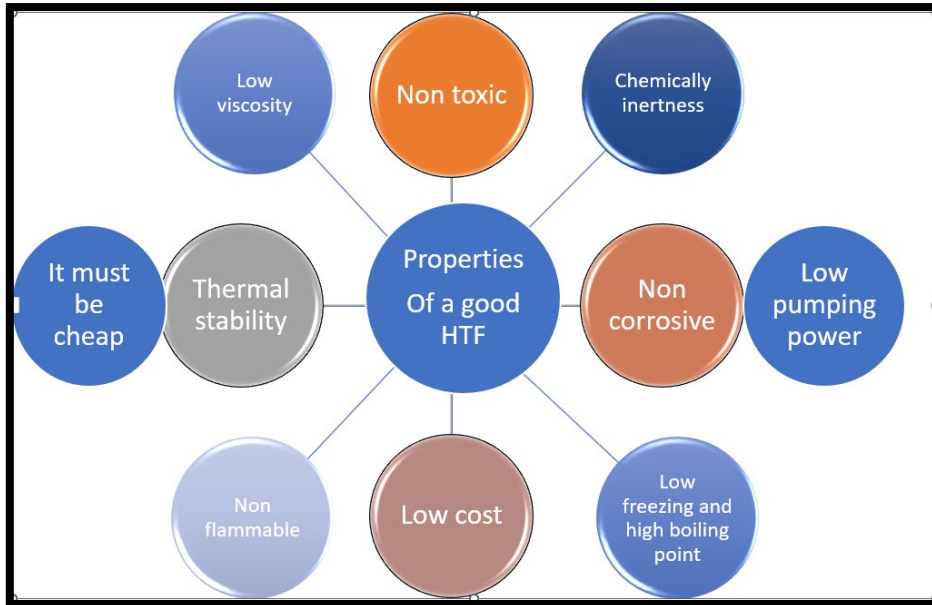
Figure 2.2 Characteristics of a good heat transfer fluid.

A decent HTF is thought to have an effective working life of a charge between 35,000 and 40,000 hours. Finally, consideration should be given to economic factors including the accessibility and affordability of HTFs. Finally High flash point is a necessity because a fluid with a high flash point is less likely to catch fire or explode and is more likely to be moderately flammable. Additionally, a fluid must be simple to maintain A good heat transfer fluid should be simple to maintain and replace as necessary, with little to no system downtime.

2.7 Enhancing Heat Transfer: Understanding the Equation of Nanofluid Thermal Conductivity

The thermal conductivity of nanofluids is calculated using the formulae below:

Using the following formula, one may determine the density of a nanofluid—a fluid that contains suspended nanoparticles—:

[84]
$$\rho_{nf} = (1 - \emptyset)\rho_f + \emptyset\rho_p$$
2-1

Using the current relationships for the two-phase mixture, the viscosity of the nanofluid may be estimated:

[85]
$$\mu_{nf} = \frac{1}{(1-\emptyset)^{2,5}}\mu_f$$
2-2

The density Specific heat is:

[86]
$$\left(\rho C_p\right)_{nf} = (1-\emptyset)\left(\rho C_p\right)_f + \emptyset\left(\rho C_p\right)_p$$
2-3

And the thermal conductivity:

[86]
$$k_{nf} = \frac{k_p + (n-1)k_f - (n-1)\left(k_f - k_p\right)}{k_p + (n-1)k_f + (\emptyset)\left(k_f - k_p\right)}$$
2-4

Where:

ρ_{nf} -Density of nanofluid

ρ_f – Density of base fluid

ρ_p – Density of nanoparticles

$\emptyset$ - Volume fraction of nanoparticles in a base fluid

μ_{nf} – dynamic viscosity of nanofluid

μ_f - viscosity of a base fluid

$\emptyset$ - volume fraction of nanoparticles in a base fluid

$\left(\rho C_p\right)_{nf}$ – Density specific heat of nanofluid

$\left(\rho C_p\right)_f$ - density specific heat of a base fluid

$\left(\rho C_p\right)_p$ - density specific heat of nanoparticles

k_{nf} - thermal conductivity of nano fluid

k_p - thermal conductivity of nano particles

k_f – Thermal conductivity of the base fluid

k_p - Thermal conductivity of the nanoparticles

The spherical particles are assumed for the nanoparticles with $n = 3$. Deciphering the complex thermal and fluidic behaviours of these designed colloidal suspensions requires an understanding of their thermophysical properties. Together, these formulations shed light on the mutual benefits that exist between the constituents of nanofluids and provide important information for a thorough examination of their thermophysical properties. These studies have important ramifications for improving our knowledge of and ability to use nanofluids in a variety of engineering applications.

2.8   Thermal enhancement of nanofluids

Scholars conducted studies using nanofluids in car engines and obtained positive findings, ,including increases in heat exchange over base fluid consumption [87]. An overview of current research efforts employing metal oxide nanofluids for electronic cooling systems shows that certain researchers, such as Gunnasegaran et al., explored SiO_2-H_2O nanofluid and discovered an average decrease of 28% - 44% in the overall thermal resistance of Loop Heat Pipe (LHP) when contrasted with pure H_2O [88]. Al_2O_3-H_2O at 5 vol% was the subject of research by Putra et al [53] and they found that employing biomaterial as a wick significantly improved LHP performance, with a thermal resistance reduction of 56.3% contrasted with sintered powder wick. Putra et al. also investigated CuO-H_2O at 0.075vol% and discovered that CuO-H_2O nanofluid's evaporator thermal resistance is lowered by 17.3% when compared to H_2O fluid [89].   In their study of SiC-H_2O using only 0.5–1 Wt%, Mohammadi et al. discovered that the maximum temperature drop was 3.7°C for maximal heat flux (15.48%) [90].   The system's total thermal performance can be improved by up to 37% using AgNPs-water (0.01-0.1 Wt%). In a laminar flow regime, Naraki et al. [91] demonstrated an improvement in the overall heat transfer coefficient of 6% and 8%. at concentrations of 0.15 and 0.4 percent copper oxide CuO-H_2O. Peyghambarzadeh et al [92] validated this when researching heat transfer performance in car radiators using Cu-H_2O and Fe_2O_3-H_2O nanofluids. For a concentration of 0.65 vol percent, the findings revealed an increase of up to 9%. The thermal conductivity of nanofluids has been the subject of numerous theoretical and experimental investigations [54, 93, 94] . Recent research has shown the complex interplay between the thermal conductivity fluctuations of nanofluids and a wide range of factors. These variables include a wide range of

influencing parameters, such as the volume fraction, size and form of the nanoparticles, the presence of additives, the pH level, temperature, the type of base fluid, and the material composition of the nanoparticles [95-97]. Many experiments on the thermal conductivity of nanofluids have been carried out utilizing a range of nanomaterials like as metals, magnetite, semiconductors, as well as graphene [93]. Nanofluids are more effective at transporting heat than traditional heat transfer fluids. This is mostly due to the scattered nanoparticles' ability to improve the thermal conductivity of nanofluids. A nanofluid's thermal conductivity is greatly influenced by its nanoparticle volume fraction [98]. Nanofluids' thermal conductivity has been a challenge to predict, despite a semi-empirical correlation for the apparent conductivity of two-phase mixtures. As previously indicated, nanofluids outperform traditional heat transfer fluids in terms of their ability to transport heat. The distributed nanoparticles significantly boost the nanofluid's heat conductivity, which explains why. The thermal conductivity of nanofluids is significantly influenced by the volume proportion of nanoparticles. The thermal conductivity of nanofluids with only minute volume fractions of nanoparticles rises noticeably as compared to the base fluid, according to experimental data. According to the study done on water-based Cu nanofluids, thermal conductivity is influenced by the volume fraction of the particles in the fluid. The proportion of the thermal conductivity of the particles to the thermal conductivity of the base fluid $\frac{k}{k_f}$ is shown to significantly increase, with values rising from 1.24 to 1.78, when the volume percent of particles is raised from 2.5% to 7.5% [99, 100]. This result highlights the crucial impact that particle concentration plays in improving the heat transfer properties of nanofluids. With a particle loading of 0.3 vol.% of Fe nanofluid (10 nm) there was a 16.5% increase in thermal conductivity at very low concentrations of 0.001 nanoparticles [93, 101-103]. Iyahraja et al [104] They noticed that the study's amazing results showed a significant improvement in heat conductivity, which peaked at an astounding 54%. This accomplishment is even the more amazing considering that it only required a volume fraction of 0.1% of silver nanoparticles, each of which was just 20 nm in size. This astounding increase in thermal conductivity demonstrates the immense potential of nanofluids despite low nanoparticle levels, emphasizing their effectiveness in aiding effective heat transfer processes. The relevance of nanofluids as a prospective route for developing cooling and heat transmission technologies is highlighted by the capacity to obtain such spectacular outcomes with a low nanoparticle presence. Lee and Choi [105-108], The researchers' thorough examination focused on the characteristics of CuO-water/ethylene glycol nanofluids that contained nanoparticles that had sizes of 18.6 nm and 23.6 nm. The properties of Al_2O_3 nanofluids comprising

nanoparticles with diameters of 24.4 nm and 38.4 nm were also studied. When the nanofluids were made up of a volume proportion of 4%, the study's remarkable conclusion showed an amazing 20% improvement in thermal conductivity. This astounding improvement in thermal conductivity shows how these nanofluids have the ability to greatly enhance heat transfer performance, even at a very low concentration of nanoparticles. The use of CuO and Al_2O_3 nanofluids in a variety of applications needing improved thermal management and effective heat transmission is greatly encouraged by our findings. Wang [109] observed a 12% increase in k_{nf} for 28 nm Al_2O_3-water and 23 nm CuO-water nanofluids with a 3% volume percentage. This demonstrates beyond a shadow of a doubt that nanofluids increase thermal conductivity and are more effective coolants than base fluids. Their usage as heat transfer fluids and electronic coolants can be very beneficial.

2.9 Exploring Factors Influencing the Thermal Conductivity of Nanofluids: A Comprehensive Analysis.

2.9.1 Nanoparticle size

In their seminal study, Michael et al [110] conducted a ground-breaking work in which they investigated the effects of dispersing alumina nanoparticles with sizes that varied from 8 nm to 282 nm in water and ethylene glycol. They carefully examined the resulting increase in heat conductivity in seven different nanofluids. The research illuminates the complex interplay between size variation, nanoparticle dispersion, and the ensuing improvement of heat transport parameters in the nanofluid medium. The primary objective of the study was to investigate how base fluid composition and nanoparticle size effect thermal conductivity increase. By exhibiting significant increases in thermal conductivity across the nanofluids, the results showed the value of alumina nanoparticles in facilitating efficient heat transfer. The thermal conductivity increase in these nanofluids declines when the particle size drops below roughly 50 nm, according to their findings. Their findings are consistent with previous research. A recent study on water-based SiC nanofluids with four distinct nominal diameters of 16, 29, 66, and 90 nm found that nanofluids with bigger particles have higher thermal conductivity (k) values [32, 93, 103]. With decreasing particle size in the region of 2 to 40 nm, k in water-based gold nanofluids decreases [111, 112]. An intriguing finding by researchers is that the improvement of thermal conductivity (k) in aqueous alumina nanofluids decreases when the

22

particle size falls below 50 nm at room temperature. This result raises the possibility that there may be a critical point below which the size-dependent improvement of thermal conductivity in these specific nanofluids is no longer meaningful. To comprehend the underlying causes of this phenomena and to investigate other strategies for improving thermal conductivity in nanofluids with smaller nanoparticles, more research is necessary.

2.9.2   Particle shape

The form of the nanoparticles has a significant influence in influencing the improvement of thermal conductivity, according to research on the thermal conductivity of alumina nanofluids. The study looked at a range of particle types, including bricks, blades, cylinders, and platelets. The results showed that platelets > blades > bricks > cylinders were   a clear hierarchy for the enhanced coefficients of heat conductivity. This finding unequivocally shows that particle form has a significant impact on the thermal conductivity increase (k) in nanofluids. These results underline how crucial it is to take particle form into account when developing nanofluids for the best possible thermal management and heat transfer applications [113, 114] . A study conducted by Elena et al [113], while investigating Particle shape effects on thermophysical properties of alumina nanofluids shows that discs contribute highest thermal conductivity (see Figure 2.3 and Figure 2.4). The experimental thermal conductivity enhancement increase in alumina nanofluids with various particle morphologies is witnessed as a result. The shapes of nanoparticles and their corresponding thermal conductivities are displayed in Figure 2.2 & Figure 2.3.
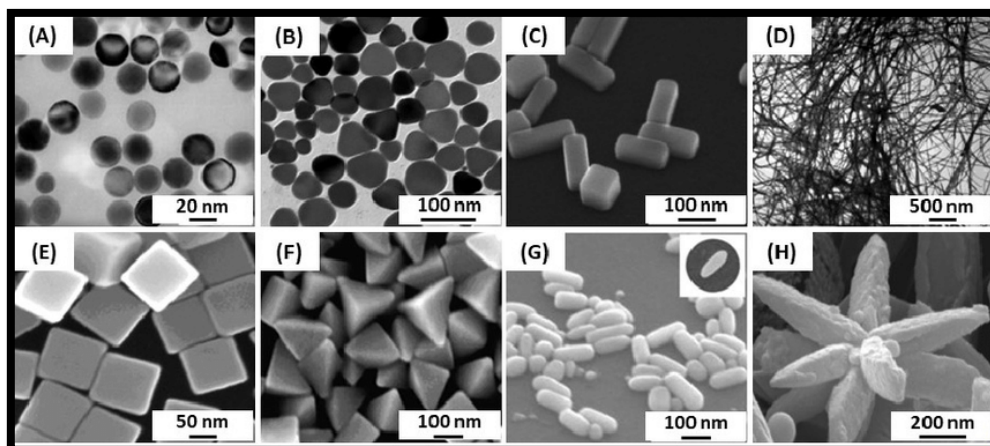
Figure 2.3: A figure showing different shapes of nano particles.

23
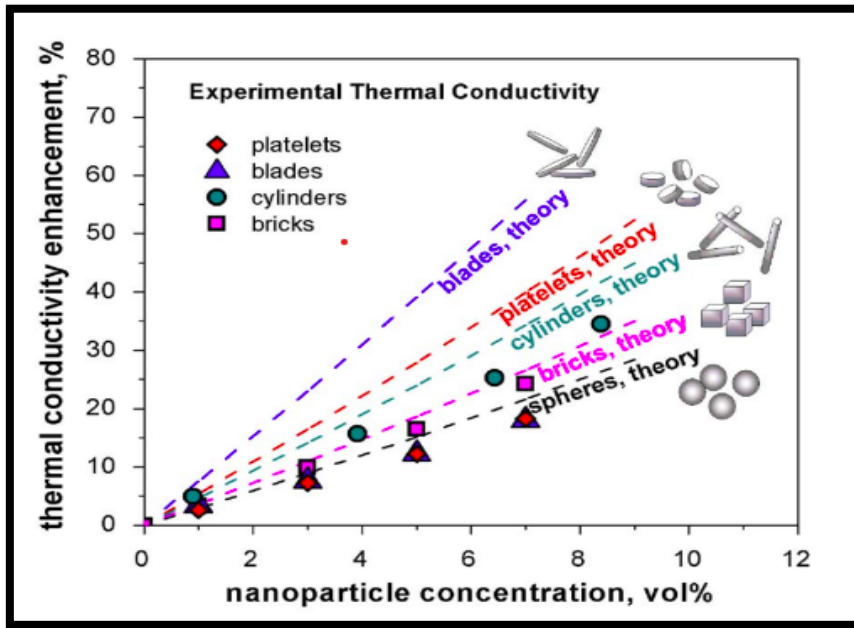
Figure 2.4: A figure showing thermal enhancement due to shape of a nanoparticle *[115]*.

Table 2-2: A table showing different nanoparticle structures.

Shape	sphere	Brick	Cylinder	Platelets	Discs
Shape structure					
Sphericity(ψ)	1	0.81	0.62	0.52	0.32

Where the nanoparticle shape parameter is given by:

$$m = \frac{3}{\psi} \qquad \text{2-5}$$

Literature as we can see reveals that shape size of nanoparticle affects thermal conductivity of a resulting nanofluid [116-118]. Blade shape is proven to have the highest enhancement of them all, with the minimal enhancement for spherical shape oof nanoparticles.

2.9.3 Temperature

The operational temperature is important when constructing heat transfer equipment because it affects the thermal conductivity of nanofluids [119-121]. This is crucial because the total effectiveness of the equipment's heat transmission can be impacted by changes in the thermal conductivity of nanofluids as a function of temperature. Designers may make sure that heat transfer equipment performs at its best across the required temperature range by taking the temperature-dependent behaviour of nanofluids into account [122, 123]. Particles vibrate and begin to move in a Brownian motion as the temperature rises. Brownian motion is a diffusive process with a diffusion constant D, and the Strokes–Einstein formula directly links it to temperature[124, 125]:

$$D = \frac{k_B T}{3\pi\mu d} \qquad \text{2-6}$$

where, k_B is the Boltzmann constant, μ is the viscosity of nanofluid and d is the particle diameter. Due to Brownian diffusion, the characteristic time scale for covering a route equal particle diameter d is.

$$\tau_D = \frac{d^2}{6D} \qquad \text{2-7}$$

Whereby the time scale required for heat to go the same distance in a fluid is given by:

$$\tau_H = \frac{d^2}{6D_T} \qquad \text{2-8}$$

25

Where D_T is a is the thermal diffusivity, which is calculated as the proportion of thermal conductivity to heat capacity per unit of fluid volume.

$$D_T = \frac{k}{\rho C_p}$$ 2-9

Thermal diffusivity relates to temperature by the mathematically as follows.

$$\frac{\partial T}{\partial t} = D_T \nabla^2 T$$ 2-10

The updated Maxwell–Garnett model for nanofluid thermal conductivity may now be written as:

$$\frac{k_{eff}}{k_{bf}} = (1 + AR_e^m \times P_r^{0.333} \varphi) \left[\frac{k_p + 2k_{bf} + 2(k_p - k_{bf})\varphi}{k_p + 2k_{bf} + (k_p - k_{bf})\varphi} \right]$$ 2-11

Effective thermal conductivity, thermal conductivity of particles, and thermal conductivity of base fluids are represented by k_{eff}, k_p, and k_{bf}, respectively. is the proportion of a particle's volume. Reynolds and Prandlt numbers are denoted by Re and Pr, respectively. Experiments may be used to determine A and m, which are empirical constants. Experimental and theoretical findings on water-based Al_2O_3 nanofluids with nominal diameters of 20, 50, and 100 nm found an increase in k/kf with increasing temperature[126-128]. This pattern was also seen in Al_2O_3 nanoparticles in paraffin emulsions [129-131]. Temperature (2–50°C) increased the value of k in water-based Al_2O_3 (36 nm) nanofluids. At 0.2 vol. percent, the boost in k for water-based Al_2O_3 nanofluids was 3.26 percent at ambient temperature (30°C), and 10.76 percent at 60°C. When the temperature was raised from 30 to 60 °C, the k enhancement rose from 6.52 to 23.98 percent for CuO nanofluids [93, 132]. The temperature affects the increase in thermal conductivity of nanofluids. Thermodynamic conductivity of nanofluids is determined using mathematical models based on Brownian motion and kinetic theory, which are easily impacted

by temperature changes. Experiments using nanofluids yield a wide range of outcomes. Mukherjee et al [115] conducted a study that showed a linear dependence of temperature and thermal conductivity.

2.10 Stability

Pinto et al [133] they conducted a study, the main goal of the study was to determine how manufacturing and storage methods affected the long-term behavior of silver nanoparticles in aqueous conditions. The results of the study allowed the researchers to draw an important conclusion: using citrate as a stabilizer makes it possible to preserve silver nanoparticles for more than a year. The study also showed that the degree of oxidation stays minimal when solutions containing the nanoparticles are sheltered from light. These findings highlight how crucial it is to use the right stabilization techniques and light protection strategies to improve the long-term stability of silver nanoparticles in aquatic settings.

The second study by Mafune et al [134] The study focused on examining the stability and structure of silver nanoparticles produced by laser ablation in aqueous solutions. An important discovery was made by the researchers, which suggests that nanoparticles can only sustain long-term stability in liquids provided they have a twofold coating of surfactant molecules. Employing surfactants with longer hydrocarbon chains will result in greater hydrophobic contact between the surfactants, which will increase the efficiency of stabilization. These findings highlight how essential surfactant properties—specifically, the length of the hydrocarbon chain—are for improving the durability of silver nanoparticles in aqueous settings.

2.11 Thermal conductivity

A fundamental feature of materials called thermal conductivity measures how quickly heat is transferred through a substance. It gives an indication of a material's capacity to transport thermal energy effectively [53]. The rate at which heat may pass through a substance is determined by its thermal conductivity; higher numbers denote stronger heat conduction

properties [135]. This trait is necessary for constructing heat transfer systems and comprehending the behavior of materials at various temperatures, which makes it important in a variety of disciplines such as engineering, physics, and materials science [136, 137]. In recent years, researchers have been exploring new ways to enhance the thermal conductivity of fluids for use in various applications [138]. One of these methods is using nanofluids, which are fluids containing nanoparticles. Among the various types of nanoparticles, silver nanoparticles have shown significant ability to increase the heat transfer capacity of fluids [139].

2.11.1 Investigating Factors Affecting the Thermal Conductivity of Silver Nanofluid

Silver nanoparticles are a well-researched option among nanoparticles for enhancing thermal performance due to their unique physical and chemical characteristics [140, 141]. Due to their large surface area to volume ratio, silver nanoparticles may interact with surrounding liquids more actively [142, 143]. Strong interatomic bonds between the nanoparticles and the liquid molecules may be possible due to the large surface area of the particles, which may significantly increase the fluid's temperature [144].

According to research, silver nanoparticles can greatly improve a fluid's thermal conductivity. For instance, Iyahraja et al work from 2015 they observed that adding silver nanoparticles to water can improve its thermal conductivity. They also noticed that thermal conductivity improvement rises as the fluid's silver nanoparticle concentration rises [104, 145].

2.1 Relationship between Thermal Conductivity and PLAL of Silver Water Nanofluids:

The relationship between the PLAL method and the thermal conductivity of silver water nanofluids has been examined in several research. For instance, Zhang et al. [146, 147] generated nanofluids with various nanoparticle concentrations by synthesising silver nanoparticles in water using PLAL. Their research showed that as nanoparticle concentration is increased, these fluids' thermal conductivity noticeably increases, peaking at a certain threshold [148]. Then, as a result of the creation of nanoparticle agglomerates, an unusual inverse pattern appears, with the thermal conductivity steadily decreasing. Our knowledge of the thermal characteristics of nanofluids is expanded by this enlightening discovery, which provides a crucial insight into the complex behaviour of these materials. Similar to this, Zhou

et al. [149] produced nanofluids with various laser fluences and synthesised silver nanoparticles in water using PLAL. They discovered that, up until a certain point, the production of bigger nanoparticles caused the thermal conductivity of the nanofluids to start decreasing as laser fluence was raised. The size and shape of the silver nanoparticles created by the PLAL process is one explanation for the association between PLAL and heat conductivity that has been reported. Depending on the laser fluence and other process variables, the high-energy laser pulse employed in PLAL can produce nanoparticles in a variety of sizes and forms. Due to their higher surface area and more effective phonon transmission, smaller, more uniformly formed nanoparticles are typically anticipated to have higher thermal conductivity than bigger, or irregularly shaped nanoparticles. However, the relationship between the size and shape of nanoparticles and thermal conductivity is complicated, and other elements like particle concentration and surface properties may also be involved.

The surface properties of the silver nanoparticles are another hypothesis explaining the observed correlation between PLAL and heat conductivity. According to other factors, such as the laser fluence, the PLAL technique can produce nanoparticles with a variety of surface characteristics. Due to the presence of insulating surface layers or elevated phonon scattering at the surface, nanoparticles with a higher degree of surface oxidation or functionalization may have poorer thermal conductivity than those with a purer surface. On the other hand, phonon transport may be more effective in nanoparticles with more uniform and clean surfaces, which could lead to better thermal conductivity.

2.2   Relationship between Morphology and PLAL of Silver Water Nanofluids:

The link between the PLAL process and the shape of silver nanoparticles produced in water has been the subject of numerous investigations. For instance, Khosroshahi et al. [150, 151]used PLAL to create silver nanoparticles in water and studied the impact of laser fluence and repetition rate on the nanoparticles' shape. They discovered that as laser fluence and repetition rate increased, the nanoparticles' shape changed from spherical to rod-like. The nanofluids made from the rod-like nanoparticles had a better thermal conductivity because they had a larger aspect ratio and surface area. Similar to this, Zhou et al. [68] looked into how laser fluence affected the shape of silver nanoparticles made using PLAL in water. They discovered that while the nanoparticles had an irregular form at high laser fluences, they exhibited a spherical shape at low laser fluences. The nanofluids made from the asymmetrically formed

nanoparticles exhibited better thermal conductivity because they had more surface area and a porous structure. By altering different process variables, including the laser fluence, repetition rate, and pulse duration, silver nanoparticle morphology can be synthesised using PLAL. The shape and size of the nanoparticles can have an impact on the thermal conductivity and other characteristics of the silver water nanofluids, and these factors can also affect the size and shape of the nanoparticles. The method by which energy is transferred from the laser pulse to the silver target is one explanation for the observed link between PLAL and morphology. The production of nanoparticles with various sizes and shapes can result from the high-energy laser pulse's ability create shockwaves and cavitation bubbles in the liquid.

2.3   Contact Angle

The angle between the tangents drawn to the liquid surface and solid surface at the point of contact and measured via the liquid phase is referred to as the contact angle. As a result, a surface's wettability by liquid can be measured to some extent [152]. Wetted surfaces are referred to as hydrophilic, while water-shedding surfaces are referred to as hydrophobic. For example, glass has a very small contact angle, but Teflon has a much larger contact angle and repels water. The chemistry and properties of the interacting medium, as well as the architecture and nature of the respective interfaces, affect the contact angle. Thomas Young and subsequently Athanase Dupré's renowned work on the adhesion and cohesion of fluids served as the foundation for the creation and significance of the contact angle in the study of three-phase systems [153, 154]. Since that time, the contact angle has been one of the most important experimentally determined quantities used to characterize solids and their wetting properties [155-158]. Wetting is crucial to many industry applications, including printing, lubrication, and heat transfer, among many others [159, 160]. To determine the extent of wetting when a solid and liquid interact, contact angles are measured as the critical information in wettability investigations. High wettability is correlated with small contact angles less than 90°, and low wettability is correlated with wide contact angles greater than 90° [156]. As a result, over the past 200 years, scientists have developed techniques to accurately measure contact angles, interpret experimental results, and understand [95, 161].

2.3.1 Wettability of nanofluids

Earlier experimental findings demonstrated that there are a range of factors linked in nanofluids wetting solids. For instance, one such study clearly demonstrated that altering the concentration of the nanoparticles improves the wetting of nanofluids on solids (i.e., silicon oxide) [162, 163]. There are several prospects for basic and application research in the study of micro- and nanoscale droplets on solid surfaces. On a fundamental level, improvements in the methods for creating and capturing these minuscule droplets will make it possible to test wetting theories at scales as small as the manometer, where they foretell the massive impact of factors like contact line tension or evaporation that can be disregarded when dealing with macroscopic drops [164]. Practically speaking, these advancements will pave the way for the characterization of a wide range of industrially significant materials, such as powdered solids, textile or biomedical micro- and nanofibers, powdered solids, and surfaces with topographically or chemically designed surfaces. These resources are useful for a range of fields, including biomedicine and petroleum engineering, among others.

Nanoparticles interact with solids, liquids, and gases to drastically affect the spreading and wettability of fluids[165]. On solid surfaces, these interactions have an impact on the wetting behaviour and contact angles[166]. Gas sheets made of nanoparticles can change the way fluid spreads. Applications for nanofluids are optimised by understanding these interactions [167-169]. According to Gopalan et al. [170], the solid-like ordering of nanoparticles in the three-phase contact zone and the deposition of nanoparticles during boiling are two important mechanisms for improving the wetting behaviour of nanofluid. Boda et al simulation study of hard spheres in a wedge-shaped cell demonstrated the formation of new layers of hard spheres in the area between the wedge's walls [171]. Earlier experimental findings demonstrated that there are a range of factors linked in nanofluids wetting solids [162]. For instance, one such study clearly demonstrated that altering the concentration of the nanoparticles improves the wetting of nanofluids on solids (i.e., silicon oxide) [162, 172]. Additionally, some investigations noted that the wettability of the solid substrate is significantly altered by the intricate interactions between the particles in the nanofluid and the solid substrate [162]. The contact angle of a fluid on a solid surface is a measure of the wetting behaviour of the fluid on that surface. Several variables, including the interaction between the fluid's surface tension, viscosity, and chemical composition as well as the roughness and chemical make-up of the solid substrate, can have an impact on the contact angle that a fluid exhibits on a solid surface [173-175].

s

2.3.1.1 Effects of Surface roughness on contact angle and wettability

Solid surfaces are not level and smooth. They typically have voids and irregularities that result in local deformations [176]. Wenzel contended that high surface roughness enhances both liquid repellence and wetting. In contrast to a smooth surface composed of the same material, surface roughness enhances liquid repellence when the contact angle is more than 90° and encourages wetting when the contact angle is less than 90° [177-180]. This is true if the surface pattern's size scale is far smaller than the size of the liquid drop. The filling of the surface cavities causes a considerable portion of the drop volume to become invisible when the size of the surface topographical structures approaches that of the drop, which in turn causes the observed contact angle to decrease.

2.3.1.2 Surface impurities or cleanliness

Williams et al [181] argues that clean and unclean must be defined first in order to measure cleanliness. Cleaning is like beauty. Beauty and cleanliness are subjective, depending on who is looking at them. As a result, there is no agreed-upon definition of "how   clean is clean." A contamination is defined as "stuff in the incorrect location," and dirty is sometimes used interchangeably with contaminated.

Contact Angle is a frequent method to determine surface impurities or cleanliness of the surface. Any kind of impurities on the surface prevents wetting and results in higher contact angle [156]. Lower contact angles, which signify greater wetting qualities, are often present on surfaces that have undergone extensive cleaning and treatment to remove impurities and pollutants [182-185]. Since the contact angle is routinely used to determine a silicon wafer's wettability, this strategy is very helpful in the manufacture of semiconductors. It is a great tool for assessing the effectiveness of production procedures and surface alterations [186-188].

2.3.1.3 Porosity

Porosity is defined as a measurement of the empty space in any substance and is defined by:

$$P = \frac{V(void\ space)}{V(total)} \qquad\qquad 2\text{-}12$$

Where $V(void\ space)$ and $V(total)$ are volumes of void space and total volume, respectively.

Another important issue to take into account is porosity. Small capillaries are formed when pores are present on a solid surface, allowing liquid to pass through. However, the particular properties of the liquid and the surface itself determine whether the liquid spreads across the surface or forms droplets [189]. That depends on intermolecular force between the liquid and substrate and the cohesive force between the liquid. The capacity of the liquid to spread over the surface gives the surface a wetting quality when the cohesive intermolecular interactions inside the liquid are higher than the intermolecular forces that exist between the liquid and the solid surface [190-194].

2.3.1.4 Surface energy

The relationship between contact angle and surface tension or energy is of utmost significance. Utilising its relevance in multiple disciplines, this connection finds several applications in a variety of real-world situations and businesses [195-200]. An actual illustration of how surface tension and surface energy interact is the interaction between ink on paper. In this situation, the paper's surface energy must be strong enough to dissipate the ink's surface tension, allowing the ink to spread across the paper's surface and flow downhill. The importance of surface energy in fostering good ink-paper interactions is highlighted by this phenomenon [201-203]. Paint or coating applications serve as another illustrative example where surface energy plays a vital role. When working with polymers or materials with low surface energy, the coating may not flow smoothly, resulting in the formation of fisheye, pinhole gaps, or air bubbles. Conversely, if the material's surface energy is excessively high, the paint may exhibit leakage and prove challenging to control. Achieving an optimal balance in surface energy is crucial for obtaining desirable paint or coating outcomes [204-206]. For effective applications, it is crucial to have a good match between the liquid's surface tension and the material's surface energy [207, 208]. This provides favourable wetting behaviour, ensuring proper adhesion, homogeneous coating, and regulated flow characteristics when these features are properly balanced. For diverse processes and applications to operate as efficiently and effectively as possible, surface tension and surface energy must coexist in harmony [209, 210]. But in general, if the surface energy is stronger than the surface tension of the liquid molecule that is

surface energy overpowers surface tension, causing liquid to spread over the solid surface [211]. The aforementioned proposition stipulates that an increase in surface energy corresponds to a decrease in the contact angle, concomitant with an elevation in wettability [212]. In the event that the surface energy is relatively weaker than the surface tension of the liquid, the mutual interaction between them will not possess sufficient strength to promote the spreading of the liquid across the surface [213]. That means lower surface energy is equal to high contact angle and low wettability. So, in summary we can say that there are several factors that affect contact angles and wettability of the solid surface[174]. All these factors must be taken into account during contact angle and wettability measurements.

2.4   Literature summary and a Gap to fill.

According to published research, base fluids have a lower thermal conductivity than metals and their oxides [214, 215]. The inability of metals and their oxides to flow, as opposed to that of fluids, limits the utilization of metals and their oxides for heat transfer. To improve the thermal conductivity of base fluids, Choi combined the two and produced the term nanofluids. According to the literature, scientists have concentrated their efforts on creating metal oxide nanofluids for electronic cooling, and they have created these nanofluids using a two-step approach. Even though metals have been utilized to create nanofluids in several experiments, most of them used a theoretical approach. Again, research relies on stabilizers and surfactants to keep nanoparticles stable, according to the literature. The purpose of this work is to generate silver nanofluid in water host fluid using the PLAL method, a straightforward technique for studying thermal enhancement. This technique is what we employ because it results in a product devoid of pollutants. The examining of surfactant free silver-water nanofluid for the contact angle will be done, we will also examine how the particles affect fluid flow.

2.5   Application of nanofluids
2.5.1   Electronics cooling

In every industrial and commercial area where an organization works with data processing, data networking, and data storage, electronics cooling is a critical concern. Thermal management is continually and significantly challenged by the rising heat generated by

computer devices. [216, 217]. The essential heat flux and heat dissipation are caused by the rapid migration of processor chips from one generation to the next. However, because of the faster processing speed, the higher heat generation cannot be avoided [218].

2.5.2   Industrial cooling

As energy prices have risen over the past 10 years, manufacturers have had to transform their operations to increase energy efficiency. A comprehensive energy integration plan incorporates heat, cooling, electricity generation/consumption, pressure/depressurization, and fuel usage. The expansion of initiatives to create more cost-effective heat exchange equipment has been motivated by considerations for conserving energy, material, space, and global economics. The physical characteristics of heat transfer fluids, such as thermal conductivity, viscosity, density, and heat capacity, determine how well they can interchange energy within a system. The primary drawback of heat transfer fluids often lies in their low thermal conductivity. However, nanofluids, characterized by their enhanced thermal conductivity, have emerged as a potential substitute for conventional heat transfer fluids. For nearly a decade, nanofluids have been utilized as coolants in American companies, leading to significant energy savings amounting to trillions of British thermal units (Btu) [219]. The use of nanofluids has saved 10-30 trillion Btu per year in the United States alone. The use of nanofluids as coolants has significantly decreased carbon dioxide, nitrogen oxide, and sulphur dioxide emissions. Particularly, the use of nanofluids has resulted in a 5600 million metric tonne reduction in carbon dioxide emissions, an 8600 metric tonne reduction in nitrogen oxide emissions, and a 21000 metric tonne reduction in sulphur dioxide emissions. [220]. Compared to pure fluids, nanofluids with extremely small amounts of metallic or non-metallic substances offer excellent thermal properties. As a result, several researchers have given them some thought. Therefore, most appliances, including heat exchangers, have an efficiency problem, according to earlier studies. Nanofluids can be used to improve their effectiveness.

2.5.3   Smart fluid

Smart nanofluids are used to manage heat transmission [221]. According to Donzelli et al [222], certain classes of nanofluids can be utilized as intelligent materials that act as heat valves to regulate the circulation of heat. A smart fluid is one whose characteristics may be altered by the application of an electric or magnetic field. Nanofluids have the potential to

function as intelligent fluids. Our lack of abundant clean energy sources and the growing use of battery-operated products, including mobile phones, computers, automobiles, and lights, have highlighted the need for intelligent technical management of energetic resources in this new era of energy consciousness.

2.5.4 Nuclear reactors

Nanofluids play a vital role in enhancing critical heat flow within various systems such as nuclear reactors, fossil fuel boilers, and fusion reactors. By incorporating nanofluids, the critical heat flow capability of these systems is substantially increased, leading to improved overall performance and efficiency. When a phase transition takes place during heating, the efficiency of heat transfer rapidly drops, leading to localized overheating of the heating surface. This occurrence is known as a critical heat flux, and it indicates the thermal limit of the event. Researchers Buongiorno et al. and Kim et al. investigated the viability of nanofluids in nuclear reactors and identified potential uses [223]. Another potential application of nanofluids in nuclear systems was described by Buongiorno et al. They proposed that nanofluids are the remedy for the catastrophic accidents during the core meltdown and relocation to the reactor vessel's bottom. If there are such mishaps, it is preferable to keep the molten fuel inside the vessel by eliminating the decay heat via the vessel wall [224]. The presence of Critical heat flux on the vessels outside surface limits this process, but research suggests that using nanofluid can boost nuclear reactors' inner vessel retention capacity by up to 40% [225]. Numerous water-cooled nuclear power plants have CHF limitations, however the use of nanofluid can significantly increase the CHF of the coolant, resulting in bottom-line economic benefits and enhancing the power plant's safety standard.

2.5.5 Nanofluid coolants

To cool internal combustion engines, radiators function as heat exchangers. To control heat, the engine system cycles through the engine coolant. It travels through the engine block, absorbing heat, before being sent to the radiator, where the heat is released into the atmosphere. Finally, the engine receives the cooled coolant back, ready to start the heat transfer cycle again.

[226]. Smaller radiators that are better positioned may be used if nanofluids were used as coolants. With improved efficiency leading to reduced fluid requirements, the size of coolant pumps could potentially be downsized. This could enable truck engines to operate at higher temperatures while complying with stringent pollution regulations. Consequently, such optimization may yield increased horsepower output while maintaining compliance with environmental standards.

2.5.6   Nanofluid in fuel.

A significant advancement in nanotechnology is the use of nanofluids as fuel. According to experimental data, the burning of diesel fuel in the presence of aqueous aluminum nanofluid significantly increases the amount of heat produced overall. Additionally, this creative strategy helps reduce the amount of smoke and the release of nitrous oxide from diesel engines' exhaust. [227, 228]. The greater breakdown of hydrogen from water during burning is made possible by pure aluminum's strong oxidation activity [229].

2.5.7   **Brake and Other Vehicular Nanofluids.**

The heat generated by braking raises the boiling point of the brake fluid, causing a vapor lock that prevents the hydraulic system from quickly dissipating the heat [230]. It will result in braking problems and provide a safety risk for cars. Nanofluids with improved properties boost heat transfer efficiency and all safety issues [231].

2.5.8   Electronic Applications

The major goal of controlling the temperature of electronic components is to keep them at or below the manufacturer's maximum stated service temperature, which is often between 85 and 100 °C [16, 232]. Chip cooling may be accomplished with nanofluid. The primary impediment to the development of smaller microchips in the electrical industry is the rapid heat dissipation. The research of a unique cooling system that uses nanofluids and an oscillating heat pipe (OHP) is presented by Ma et al [233]. It was another invention that made it possible for cooling technology to advance at the same rate as advances in electrical technology. From this data, it

is anticipated that the upcoming generation of computer processors would create a localized heat flux more than 10 MW and a total power greater than 300 W. The study also emphasized the lack of an affordable cooling system that could successfully control heat generation at such levels. This research project will hasten the creation of cutting-edge cooling techniques created especially for electronic systems with extraordinarily high heat fluxes [234]. Even while OHPs and nanofluids are not brand-new scientific discoveries, their complementary properties enable the nanoparticles to be entirely suspended in the base liquid, boosting their capacity for heat transfer [32, 235, 236].

CHAPTER 3 : LASER THEORY

3.1 Pulsed laser Ablation in liquid (PLAL)

Light Amplification by Stimulated Emission of Radiation, or LASER, has become so well-known and widely used in daily life. They are particularly unique because they are monochromic (the same colour), coherent (all light waves are in phase with one another both geographically and temporally) and collimated (all rays are parallel to one another and do not diverge appreciably even over long distances). In 1917, Einstein published "Zur Quantum Theorie der Strahlung," which listed notions of stimulated and spontaneous emission and absorption. This was the year that lasers were first thought about. Dr S. Arthur Schawlow and Charles Townes expanded the use of lasers into the optical frequency range in 1956, [237]. Theodore H. Maiman invented the first pulsed laser on May 16, 1960. It used a ruby crystal and produced light with a wavelength of 694 nm. Since that day, lasers were widely used in both fundamental research and the production of materials. In reality, the laser-assisted fabrication of nanomaterials has been one of the many applications for pulsed lasers [238]. When producing nanoparticles by processes like milling, grinding, and chemical reactions, other undesirable particles could be included. However, to stabilize the colloidal solution during chemical reactions, surfactants are typically required. These two methods are therefore limited in their purity. Precisely during pulsed laser ablation in liquid (PLAL), nanoparticles are produced without impurities [239]. The decrease of particle size was the subject of numerous efforts. As a result, subsequent tests have produced narrow particle sizes. It was also demonstrated that a variety of factors influence the ultimate size and shape. It has been demonstrated that the creation of a highly narrow NP particles size depends heavily on the presence of surfactant molecules [240]. It is essential to correctly set a number of laser parameters, such as laser fluence, pulse length, beam focusing, and repetition rate, in order to obtain a desired size dispersion. The size distribution of the particles or features produced by laser processing is influenced by these variables. The intended output for the specific application is achieved with proper adjustment of these parameters, which guarantees exact control over the size dispersion [241-243]. Additionally, the parameters of the plasma plume are influenced by the material's properties, which determine absorption and the amount of ablated material. Conditions of strong confinement have an impact on both the dynamics and generation of laser plasma[244]. Diverse target materials (elemental, alloys, powders) can be

employed with pulsed laser ablation in liquid, making it a flexible technology [245, 246]. Most recently, researchers have used various target geometries to increase the productivity of the laser ablation process. Another noteworthy benefit is that, in contrast to chemical approaches, nanoparticle manufacturing is free of hazardous substances. Numerous studies have used PLAL to create stable nanomaterials in colloidal solution without using any size-modifying surfactants.

3.2   Laser Theory

A flat, optically transparent media experiences partial reflection, absorption, scattering, and transmission of a ray of light incident on it (see Figure 3.1). The wavelength, material type, and thickness of the material all affect how much light is absorbed [247]. The optical absorption in each absorber is given by Equation:

$$E = E_0 e^{-\alpha z} \qquad\qquad\qquad 3\text{-}1$$

E – transmitted irradiance

E_0 – incident irradiance

α – Target attenuation coefficient

z – absorber thickness in the same units of length as α
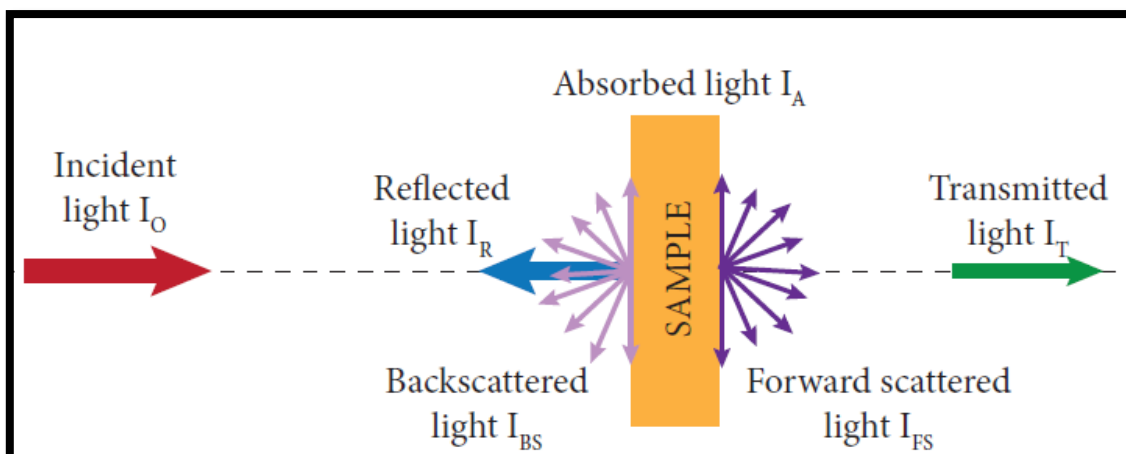
Figure 3.1: The figure demonstrates the interaction of light as it passes through a transparent medium of thickness z. The incident light undergoes absorption, reflection, and transmission upon encountering the medium, resulting in changes in its intensity and direction.

$$I_0 = I_R + I_A + I_T \qquad\qquad \text{3-2}$$

The Beer-Lambert law establishes a relationship between the attenuation of light and the properties of the medium it traverses. The absorbance is.

$$A = \varepsilon l c \qquad\qquad \text{3-3}$$

The transmittance, defined as the amount of light passing through an absorber is frequently described using the symbol T is written as:

$$T = \frac{E}{E_0} \times 100\% \qquad\qquad \text{3-4}$$

All opaque materials absorb, scatter, and reflect a range of visible wavelengths that give them their color, as well as a range of UV and NIR wavelengths. Transmittance is the measurement of a material's ability to transmit light of a certain wavelength to a detector placed behind it. Any decrease in intensity observed by the detector when compared to the original beam indicates that the sample has either absorbed, reflected, or scattered some of the light at that wavelength. This phenomenon is referred to as extinction. Due to the disparity in refractive

41

indices, reflection occurs when two media come into contact. Equation represents a relationship between the percentage of reflection R and the angle of incident light on the interface.

$$R(\%) = \left(\frac{n_2 - n_1}{n_1 + n_2}\right)^2 \times 100\%$$
<div align="right">3-5</div>

n_1 & n_2 – are materials' refractive indices.

When working with lasers, protective goggles must always be worn for safety reasons because the radiation level is typically significant. Radiance is given by:

$$E = \frac{Power(mW)}{Area(cm^2)}$$
<div align="right">3-6</div>

3.3   Population inversion

Lasers rather than creating energy, lasers change it. They generate photons from the electrical energy used to excite atoms or molecules, regulate those photons to produce a focused beam of light [248]. According to Chen et al [249] Population inversion, the threshold phenomena, and optical feedback are the three prerequisites that laser generation must satisfy (see Figure 3.2). Population inversion indicates that there should be a greater population at the upper level than in the lower level. Most atoms tend to be in their lowest energy state under normal circumstances, while just a limited fraction is in a higher state. In some circumstances, both achieving population inversion and high-speed gas flow require energy. To produce a laser, an atom in ground state 1 in a four-level model is excited to level 4 by absorption of a photon with a specific energy. Before being pumped into the cavity, the atom undergoes a quick, nonradioactive relaxing phase that causes it to fall from level 4 to level 3. It is significantly simpler to establish population inversion between populations in energies E3 and E2 due to the quick non-radiative processes and the vacant energy E2. Particles are pushed from ground state 1 to level 3 in a laser system with three levels, as depicted in Figure 1B. Once level 2 is reached, they decay quickly between level 2 and ground state 1, the population inversion is accomplished. Due to the equal likelihood of an electron being raised to the upper level and falling to the ground position, a two-level energy system like the one depicted in Figure 1C is not frequently utilized for lasing.
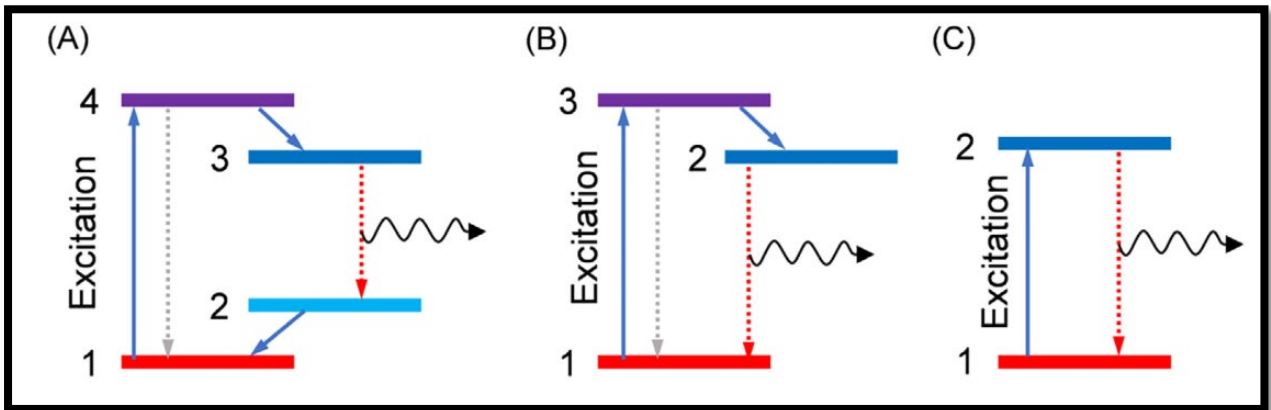
Figure 3.2: A Figure Exploring Three Models for Achieving Laser Emission. This figure illustrates the three distinct models employed to achieve lasing: (A) a four-level system, (B) a three-level system, and (C) a two-level system. Each model represents different energy level configurations involved in the process of laser emission.

3.4   Types of lasers

Pulsed lasers are classified as either solid state (such as Nd-YAG and Ti-Sapphire) or gas phase (such as Excimer and carbon dioxide laser sources). This thesis focuses on Nd-YAG, which was used to create the nanofluid. Arc lamps or laser diodes are used to power the solid-state source. Arc lamps have a higher power density than diodes. The output laser light is infrared at 1064nm and can be doubled, tripled, or even quadrupled. Optics is employed to give it life and can produce pulses lasting tens of nanoseconds. Due to their little product loss, minimal operation requirements, and precise size control, these lasers are the most often used for research. The sluggish pace of nanoparticle manufacturing, high energy consumption, and high cost of laser equipment are its key drawbacks. Neodymium Yttrium-Aluminium-Garnet (YAG) is composed of $Y_3Al_5O_{12}$ with some Nd3+ ions replacing the Y_3^+ ions. The insulated inner 4f states are the active electronic states in the rare earth metal neodymium. The Nd: YAG laser has four levels. At 1.064 m, Nd: YAG emits most of its energy[250]. It has many applications such as laser lipolysis[251], labelling of ceramic and plastic IC packages [252], thin film deposition [253], and synthesis of nanomaterials [254].
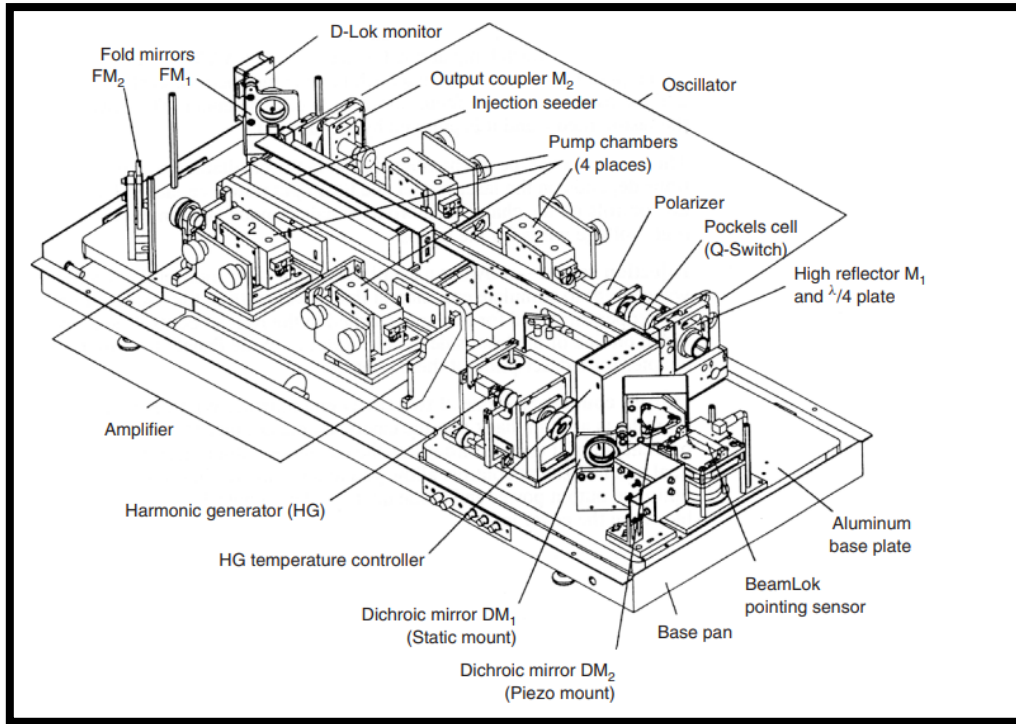
Figure 3.3: **Figure showing an Integration of Components in the Head of an Nd: YAG Laser System.**

3.5 Laser Matter interaction

The material properties govern the laser performance requirements while using pulsed laser ablation [255]. The properties that matter have to do with how much energy is required to vaporize or alter a material's phase, as well as how much light and heat it can absorb [256, 257]. These properties include thermal diffusivity D_T, attenuation coefficient at the wavelength of the laser α, the heat of vaporisation H_v and density ρ [258, 259] .One may start selecting the laser settings required to achieve ablation at the desired scale after the material has been understood (see Figure 3.40) [260]. The two most important parameters to comprehend are the pulse duration, which measures how long the energy is focused on the surface [261].
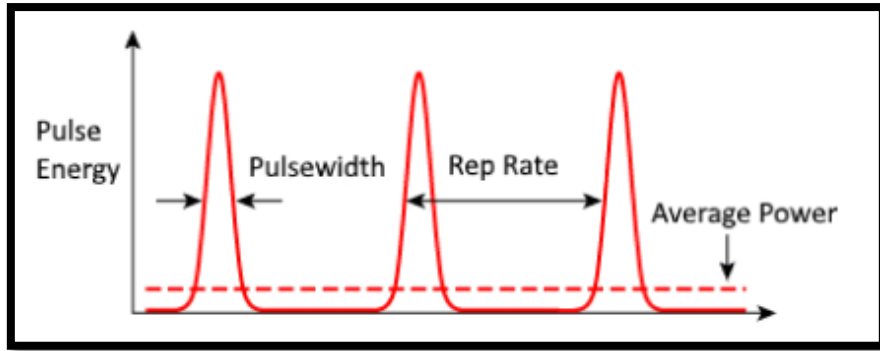
Figure 3.4:LASER Pulse width and duration.

The second is the quantity of energy that is deposited on a beam spot region, or laser fluency. The idea of optical and thermal penetration is important to grasp to comprehend how fluence and pulse duration work. When a laser beam strikes a material, its energy travels a distance:

$$l_\alpha = \frac{1}{\alpha} \qquad \text{3-7}$$

which is determined by the substance's attenuation coefficient. The thermal diffusivity determines the thermal penetration depth during the ablation during a pulse, and is given by:

$$l_t = \sqrt{D_T \tau_L} \qquad \text{3-8}$$

The amount of energy required to accomplish vaporization per unit volume to ablate a material is known as the threshold fluence. The volume and heat impacted zone for short pulses may be thought of as being confined by optical penetration depth, providing a threshold fluence F_{th} independent of pulse length. F_{th} for $\tau_L \ll 10^{-11}s$ is given by:

$$F_{th} = \frac{\rho H_v}{\alpha} \qquad \text{3-9}$$

45

The threshold fluence increases with pulse duration for pulses above around $10\ ps$ because the thermal penetration depth is greater than the optical one. F_{th} for $\tau_L \gg 10^{-11}s$ is given by

$$F_{th} = \rho H_v l_\tau \qquad\qquad \text{3-10}$$

The two-temperature model follows the gradual transfer of thermal energy to the lattice while accounting for the electrons' energy absorption. The electrons in the lattice's heat capabilities are used in the model.

$$C_e \frac{\partial T_e}{\partial t} = \frac{\partial}{\partial z}\left(k_e \frac{\partial T_e}{\partial z}\right) - \Gamma_{e-p}(T_e - T) + (1 - R)\alpha I(t)e^{-\alpha z} \qquad \text{3-11}$$

$$C \frac{\partial T_e}{\partial t} = \Gamma_{e-p}(T_e - T) \qquad\qquad \text{3-12}$$

C_e - Electron volumetric heat capacity

C - Lattice volumetric heat capacity

T_e – Electron temperature

T - Lattice temperature

k_e – Electron Thermal conductivity

Γ_{e-p} – Electron-Lattice temperature coefficient

α – Target attenuation coefficient

R – Target Reflectivity

I – Laser intensity

3.6   Mechanism of Pulsed laser Ablation in Liquid (PLAL)

In a prior work, Maaza et al [254]. Short time scales, typically referred to as the "nanosecond regime," have been seen to cause a variety of events when a pulsed focused laser beam interacts with a metallic solid object submerged in liquid. The following list of essential processes, which are all included in the laser ablation procedure, may be summarised in Figure 3.5 and Figure 3.6:

I) A fast and temporary event arises from the interplay between a pulsed laser beam and a solid object, leading to the creation of an atomic plasma on the surface of the object. This phenomenon is characterized by its quick initiation and short-lived duration.

II) The plasma is formed as a result of the rapid expansion of the material when exposed to intense laser radiation. This expansion leads to high temperatures and pressures within the plasma. These extreme thermodynamic conditions create an environment where significant dynamics of energy transfer occur.

III) Interaction-induced high-temperature plasma leads to shock waves in the immediate vicinity. These shock waves propagate through the surrounding medium, further complicating system dynamics.

IV) Simultaneously, a subtle vapor layer materializes around the plasma volume, indicating cavitation bubble formation. This vapor layer, a temporary manifestation, adds intricacy to the multiphase dynamics observed during the laser-material interaction.

V) As the plasma cools down, a critical phase occurs marked by the formation of nanoparticles within the plasma volume. These nanoparticles exhibit colloidal characteristics and disperse within the surrounding fluid as shock waves induce cavitation bubble contraction. This process leads to a colloidal suspension, emphasizing laser-induced plasma dynamics and nanoparticle formation.

During the laser ablation procedure, distinct phenomena manifest, including the visually striking spark and the audible cracking sound. It is noteworthy that the nature of the experimental setup ensures that the expanding plasma plume remains fully submerged within the liquid. This prevents any unintended splashing of water. This is achieved by submerging

both the solid target and the laser beams beneath the liquid's surface, ensuring confinement and containment of the plasma within the liquid environment.
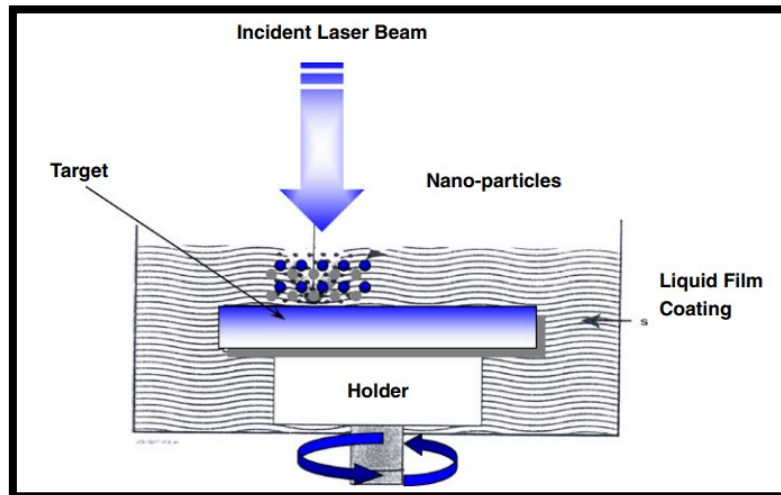
Figure 3.5 : A Figure Illustration depicting a simplified setup for laser liquid solid interaction, where a silver target is subjected to a normal incidence laser beam with precise focus [262].
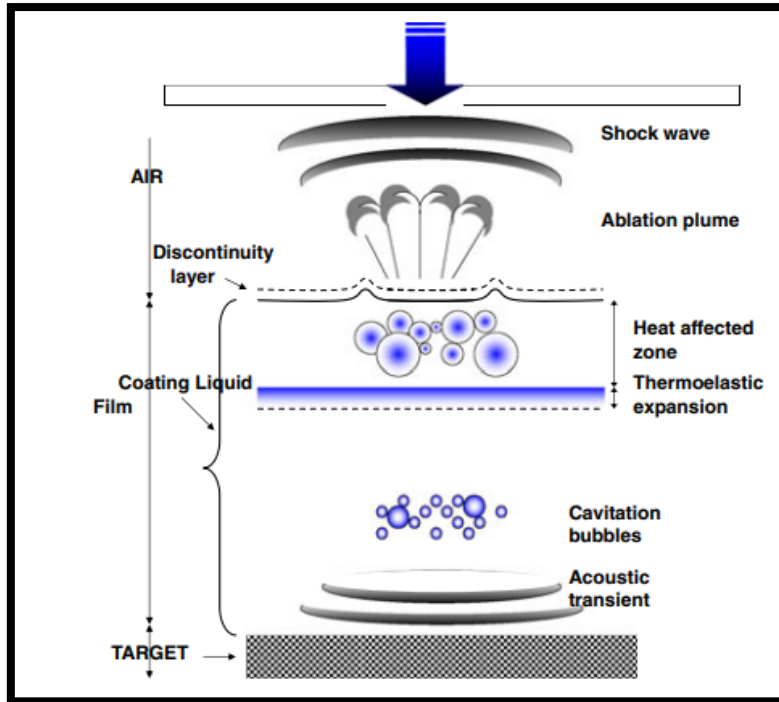
Figure 3.6: **A Figure showing Ablation Mechanisms during Laser Liquid Solid Interaction - Analysing the Role of Cavitation and Implosion of Formed Vapor Bubbles [262].**

As nanoparticles were being created, the base liquid's colour began to change toward the end of the ablation process, as seen in the Figure 3.7.
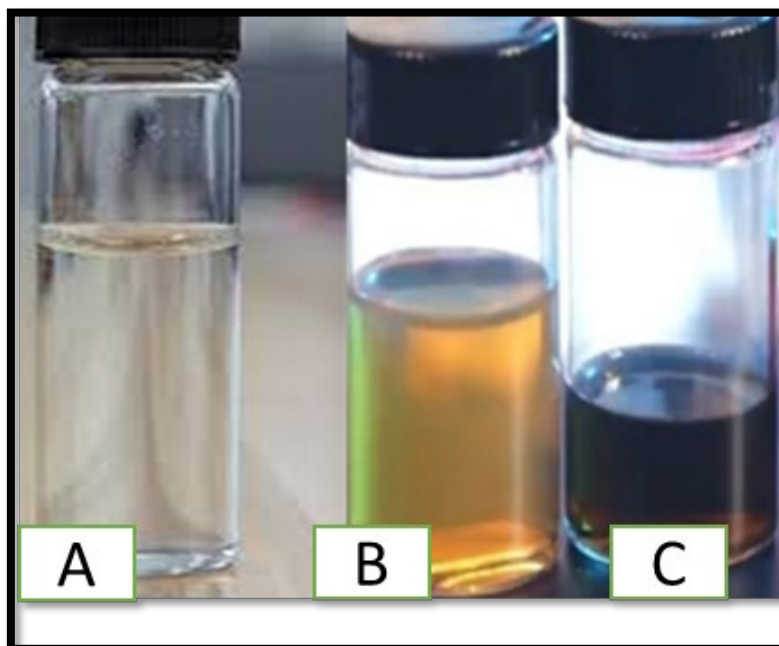
Figure 3.7: (A) De Ionized water, (B) &(c) Silver -De Ionized water nanofluid.

3.7 Particle shape and size

Particle size and shape is adjustable based on the difference parameters in the set up. So, like Laser power or frequency or the type of solution, you are using. So, for example, this vial of brown nanoparticles that I showed in the beginning, this was generated with a high-power pulse. The large pulse ablates bigger fragments of metal, and so when those quench, you turn to get larger nanoparticles. Whereas this vial was done at a lower power, so you get smaller Ablation products. And thus, smaller nanoparticles.

3.8 Why PLAL

Now there are dozens of different ways to generate nanoparticles that the literature is filled with different ways to make it. So, the question is why is this preferable to those other technics. Well, for one, it is simple, you do not need anything other than your metal, liquid, and your Laser. And so, the setup is easy to get up and running quickly. It is clean, meaning that the only thing that is in your vial, is the liquid, which is usually pure distilled water and the nanoparticles.

CHAPTER 4 : "Synthesis and Characterization of Silver-Water Nanofluid using Pulsed Laser Ablation in Liquid (PLAL)"

4.1 Material and instrumentation

Chemicals and reactants: For this experiment, the only necessary base fluid was distilled water and Silver from Sigma-Aldrich, purity: 99%.

Chemical apparatus: This experiment's equipment included beakers, a funnel, a sample container, a dropper, a clamp, and other items.

Machines and instruments: Rotating stand (The target is put on a revolving stage to maintain the surface and avoid overheating and cracking.), UV-Vis Spectrophotometer (for optical properties studies), Scanning Electron Microscopy (SEM) for morphology studies with Energy Dispersive Spectrometer (EDS) for composition studies, hot wire method equipment (for thermal conductivity studies) and goniometer (for contact angle measurement).

Software's: Origin and Sigma plot

4.2 synthesis of Ag-H_2O nanofluids by Pulsed Laser Ablation

An overview of the PLAL process, which was utilized to create silver nanoparticles, is given in this chapter, the results are additionally explored (see Figure 4.1).
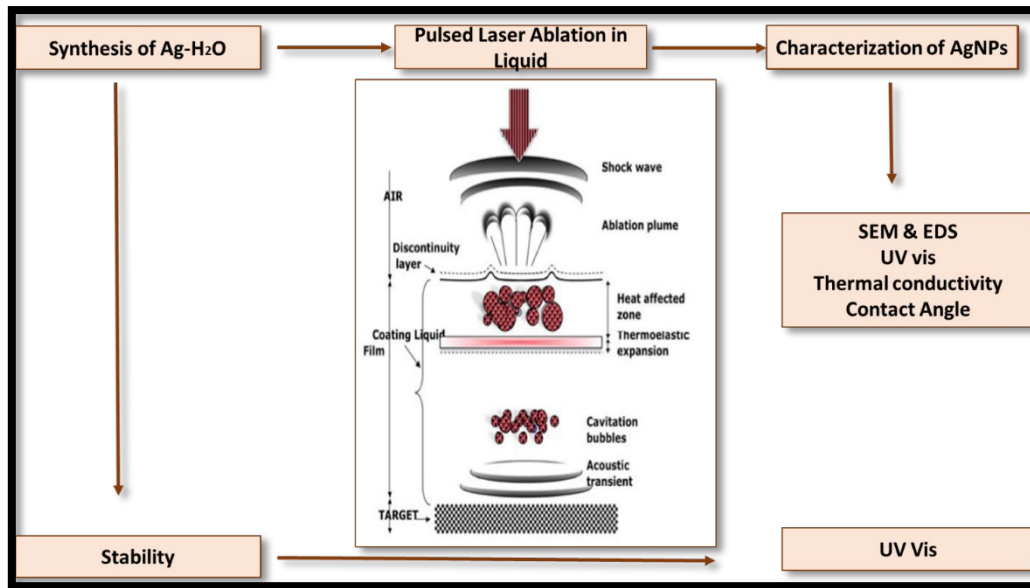
Figure 4.1: Synthesis and characterization of Ag-H2O nanofluid

4.3 Experimental design

Figure 4.2. is the fabrication method of AgNPs-H₂O nanofluid through laser ablation of solid Ag target in base fluid (H₂O)"
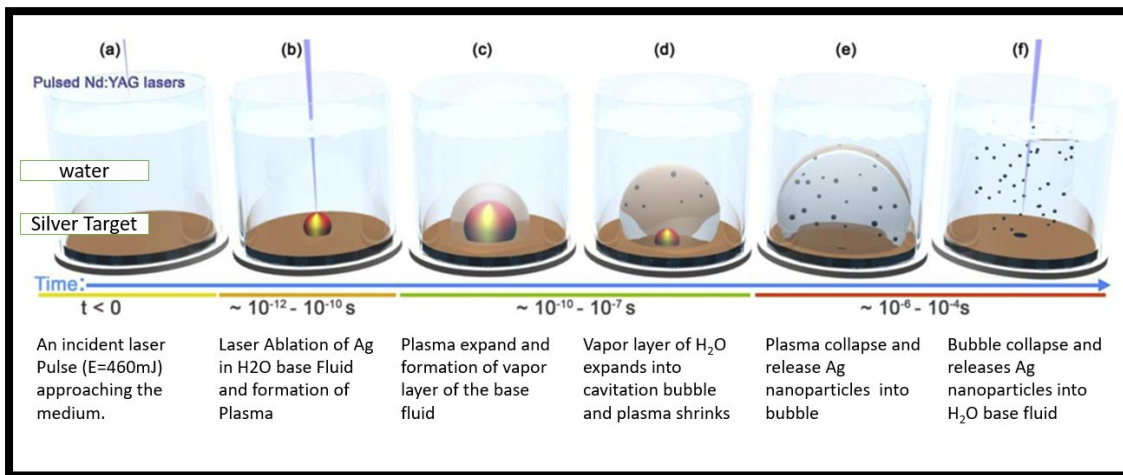
Figure 4.2: Mechanisms causing the ablation of solid Silver Target (Ag) in water (H₂O).

The experimental setup consisted of the following components and parameters:

1. Ag Target: A 10 mm diameter and 6 mm thick Ag target, obtained from Sigma-Aldrich with a purity of 99%.

2. Beaker: A glass beaker filled with 15 mL of H_2O (water).

3. Laser: A pulsed Nd: YAG laser with the following specifications:

   - Wavelength: 1064 nm

   - Pulse Duration: 10 ns

   - Output Energy: 465 mJ/pulse

   - Laser Power: 4.65 kW

   - Beam Focus: 2.5 mm

4. Laser Operation: The pulsed laser beam was operated at a repetition rate of 10 Hz.

5. Converging Lens: A converging lens with a focal length of 1200 mm was placed above the beaker to focus the pulsed laser beam.

6. Reflective Mirrors: Coated mirrors, optimized for 1064 nm, with a diameter of 45 mm and a thickness of 15 mm, were utilized to guide and direct the laser light during the experiments.

7. Placement: The Ag target was positioned at the bottom of the beaker, approximately 2 cm below the top surface of the H_2O.

This experimental design made it possible to see and analyze the phenomena that resulted from the interaction of the pulsed laser beam with the Ag target submerged in water.
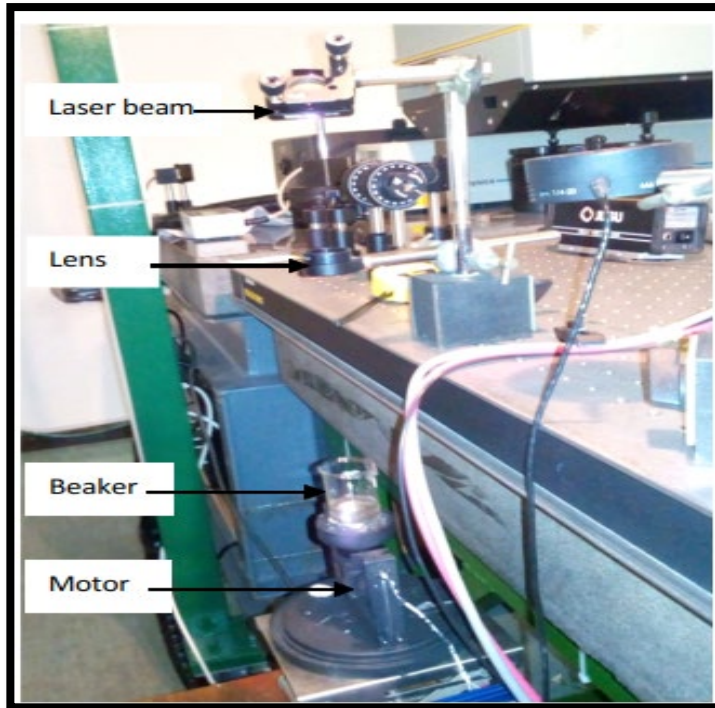
Figure 4.3: The method of fabricating AgNPs-H2O using PLAL.

4.4   Experimental technique

The laser was turned on for a 30- to 60-minute warm-up period. This was done to reach operational temperature for the Nd: YAG laser rods and lamps. After each production of the nanofluid, the alignment of the laser entering the beaker was checked.

Then, the following procedures were used to synthesize silver nanoparticles:

1. A pure silver target was put inside a beaker containing 15 milliliters of deionized water.

2. To improve the distribution of silver nanoparticles in a water host fluid, the beaker was mounted on a revolving stand.

3. The silver target underwent ablation for 2.5, 5, 10, 15, 20, and 25 minutes, yielding six distinct nanofluids of varying concentrations.

4. The samples were taken and clearly marked, for example, "sample ta=2,5 min," "ta=5 min,"...

4.5   Characterization

4.5.1   AgNPs-H$_2$O nanofluid, fabrication

The AgNPs-H$_2$O nanofluid, fabricated through laser ablation of a solid Ag target in H$_2$O, was subjected to various characterizations to understand its properties. The morphology and composition analysis of the obtained AgNPs were conducted using Scanning Electron Microscopy (SEM) and Energy-Dispersive Spectroscopy (EDS), respectively.

4.5.2   Morphology analysis

SEM, or scanning electron microscopy, was used to carry out the morphological investigation. A little portion of the sample, which was probably made up of AgNPs, was spread out over a substrate and allowed to dry. The sample was then covered with a thin coating of carbon, a conductive substance. This process contributes to the final photographs' improved quality. The surface morphology of the AgNPs was examined, and their size distribution was evaluated, using the SEM method.

4.5.3   Elemental composition

To determine the elemental composition, EDS was employed. EDS is a technique that measures the characteristic X-ray emission from the sample when bombarded with an electron beam. A high-resolution detector was used to analyze the emitted X-rays and identify the elemental composition of the AgNPs.

4.5.4   Optical properties and stability of the nanofluid

The optical properties and stability of the nanofluid were studied using UV-Vis spectroscopy. A UV-Vis spectrophotometer was employed to measure the absorption and scattering of light by the nanofluid. The nanofluid was placed in a cuvette, and its absorbance spectrum was recorded in the ultraviolet-visible range. The stability of the nanofluid was assessed by monitoring any changes in the UV-Vis spectra over time.

4.5.5 Thermal conductivity (k)

The thermal conductivity (k) of the fabricated AgNPs-H_2O nanofluid was determined experimentally using a homemade guarded hot-plate apparatus. The apparatus consisted of two plates with a temperature gradient, and the nanofluid was sandwiched between them. The heat flow through the nanofluid was measured, and the thermal conductivity was calculated using Fourier's law of heat conduction.

4.5.6 Contact angle

The contact angle of the nanofluid on a solid surface was measured directly using a Telescope-Goniometer. A droplet of the nanofluid was placed on a solid substrate, and the angle formed between the droplet and the surface was measured using the goniometer. The contact angle provided information about the wetting behavior of the nanofluid and its interaction with the solid surface.

4.5.7 Conclusion

In conclusion, the characterization of the AgNPs-H2O nanofluid involved SEM and EDS for morphology and composition analysis, UV-Vis spectroscopy for optical property and stability assessment, a homemade guarded hot-plate apparatus for thermal conductivity determination, and a Telescope-Goniometer for contact angle measurement. These characterizations provided valuable insights into the physical, chemical, optical, thermal, and wetting properties of the nanofluid, contributing to a comprehensive understanding of its potential applications.

CHAPTER 5 : Morphological properties of the Ag-H₂O PLAL synthesized nanofluids.

5.1   Introduction

The two types of silver water nanofluids are aggregated and scattered. As contrast to dispersed nanofluids, which have individual nanoparticles disseminated evenly throughout the base fluid, aggregated nanofluids feature nanoparticles that have agglomerated into larger clusters. Silver nanofluids' shape has a big impact on their physical, chemical, and optical characteristics. The goal of this chapter is the use of SEM and EDX for characterising nanofluids by revealing details about the morphology, elemental content, and impact of the nanoparticles on the characteristics of the nanofluid. These technologies enable the improvement of synthesis procedures and the creation of custom nanofluids for purposes by providing researchers with a thorough grasp of nanofluid behaviour.

5.2   Techniques for characterizing and examining the morphology of silver nanoparticles (SEM and EDS)

Energy dispersive spectroscopy (EDS) with scanning electron microscopy (SEM) investigations of the produced Ag nanoparticles were carried out to gain a better understanding of   their   morphology   and   composition.   Figure   5.1

Figure 5.1: figure showing SEM with EDS

5.3 measurement of the size, shape, and surface properties of nanoparticles results

SEM image was taken at a scale of 500 nm at 100 K X magnification. *Ag-H₂O* was composed of clustered aggregates of varied sizes, but with varying degrees of aggregation. To establish the dimensions of the nanoparticles, such as diameter, length, or area, the SEM picture was processed using measuring tools in ImageJ.

5.3.1 SEM ANALYSIS

Figure 5.2 to Figure 5.7 shows typical scanning electron microscopy (SEM) findings for PLAL produced Ag-H$_2$O nanofluid at various concentrations. The synthesised silver water nanofluids used in this investigation were identified by the notations NF1, NF2, NF3, NF4, NF5, and NF6. Every identifier corresponds to a certain ablation time in the synthesis procedure. NF1 denoted, for example, the nanofluid that was synthesised and had an ablation duration of 2.5 minutes; NF2 denoted an ablation period of 5 minutes, and so on. This notation scheme was used to improve clarity and make it easier to compare the various nanofluids that were synthesised at different ablation times by streamlining the referencing to them. At low concentrations there is less aggregation while for high concentration there is more aggregation. There is evidence in the literature that as nanoparticle concentration increased, the stability of the nanofluids decreased [263].
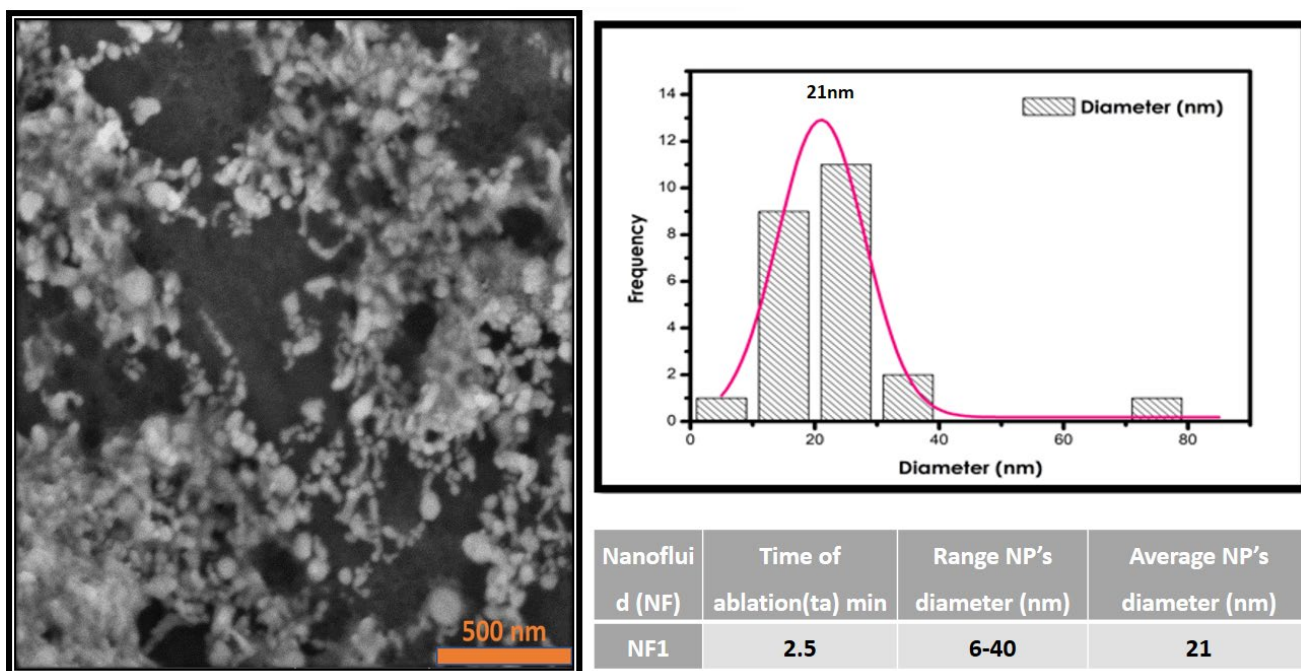
Figure 5.2: SEM results and Histogram of diameter distribution for Ag-H$_2$O synthesised by PLAL ablated for 2.5min (NF1) at 100 K X magnification.

Nanofluid (NF)	Time of ablation(ta) min	Range NP's diameter (nm)	Average NP's diameter (nm)
NF1	2.5	6-40	21
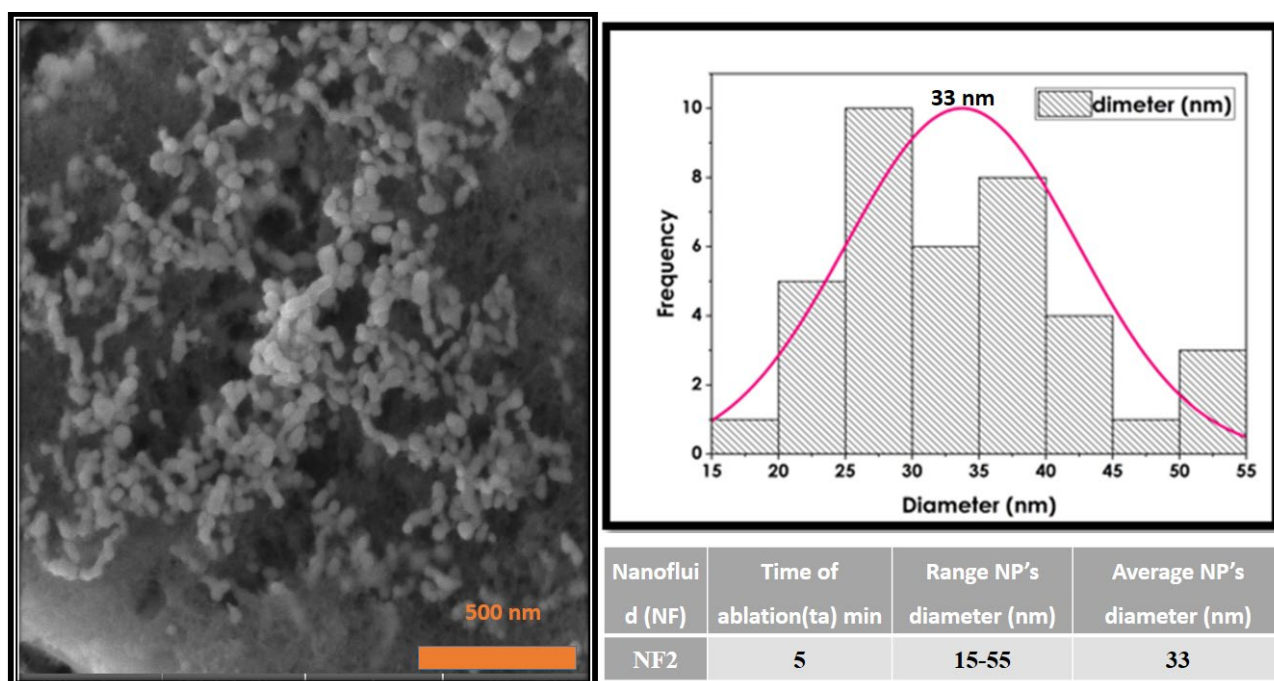
Figure 5.3: SEM results and Histogram of diameter distribution for Ag-H$_2$O synthesised by PLAL ablated for 5 min (NF2). at 100 K X magnification.

Nanofluid (NF)	Time of ablation(ta) min	Range NP's diameter (nm)	Average NP's diameter (nm)
NF2	5	15-55	33

Nanoflui d (NF)	Time of ablation(ta) min	Range NP's diameter (nm)	Average NP's diameter (nm)
NF3	10	10-55	37
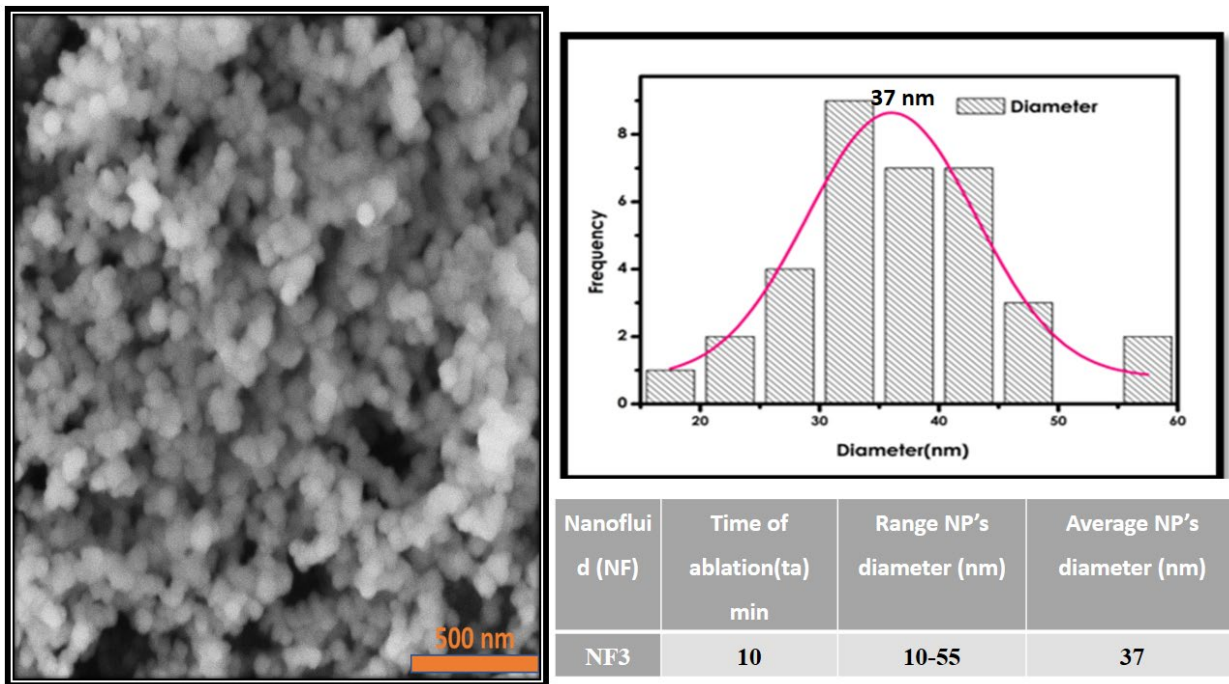
Figure 5.4 SEM results and Histogram of diameter distribution for Ag-H$_2$O synthesised by PLAL ablated for 10 min (NF3) at 100 K X magnification.

Nanoflui d (NF)	Time of ablation(ta) min	Range NP's diameter (nm)	Average NP's diameter (nm)
NF4	15	11-40	23
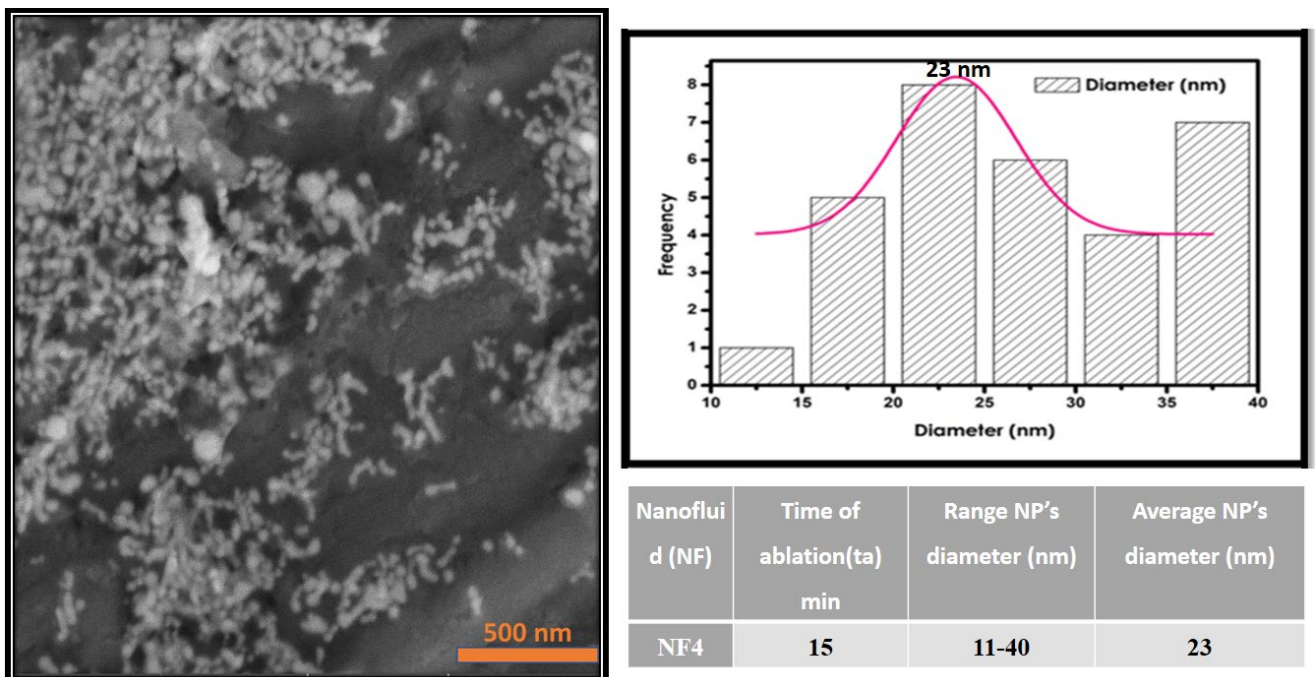
Figure 5.5: SEM results and Histogram of diameter distribution for Ag-H2O synthesised by PLAL ablated for 15 min (NF4) at 100 K X magnification.

.

60

Figure 5.6: SEM results and Histogram of diameter distribution for Ag-H₂O synthesised by PLAL ablated for 20 min (NF5) at 100 K X magnification.
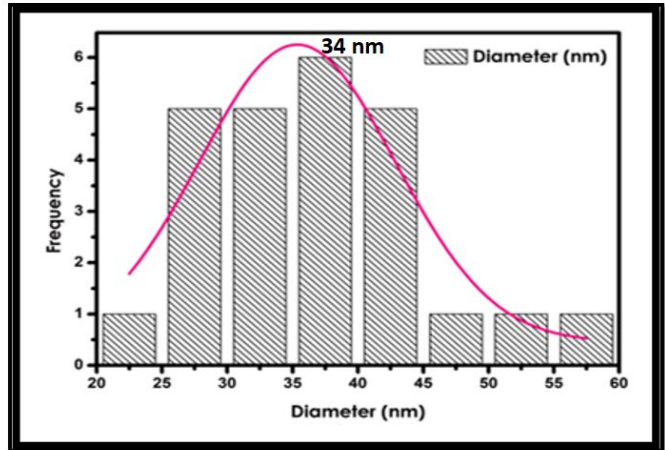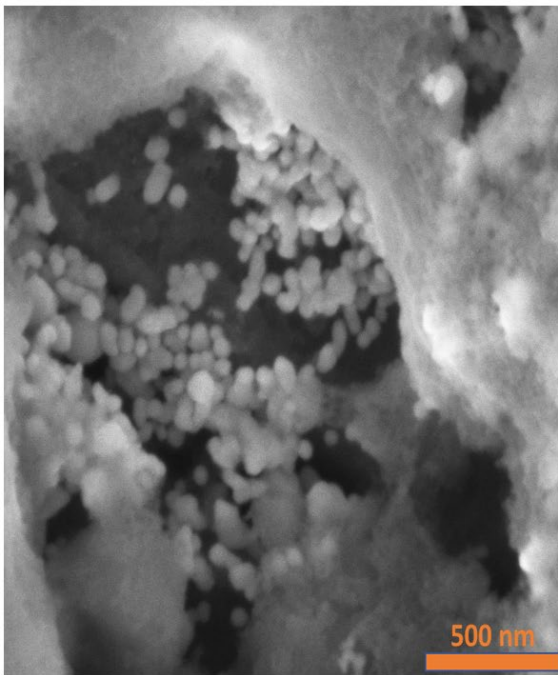
Nanofluid (NF)	Time of ablation(ta) min	Range NP's diameter (nm)	Average NP's diameter (nm)
NF5	20	35-65	34

Figure 5.7: SEM results and Histogram of diameter distribution for Ag-H₂O synthesised by PLAL ablated for 25min (NF6) at 100 K X magnification.
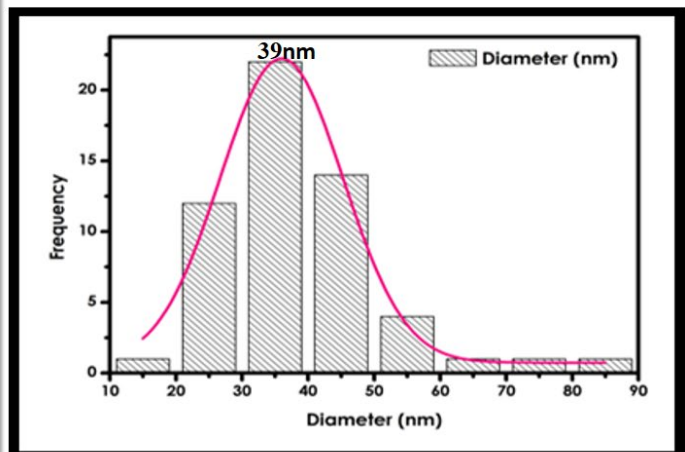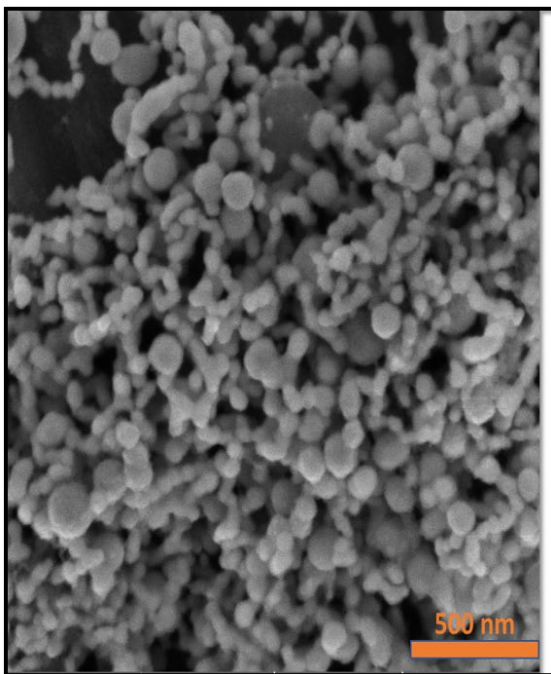
Nanofluid (NF)	Time of ablation(ta) min	Range NP's diameter (nm)	Average NP's diameter (nm)
NF6	25	15-85	39

61

5.3.2 Size distribution of silver nanoparticles in Water

Using scanning electron microscopy (SEM), the morphology of the nanofluids was identified. The average particle size and size distribution of the nanofluids were calculated using ImageJ software after analysis of the SEM images. To create nanoparticles, it is important to understand how long the ablation process lasts. The t_a values in this table indicate the nanofluid synthesis timeframes for each nanofluid sample, which vary from 2.5 minutes to 25 minutes. The smallest and greatest nanoparticle sizes found in each nanofluid sample are represented by the range of NP's diameter. The ranges differ between samples, demonstrating the variety of nanoparticle sizes. For instance, while the diameter range of NF1 is 6–40 nm, that of NF6 is 15–85 nm.

5.3.2.1 nanoparticles distribution

The comparatively restricted range of nanoparticle dimensions (6–40 nm) that NF1 exhibits is suggestive of a more carefully managed production process. Given the shorter ablation duration of 2.5 minutes, this tight distribution points to a high degree of particle size uniformity. Comparing NF2 and NF3 to NF1, the ranges of nanoparticle diameters are wider (15-55 nm and 10-55 nm, respectively). The longer ablation times (5 and 10 minutes) may be responsible for the larger spread since they allowed for more thorough nucleation and growth processes. The wider distribution might be more adaptable in uses where a variety of nanoparticle sizes are needed, but depending on the use case, it might also result in performance variations. Even wider ranges of nanoparticle diameters (11–40 nm, 35–65 nm, and 15–85 nm, respectively) are shown by NF4, NF5, and NF6. The longer ablation times (15, 20, and 25 minutes) may have allowed for more widespread nucleation and growth, which is why the distributions are wider. The wide distribution, however, can also make it more difficult to achieve reliable results in applications that call for stable nanoparticle sizes.

5.3.2.2 Average nanoparticles diameters

The average nanoparticle diameters of NF1 and NF4 are smaller—21 and 23 nm, respectively—which may indicate that smaller nanoparticles are prevalent as. NF4's lower average nanoparticle diameter may suggest that nanoparticle growth was constrained, even

though it had a longer ablation period. The average sizes of the nanoparticles produced by NF2 and NF5 are 33 nm and 34 nm, respectively, suggesting a balance between the nucleation and growth processes. With typical nanoparticle sizes of 37 nm and 39 nm, respectively, NF3 and NF6 show considerable expansion during synthesis. Larger average sizes could have resulted from intensive nucleation and growth processes made possible by the extended ablation periods.

5.3.2.3   Analogy and Consequences:

The data demonstrates how ablation duration affects the distribution and average size of nanoparticles, with longer times often leading to bigger average sizes and broader distributions. Comprehending these correlations is crucial in customizing the synthesis settings to attain the intended nanoparticle attributes for particular uses. By precisely controlling the size and distribution of nanoparticles using optimization techniques, future research may be able to fully realize the potential of silver water nanofluids in a variety of technological and biological applications.

5.4   Ag-H$_2$O Element Composition studies

EDS investigations were conducted to ascertain the materials' chemical make-up. Except for Carbon and Aluminium from the Carbon coated aluminium grid, there are no other elements visible in the sample's EDS spectra besides silver (Ag) peaks. Figure 5.8 to Figure 5.13 shows a typical EDS spectrum on a silver water nanofluid.   The nanofluid samples were subjected to EDX analysis in order to determine the percentage composition of silver and other elements, including carbon. The elemental makeup of the nanofluids and the production method were revealed by the EDX data, namely the % content of silver. To comprehend the variability in elemental composition with increasing time of ablation, the changes in the percentage composition of silver seen throughout samples (NF1 to NF6) were analysed in conjunction with the results of the EDX. The efficacy of the synthesis procedure as well as the concentration and dispersion of silver nanoparticles in the nanofluids were assessed using the EDX data.
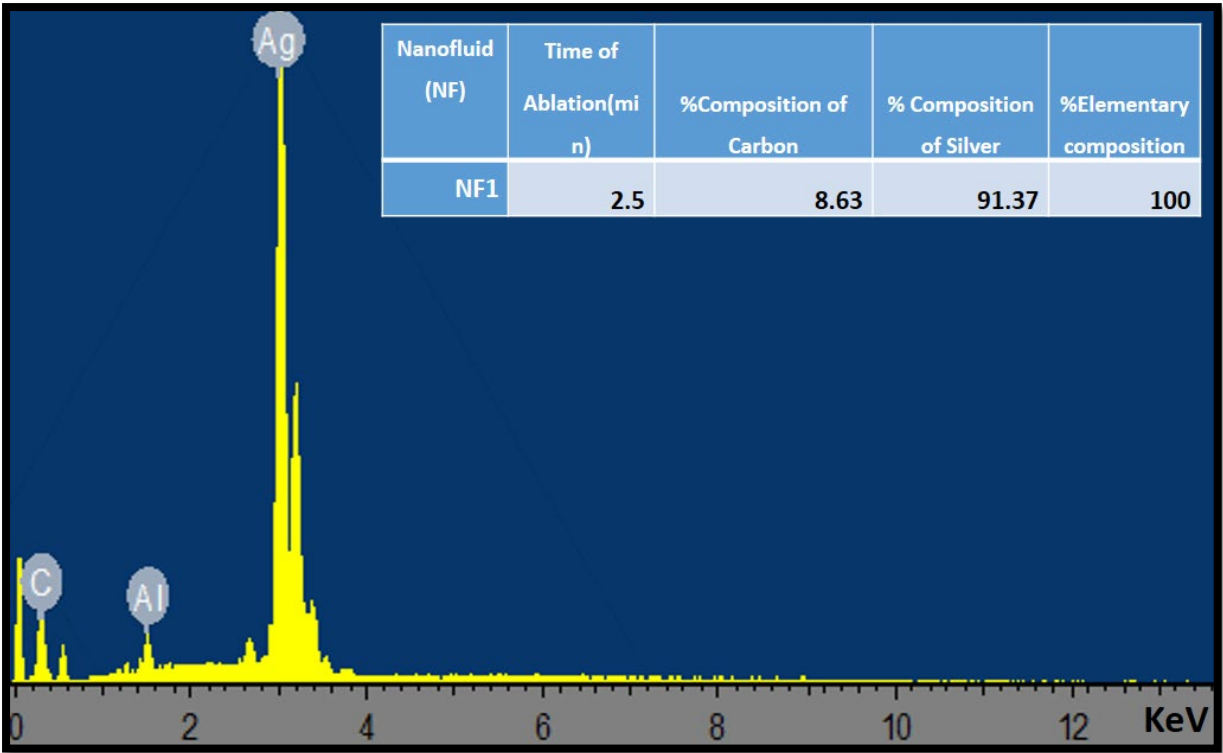
Figure 5.8: EDX Analysis Results for NF1.

Nanofluid (NF)	Time of Ablation(min)	%Composition of Carbon	% Composition of Silver	%Elementary composition
NF1	2.5	8.63	91.37	100
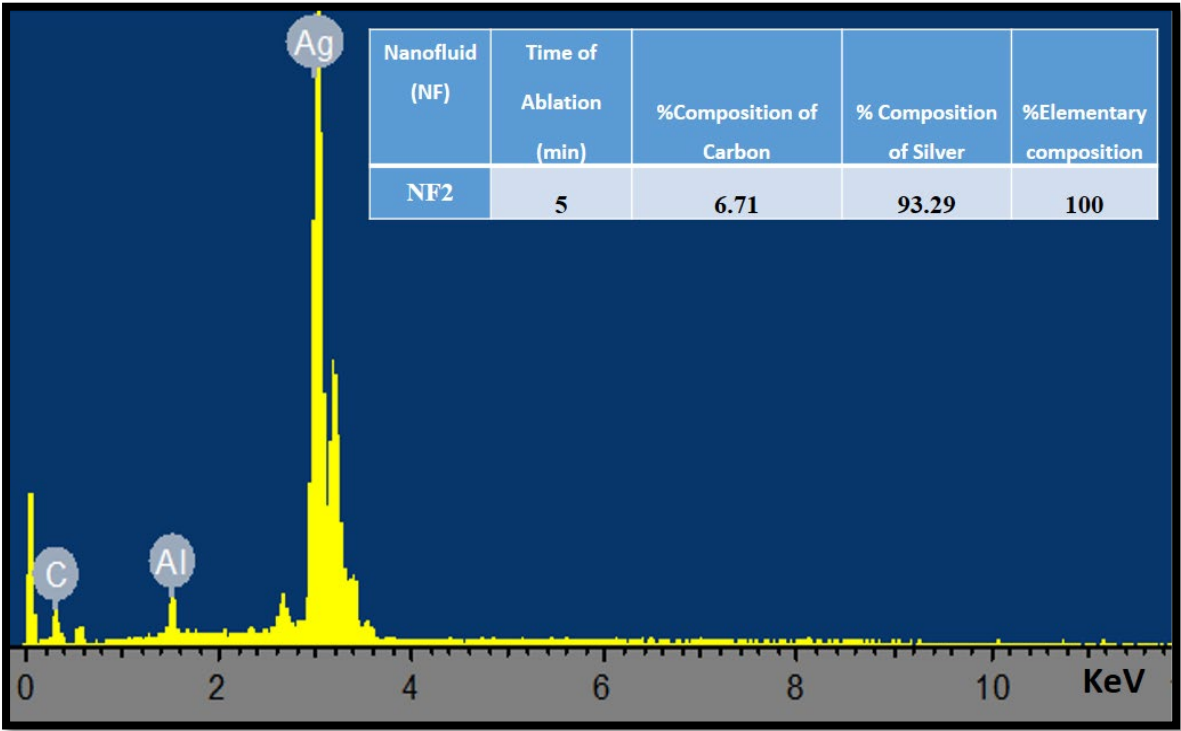
Figure 5.9: EDX Analysis Results for NF2

Nanofluid (NF)	Time of Ablation (min)	%Composition of Carbon	% Composition of Silver	%Elementary composition
NF2	5	6.71	93.29	100
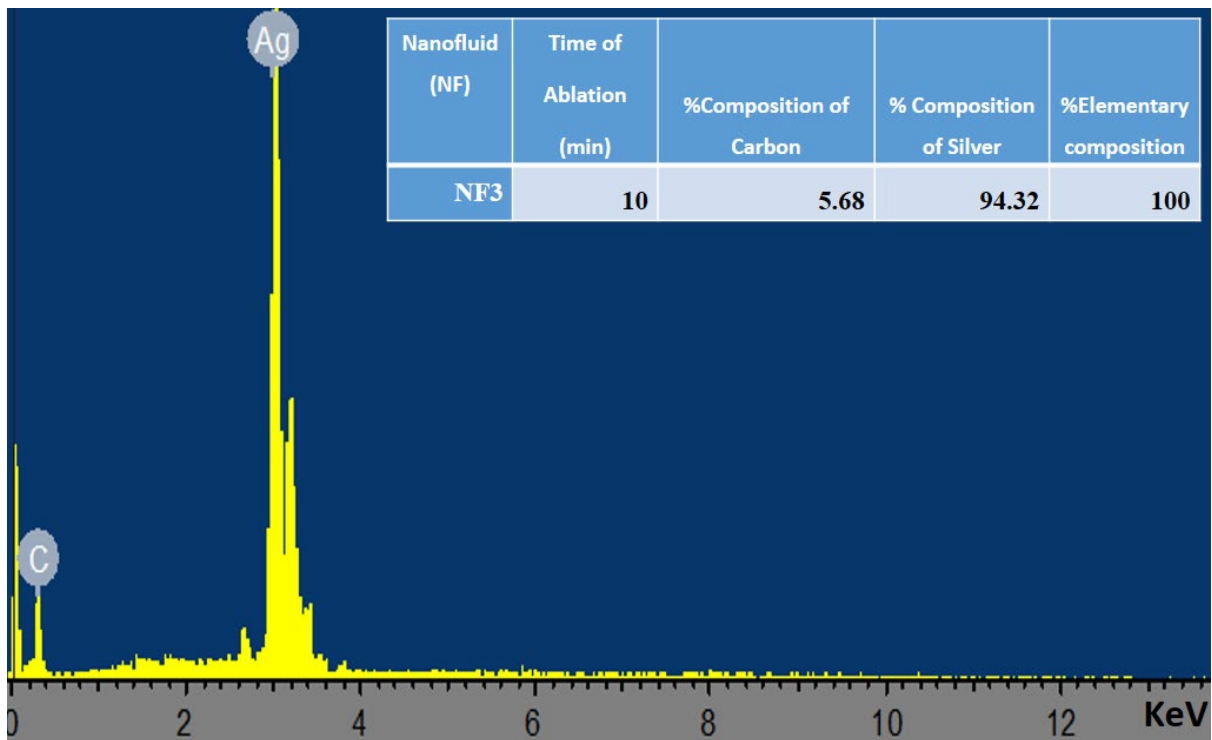
Figure 5.10: EDX Analysis Results for NF3

Nanofluid (NF)	Time of Ablation (min)	%Composition of Carbon	% Composition of Silver	%Elementary composition
NF3	10	5.68	94.32	100
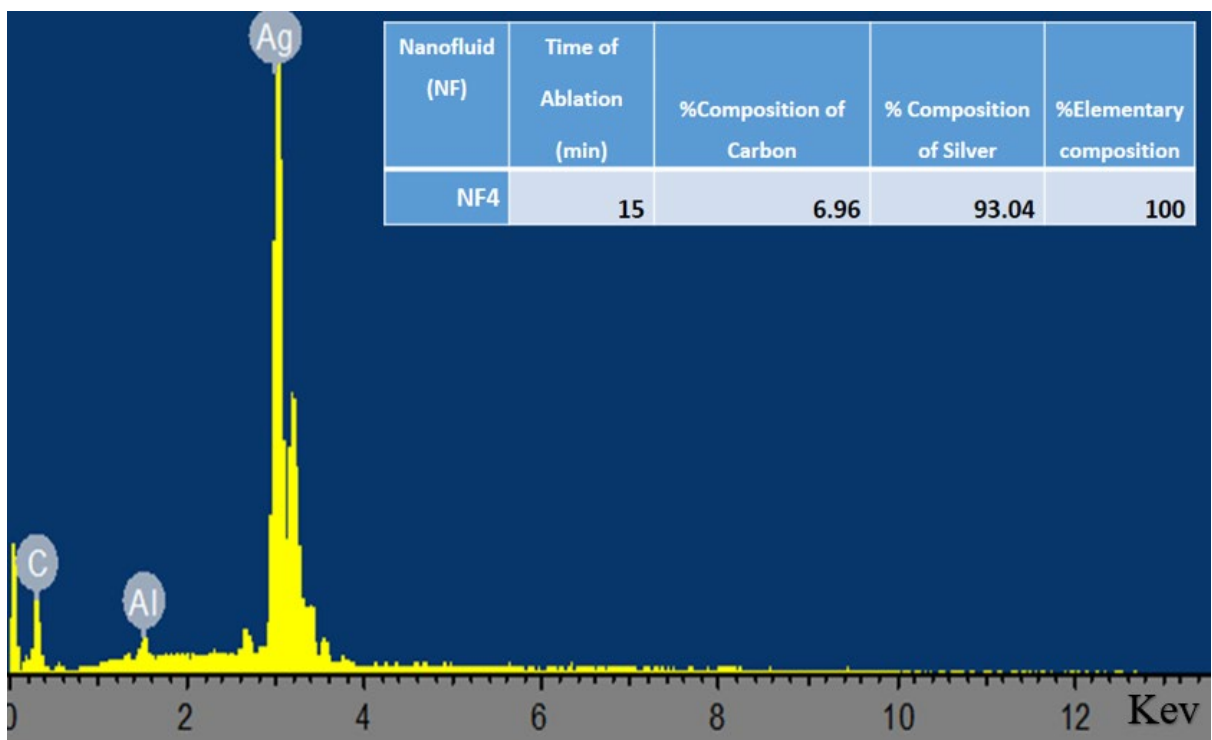
Figure 5.11: EDX Analysis Results for NF4

Nanofluid (NF)	Time of Ablation (min)	%Composition of Carbon	% Composition of Silver	%Elementary composition
NF4	15	6.96	93.04	100

Nanofluid (NF)	Time of Ablation (min)	%Composition of Carbon	% Composition of Silver	%Elementary composition
NF5	20	3.65	96.35	100
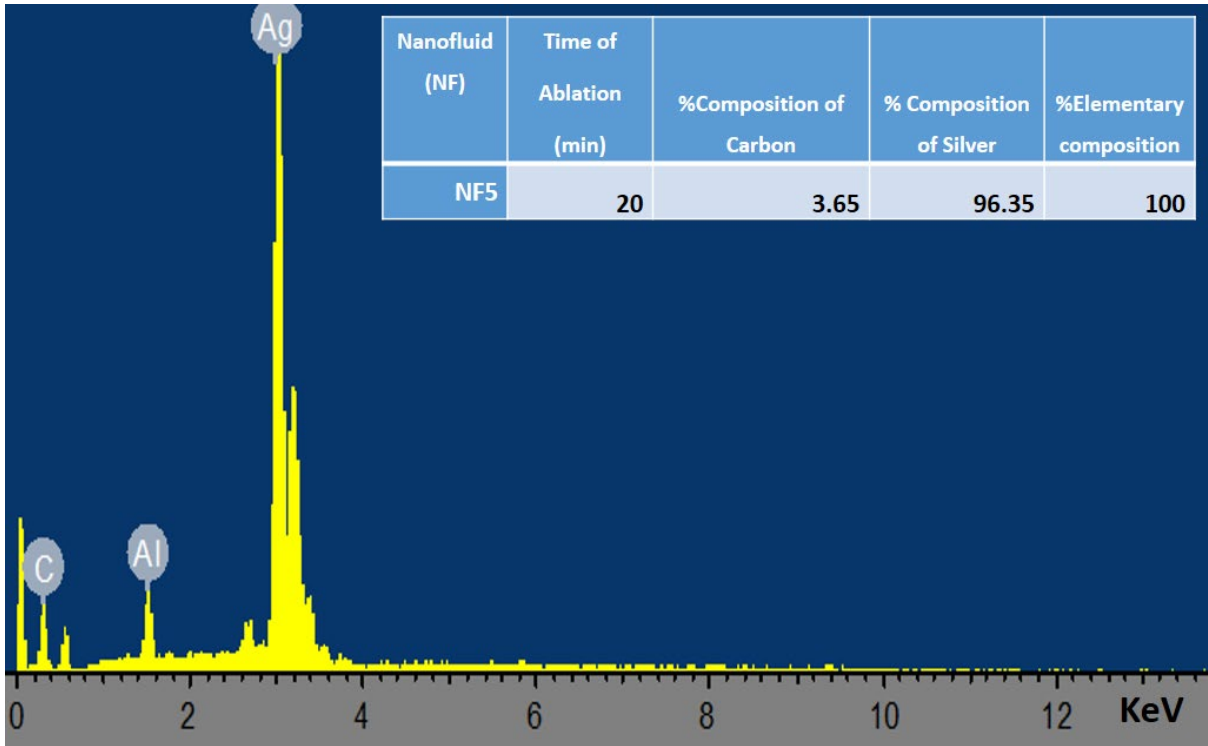
Figure 5.12: EDX Analysis Results for NF5.

Nanofluid (NF)	Time of Ablation (min)	%Composition of Carbon	% Composition of Silver	%Elementary composition
NF6	25	5.89	94.11	100
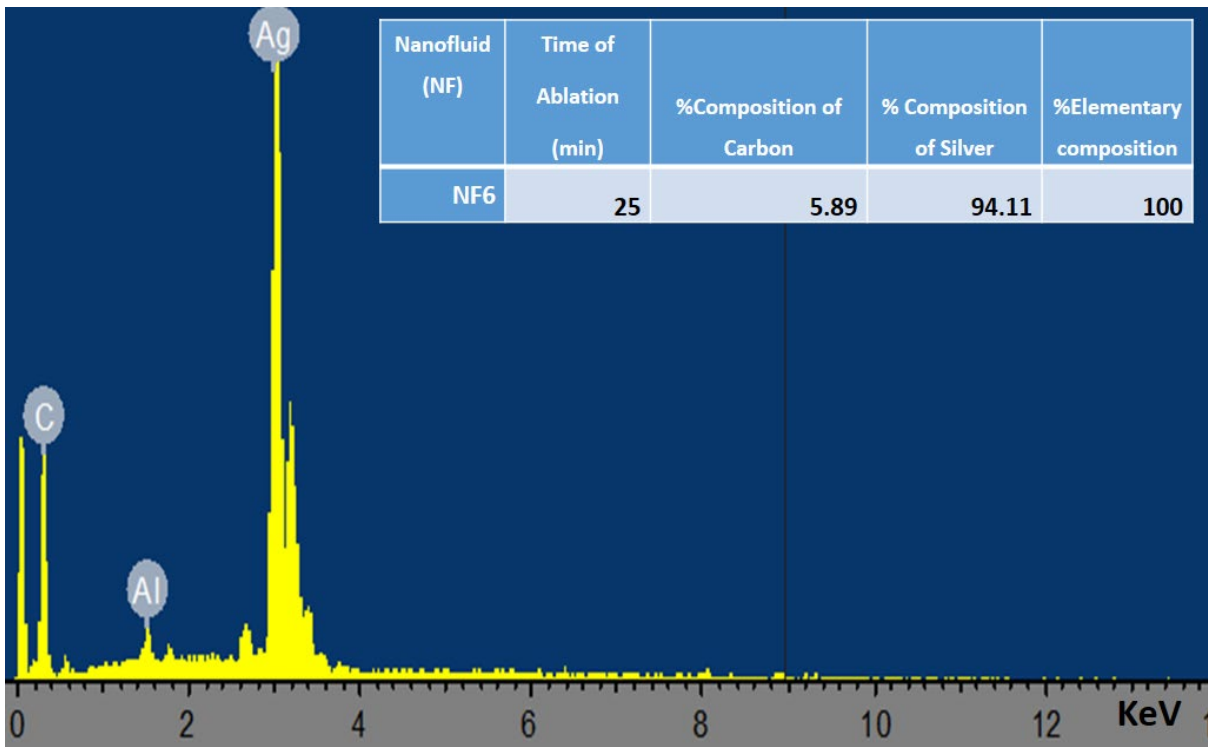
Figure 5.13: EDX Analysis Results NF6.

5.4.1 Current Trends in Elements Composition:

The effective production and dispersion of silver nanoparticles with increasing ablation time is indicated by the gradual increase in silver percentage from NF1 to NF5. Higher percentages of silver can be found in the resultant nanofluids due to longer ablation periods allowing for more thorough fragmentation and dispersion of the target material. Higher concentrations of silver can be achieved by more effectively fragmenting and dispersing the silver target material, which can be achieved with a longer ablation duration. Prolonged ablation durations can, however, eventually cause nanoparticles to aggregate or re-deposit, which could result in variations or saturation in the silver percentage that is being measured. Agglomeration of nanoparticles may change the distribution and detection of individual nanoparticles, which may have an impact on the reported elemental composition, particularly for longer ablation periods.

Conversely, enhanced dispersion makes it possible for nanoparticles to be distributed more uniformly throughout the nanofluid, which may result in greater measured silver percentages.

% Composition of Carbon: The amount of carbon that was introduced during the characterisation procedure is shown in this column. From NF5 to NF1, the carbon content ranges from 3.65% to 8.63%. These ratios represent the volume of carbon added to the nanofluid throughout the characterisation process. The amount of silver in each nanofluid sample falls between 91.37% (NF1) and 96.35% (NF5). It shows that all the nanofluid samples had a significant silver concentration.

CHAPTER 6 : AgNPs-H$_2$O Optical investigation

6.1 Characterization

6.1.1 Introduction.

UV-vis spectroscopy was used to investigate the formation and stability of silver nanoparticles from an ablation process of silver-submerged underwater host fluid. Throughout the experiment, distilled water was used as a blank solution, and measurements were made at room temperature with a resolution of 1 nm in the wavelength range of 200 to 800 nm. The samples had different concentrations of silver-water nanofluid. These concentrations were suitable for various ablation times of 2.5, 5, 10, 15, 20, and 25 minutes. Nanomaterials are elusive to the naked eye. UV-vis shows that Wavelengths between 380 and 470 nm are often absorbed by silver nanoparticles smaller than 100 nm in diameter. Smaller particles absorb light with shorter wavelengths. With a diameter of 10 nm, spherical silver nanoparticles can absorb light between 400 and 410 nm. Smaller AgNPs exhibit a blue shift in the spectral curve while larger particles exhibit a red shift [264]. This is because AgNPs with smaller sizes exhibit better electron confinement, which raises the plasmon resonance energy level. The spectral curve shifts to the blue at this higher energy level because shorter light wavelengths are absorbed or dispersed at these levels. Put differently, smaller AgNPs scatter or absorb light at shorter wavelengths, usually in the blue part of the spectrum [265-268]. On the other hand, when AgNPs get bigger, the electrons are less strongly confined, which lowers the energy at which their plasmon resonance occurs [269]. The spectral curve is redshifted as a result of longer light wavelengths being scattered or absorbed at this lower energy level. Stated differently, larger AgNPs scatter or absorb light at longer wavelengths, which are generally in the red part of the spectrum [265, 270].The peak of the spectrum can change depending on the predominate form of the nanoparticles. The plasmonic band would noticeably widen toward longer wavelengths because of the nanoparticles aggregating [271-273].

6.1.2 Methods for evaluating the stability of nanofluids.

The following procedures are involved in the examination of nanofluids using UV-Vis spectroscopy:

Sample Preparation: The silver-water nanofluid was synthesized by PLAL method.

Setup of the Instrument: UV-Vis spectrophotometer was switched on and allowed some time to warm up. A wavelength range of 200-800nm was used.

Measure the baseline or "blank" using de-ionized water that doesn't contain any nanoparticles. This takes into consideration any background scattering or absorption caused by the base fluid itself.

Sample measurement: Measure the produced nanofluid sample by placing it in a suitable cuvette and placing the cuvette inside the spectrophotometer. The sample was properly positioned in relation to the light beam. By scanning the necessary wavelength range, the absorbance or transmission spectra of the nanofluid was determined.

Data analysis: The spectrophotometer data were used to determine the absorbance. data analysis was carried out utilizing original software or tools. Calculations were made to determine the absorbance values of the nanoparticles at wavelengths.

Figure 6.1: A Figure showing UV-Vis spectroscopy.

Throughout the investigation, distilled water served as a blank solution for the measurements, which were conducted in the wavelength range of 200 to 800 nm.

6.2 Optical Results of AgNPs-H$_2$O:

Silver nanoparticles have a plasmon resonance peak that is generally observable in the visible spectrum between 400 and 500 nm. The plasmon peak obtained was around 400nm indicating Silver nanoparticles correspond to those from prior research on Ag nanospheres [274]. As

expected, since we only used water and silver nanoparticles to synthesize our nanofluid. Figure 6.2 to Figure 6.7 shows the effect of ablation time on Plasmon absorption resonance.
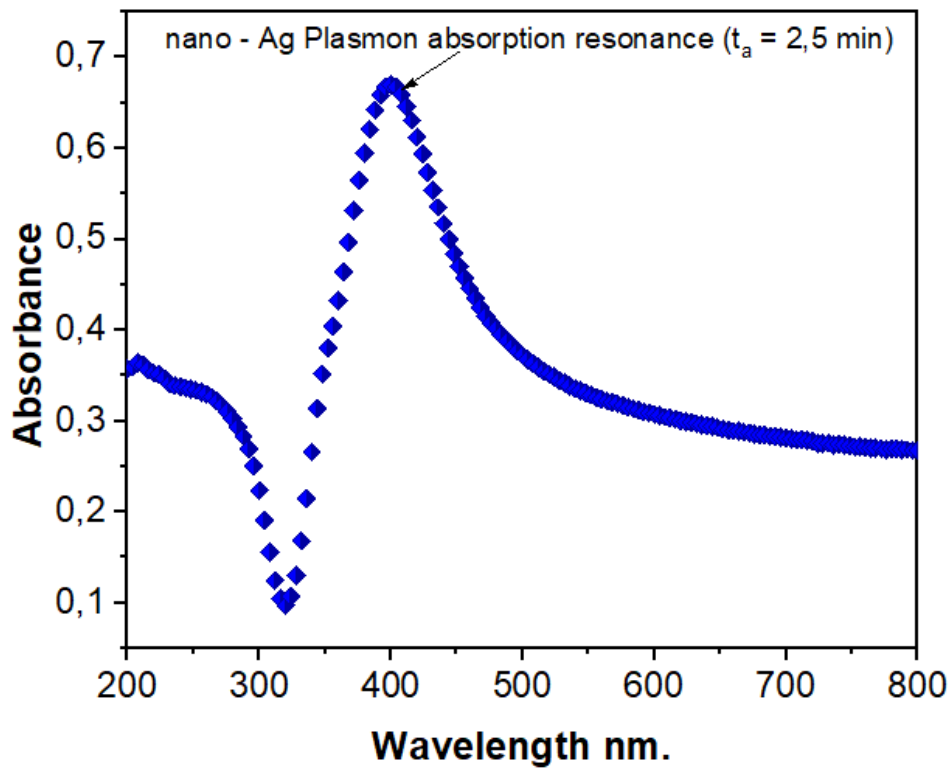
Figure 6.2: NF1 Absorbance analyses (June 2022).
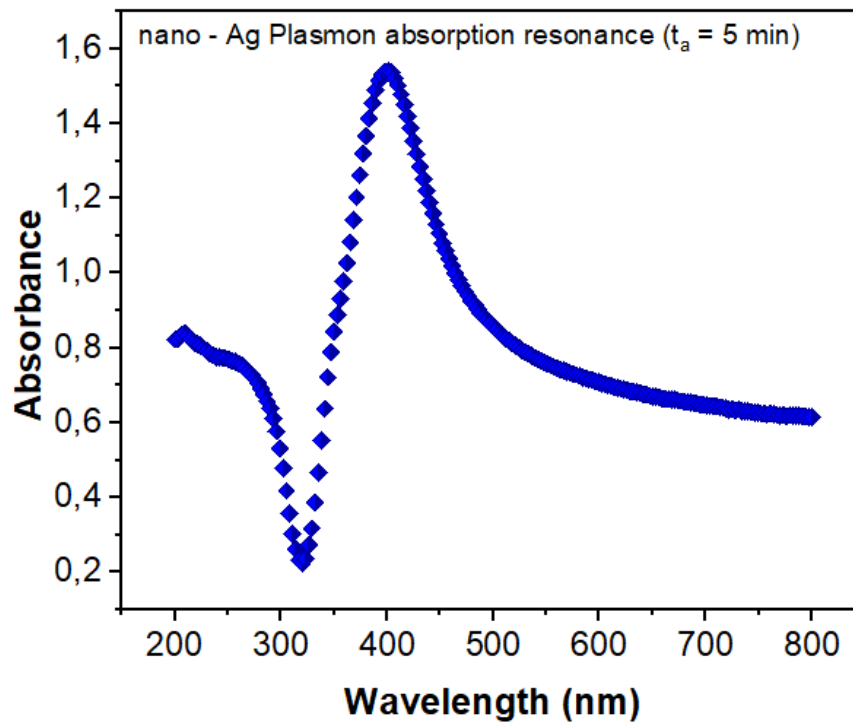
Figure 6.3: NF2 Absorbance analyses (June 2022).

70
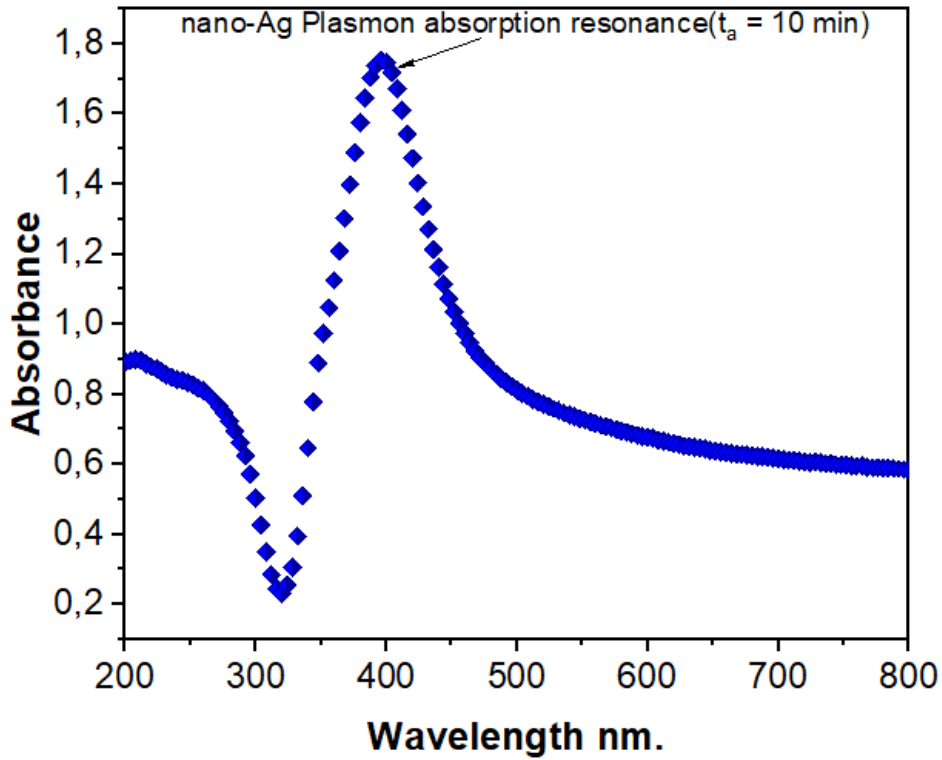
Figure 6.4:NF3 Absorbance analyses (June 2022).
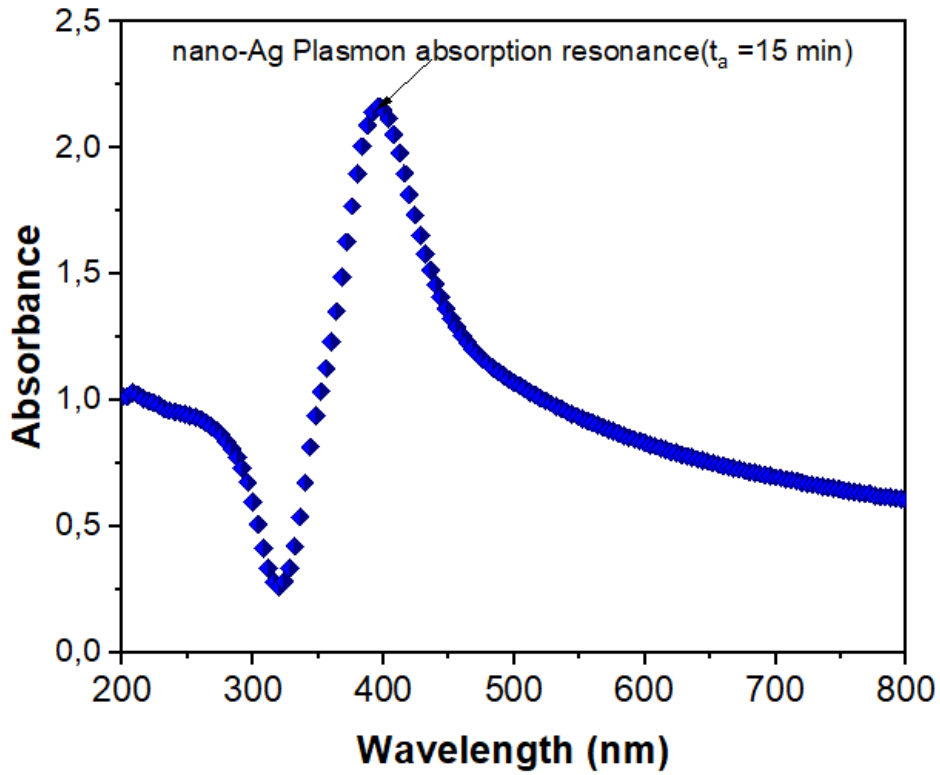
Figure 6.5: NF4 Absorbance analyses (June 2022).
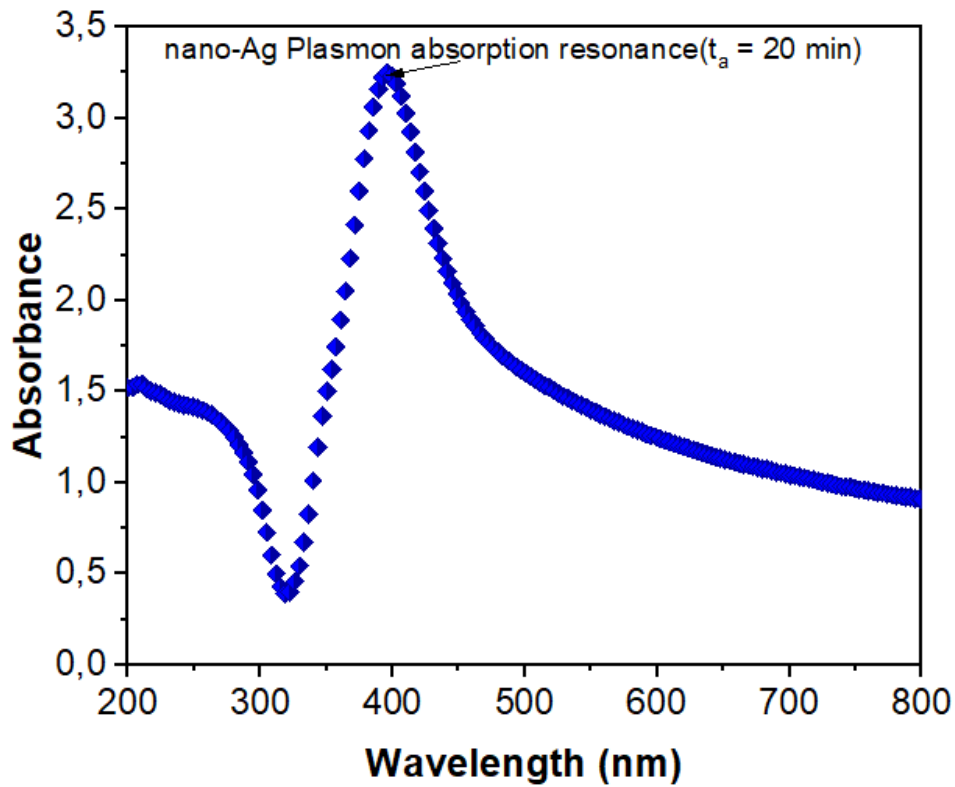
Figure 6.6: NF5 Absorbance analyses n (June 2022).
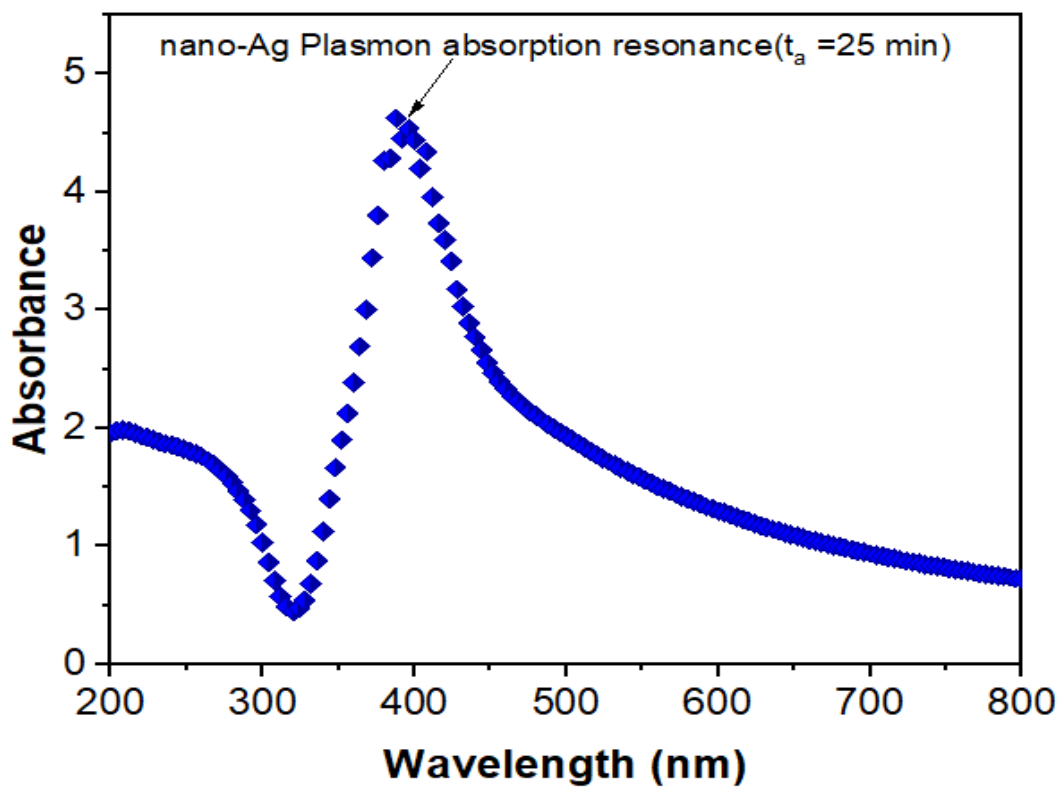
Figure 6.7:NF6 Absorbance analyses (June 2022).

The data demonstrates a strong relationship between the absorbance values of plasmon peaks and the ablation time. Ablation times as short as 2.5 and 5 minutes' result in absorbance values that are comparatively lower, which suggests that there is limited production of nanoparticles in the solution. This is explained by the fact that there was not enough time for the vaporisation caused by the laser and the ensuing nucleation and growth processes. On the other hand, larger absorbance values are seen during prolonged ablation times (such as 10 minutes and more), which may indicate increased nanoparticle formation and dispersion. This is anticipated since longer times lend more energy to vaporisation and subsequent nucleation, raising the quantities of nanoparticles in the solution.

6.3   Utilizing UV-vis spectroscopy to assess stability throughout time of Ag-H$_2$0 nanofluid.

A nanofluid's stability can be described as its capacity to maintain its dispersion condition over time without settling or agglomerating nanoparticles. Due to the silver nanoparticles' small size and improved ability to interact with the fluid molecules, silver nanofluids are well known for having good thermal conductivity. However, several variables, including particle size, surface charge, agglomeration, and pH, have an impact on their stability.

The stability of silver water nanofluids under various circumstances has been examined in several studies. Wang et al. [275], for instance, looked at the stability of silver water nanofluids at various pH levels and nanoparticle concentrations. They discovered that the stability of the nanofluids was reduced with increasing nanoparticle concentration and more acidic fluid pH. However, they discovered that as the pH rose towards alkalinity, the stability of the nanofluids improved.

According to Mafuné, an inter - band transition causes the plasmonic peak of the silver nanoparticles' optical absorption to appear at about 400 nm on the broad band. The silver nanoparticles are assumed to be spherical based on the single surface-plasmon peak's presence. Important to remember that the absorption spectra would show two plasmon peaks for ellipsoidal particles [276]. The absorption spectra of nanoparticles revealed one surface plasmon absorption peak in the 402 nm range that corresponds to silver, since it in the range 380 and 470 nm.

6.4   Stability of AgNPs-H₂O (May-October 2022)

The stability of the nanofluid was assessed using UV-vis spectroscopy over an extended period. From June and October, the UV inspection was done every month. The data was utilised to assess whether the nanoparticles are aggregating or going through sedimentation, which indicates instability, by tracking variations in absorbance. The drop in absorbance values at longer ablation times—especially after 15 minutes—is an interesting finding. This phenomenon suggests that the system may be experiencing saturation or degradation. One possible explanation is the agglomeration of nanoparticles, where longer ablation causes larger clusters to form, which scatter light less effectively and lower the measured absorbance. Extended periods of time may also witness chemical changes in nanoparticles, such as oxidation or dissolution, which would further contribute to the absorbance drop [277]. This observation is witnessed in Figure 6.8 to Figure 6.13 where stability declines as shown by the loss of plasmonic peaks.
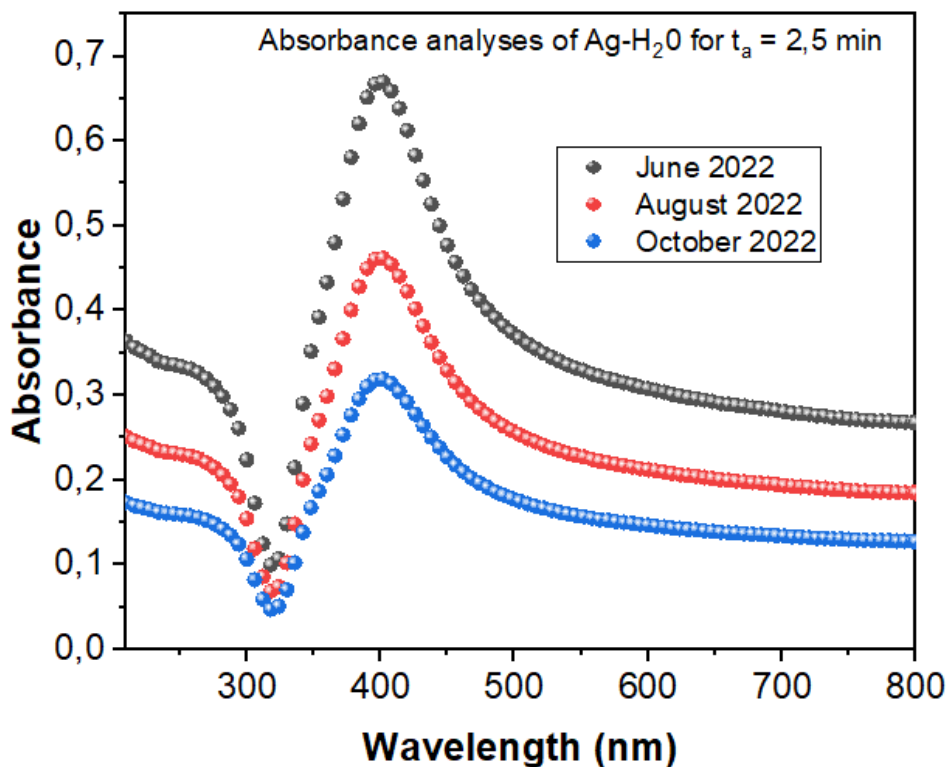
Figure 6.8: NF1 Absorbance analysis for long term stability.
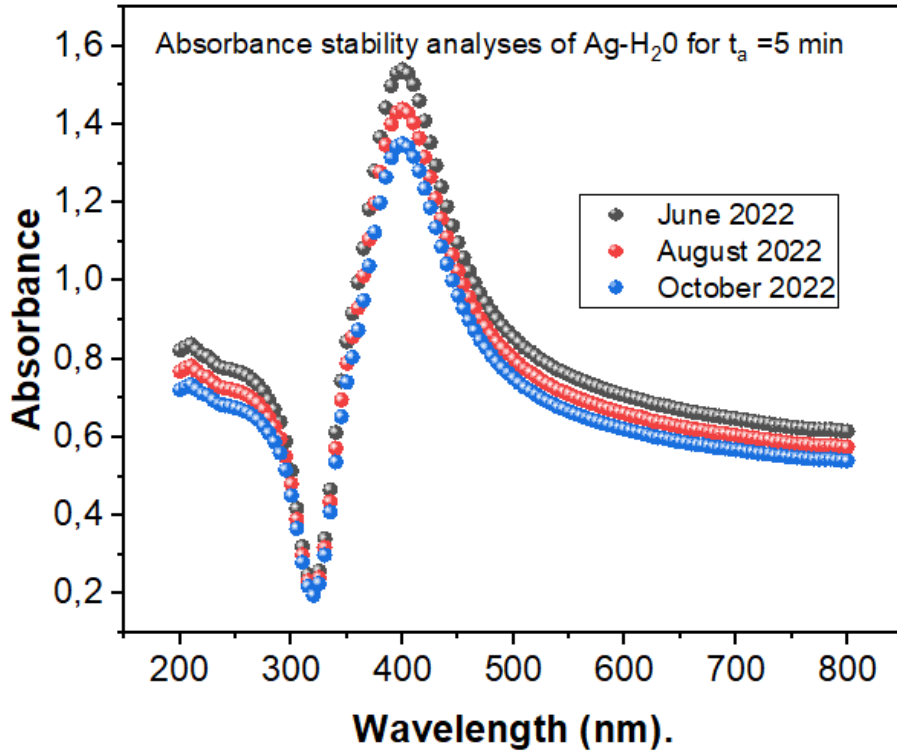
Figure 6.9: NF2 Absorbance analysis for long term stability
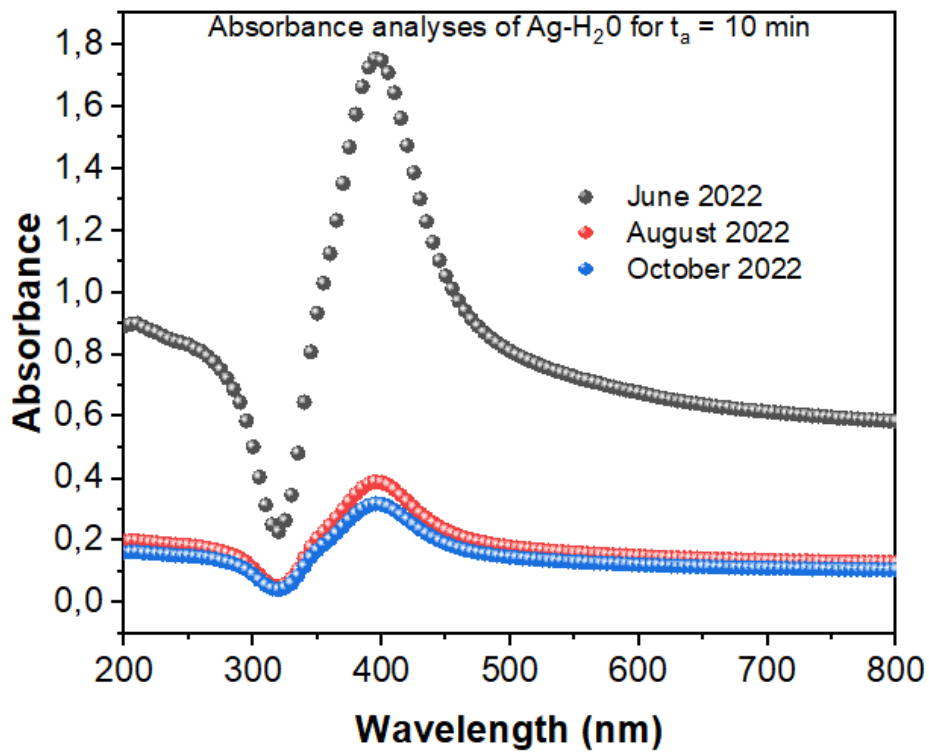
Figure 6.10 :NF3 Absorbance analysis for long term stability.
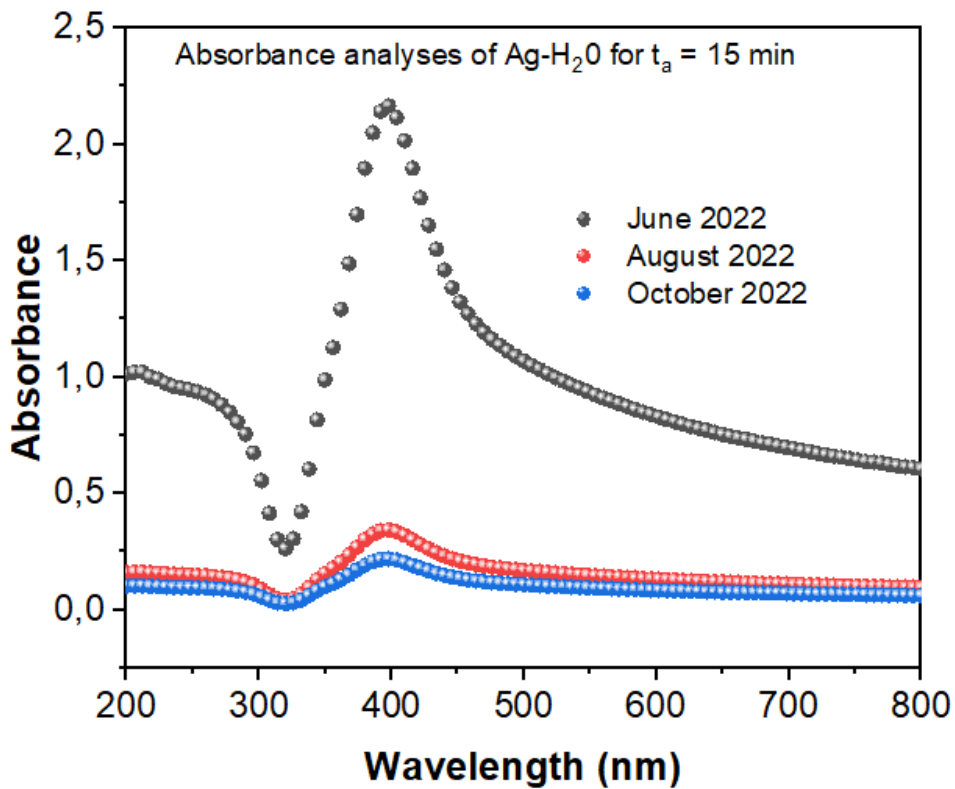
Figure 6.11: NF4 Absorbance analysis for long term stability
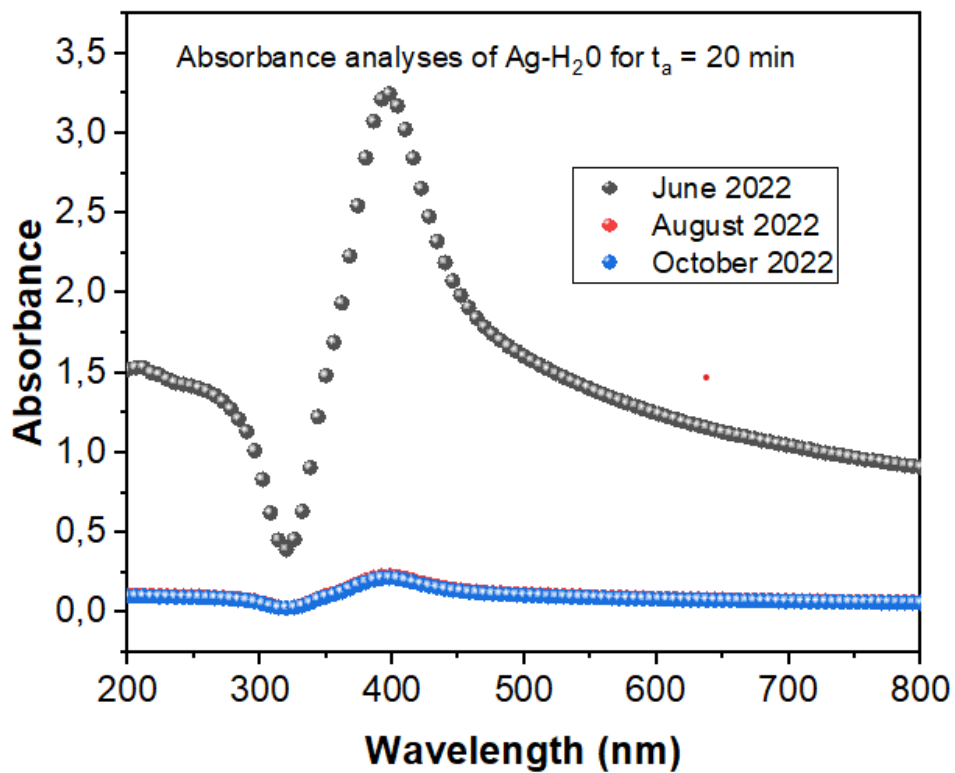
Figure 6.12: NF5 Absorbance analysis for long term stability
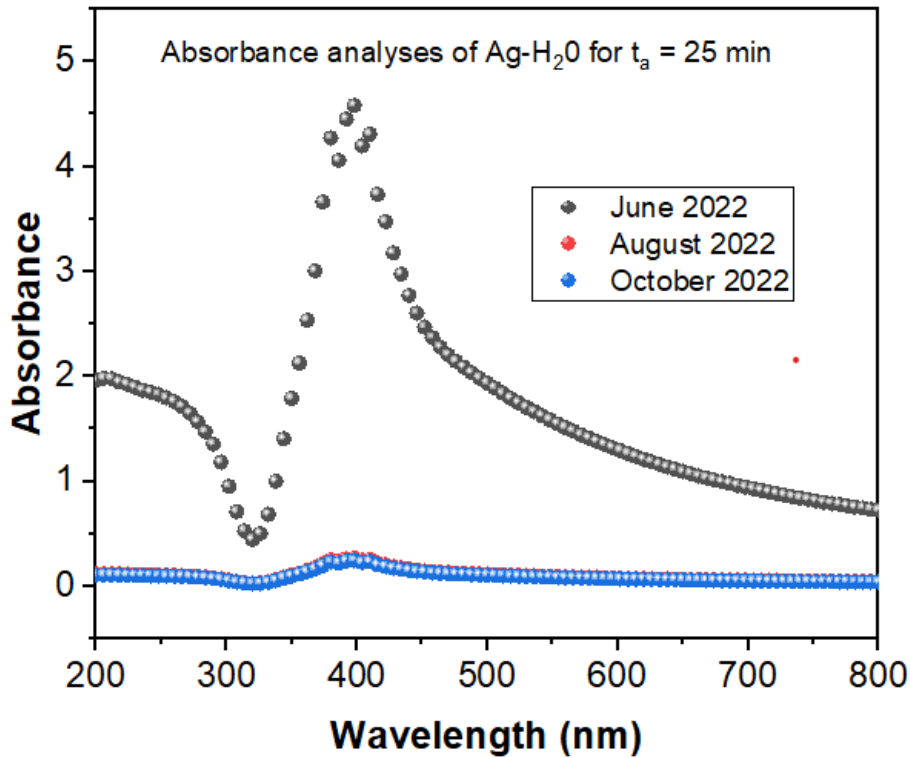
Figure 6.13: NF6 Absorbance analysis for long term stability.

To achieve improved thermal performance, it is crucial to take the stability of nanofluids into account. Electrostatic and van der Waals interactions among nanoparticles are prevalent [278-280]. Both sedimentation (produced by the density difference between the nanoparticles and base fluid) and clustering of nanoparticles (induced by the van der Waals contact between nanoparticles) create instability [36, 281-283]. Additionally, instability is brought on by a number of factors, including the Soret effect, the structure and morphology of nanoparticles, the duration of ultrasonication, Brownian motion, particle-particle interaction, base fluid-particle interaction, and particle-particle contact [27, 33, 284, 285]. The information points to a trade-off between the amount and calibre of nanoparticles that are produced. Longer ablation times initially result in greater plasmonic signals and higher concentrations of nanoparticles; however, the eventual fall in absorbance values suggests a compromise in the quality of the nanoparticles see Figure 6.10 to Figure 6.13. The initial plasmonic peak in relation to ablation time with varying absorbance, with higher absorbance for longer ablation times and lower absorbance for shorter ablation times. The study reveals that particles agglomerate and settle in water due to gravity at larger concentrations over time [286]. This suggests that a lower particle concentration is required for the synthesis of more stable nanofluids see Figure 6.8 and

Figure 6.9. This can also be stregthen by a comparative study of of NF1 to NF6 for optical properties as depicted by Figure 6.14 to Figure 6.16. NF1 and NF2 are more stable than the rest.
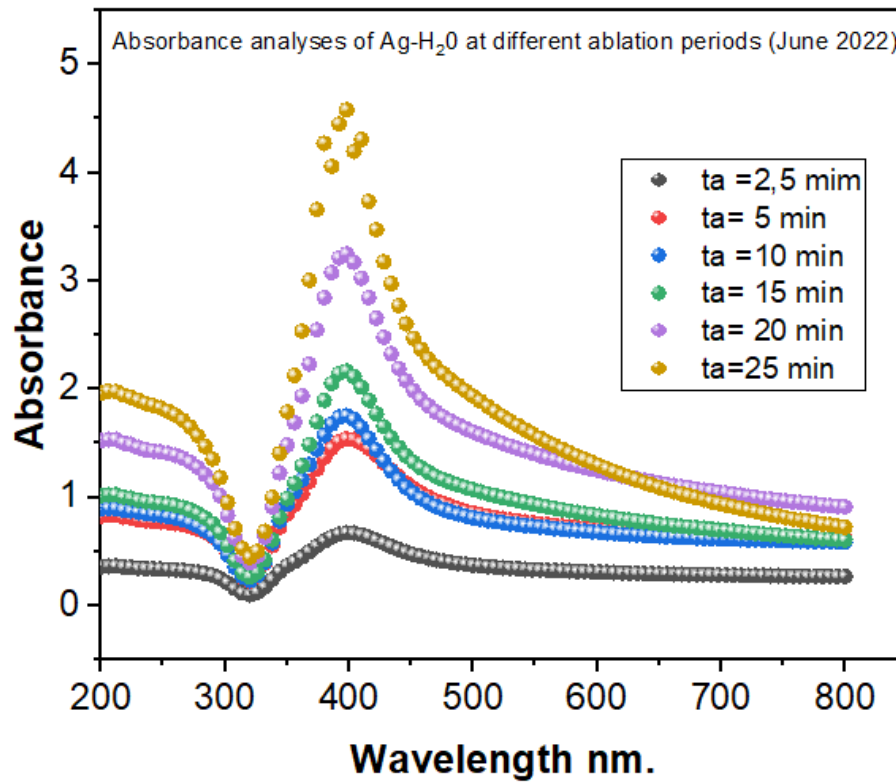
Figure 6.14: A comparative study of Absorbance for long term stability (June 2022)
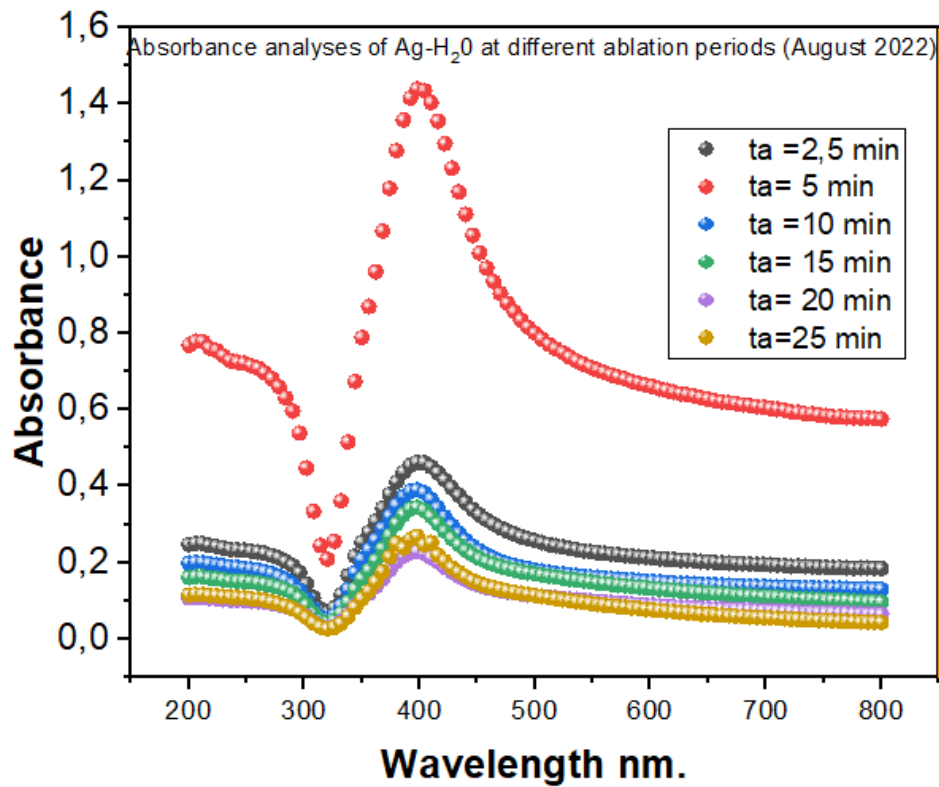
Figure 6.15: A comparative study of Absorbance for long term stability (August 2022)
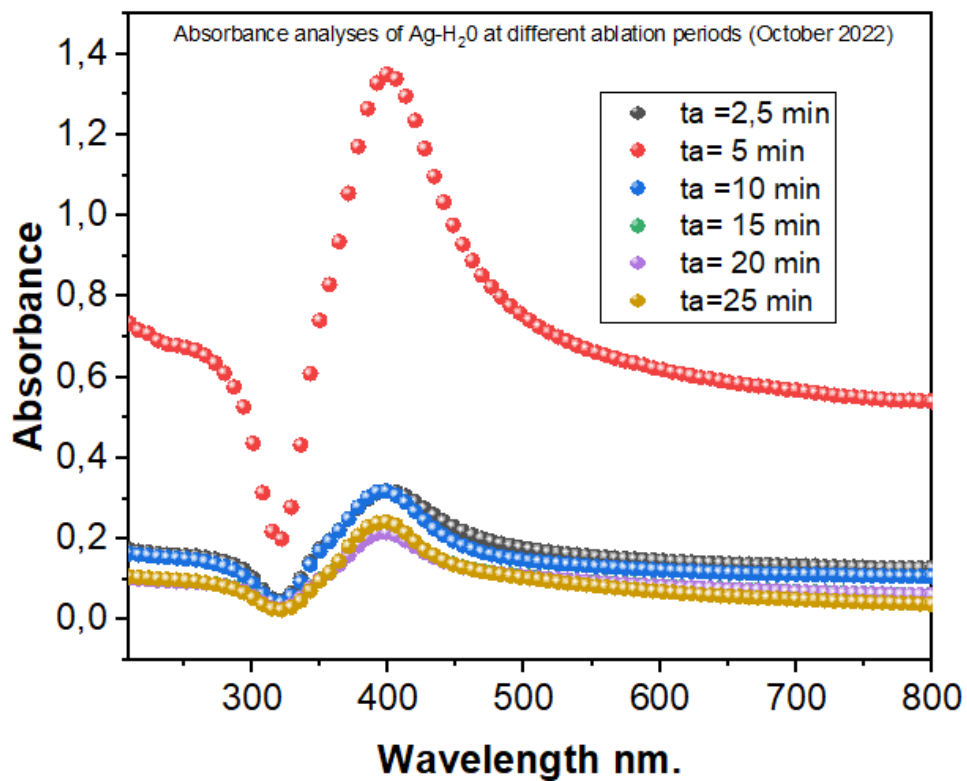
Figure 6.16A comparative study of Absorbance for long term stability (October 2022)

79

6.5 Examination of variables influencing the stability of nanofluids, such as nanoparticle concentration and surface alterations

Table 6-1 shows how absorbance was changing with respect to concentration for different months. In June it is higher and lower for October 2022 the results are clearly shown in Figure 6.17

Table 6-1: Table showing the relationship between the absorbance vs time of ablation (concentration) from June to October 2022.

Nanofluid	Absorbance (June 2022)	Absorbance (August 2022)	Absorbance (October 2022)
NF1	0.7	0.25	0.222
NF2	1.6	1.5	1.4
NF3	1.8	0.4	0.325
NF4	2.1	0.331	0.212
NF5	3.2	0.225	0.213
NF6	4.5	0.2625	0.2415

The absorbance readings of the nanofluid samples at various time intervals are shown in the table. Absorbance, a measurement of how much light a material absorbs, can provide light on the concentration or optical characteristics of the samples.

6.5.1 The following tendencies are visible when we examine the data:

The absorbance values for the same time points in June 2022 were 0.7, 1.6, 1.8, 2.1, 3.2, and 4.5. These numbers represent the samples' initial absorbance immediately after synthesis. In comparison to the baseline values, the absorbance levels dropped in August 2022. The samples had absorbance readings of 0.25, 1.5, 0.4, 0.331, 0, 225, and 0.2625, which indicated a decline

in absorbance with time. In comparison to the last time point, the October 2022 absorbance levels fell much more. These were the numbers: 0.222, 1.4, 0.32, 0.212, 0.231, and 0.2415. These decreased absorbance readings imply that the samples' concentration or optical characteristics are continuing to decline.

The stability of each generated Ag-H_2O nanofluid at various ablation periods is shown in Table 6-2 at various concentrations. From June to October 2022, higher concentration samples had greater agglomeration rates. As fewer particles were remained in a host fluid from August to October, it is also evident that the rate of aggregation decreased (see Figure 6.18). Absorbance is slowly declining at low concentrations, indicating poor agglomeration at 2.5 and 5 minutes, the most stable nanofluids are created; nevertheless, it is also noted that there is a concentration beyond which the pace of agglomeration accelerates.
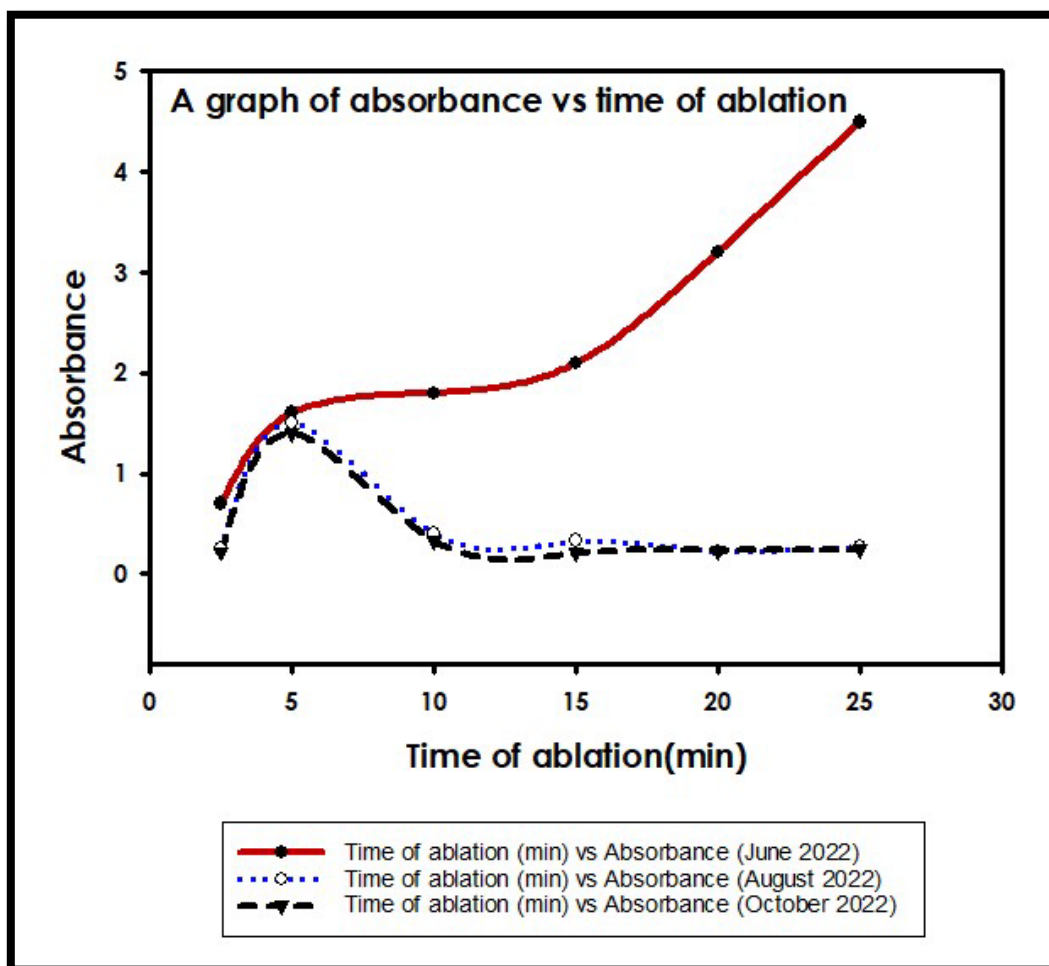
Figure 6.17:Figure showing the relationship between the absorbance vs time of ablation from June to October 2022.

6.6 The rate of agglomeration based on the plasmonic peaks information.

Table 6-2 displays absorbance values for silver water nanofluids recorded at various time periods (months). The table displays the absorbance values for the months of June 22, August 22, and October 22 for various ablation times ranging from 2.5 min to 25 min. The quantity of light that a substance absorbs is measured as its absorbance, which might reveal details about the chemical makeup or characteristics of the sample. Various time periods were used to evaluate their effects on the absorbance values in relation to the concentration of silver nanoparticles in water.

Table 6-2:Stability of Ag-H20 of nanofluid synthesized by PlAL.

Absorbance per month	NF1	NF2	NF3	NF4	NF5	NF6
Jun-22	0.7	1.6	1.8	2.1	3.2	4.5
Aug-22	0.45	1.5	0.4	0.331	0.225	0.263
Oct-22	0.322	1.4	0.325	0.212	0.231	0.242
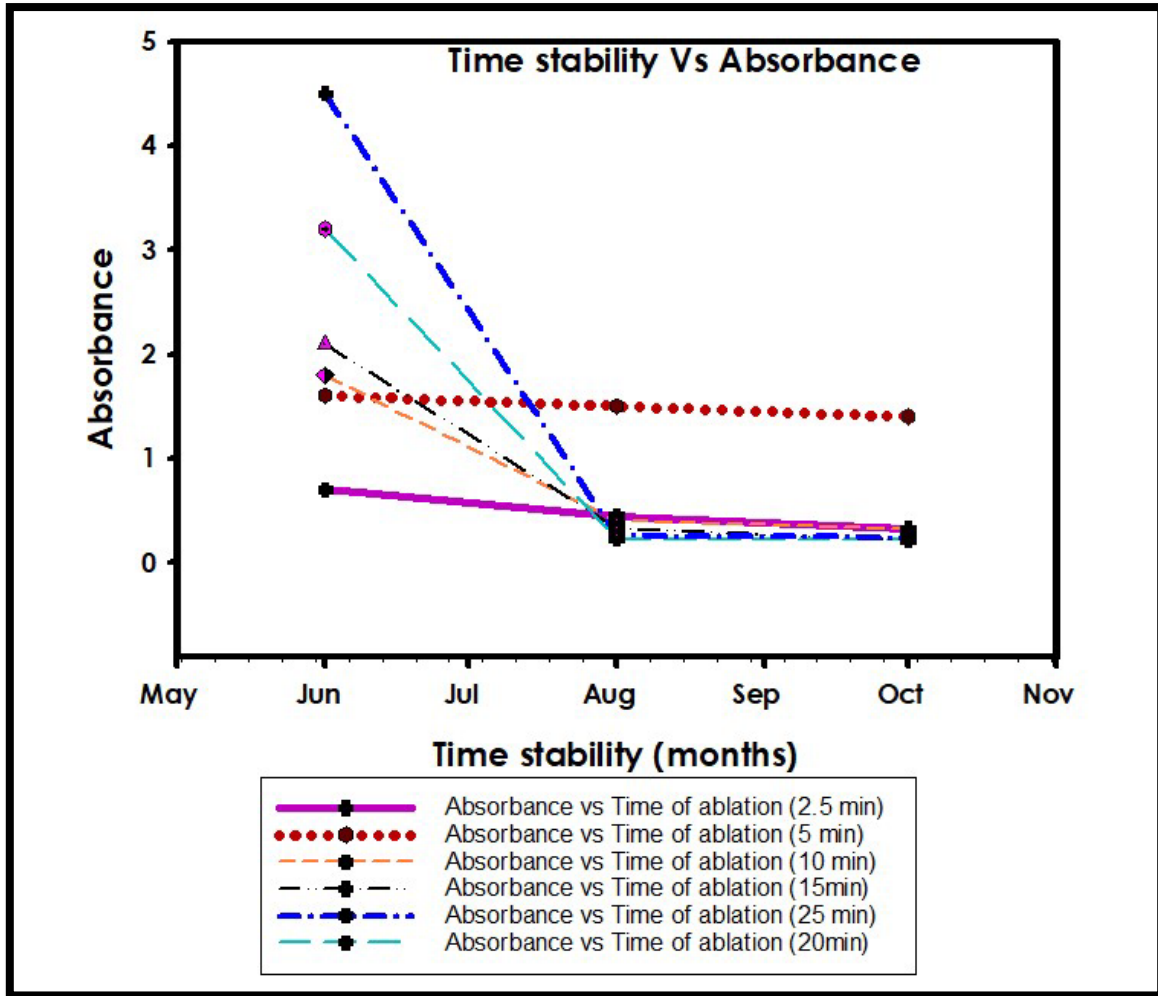
Figure 6.18: Stability of Silver water nanofluid synthesized by PlAL.

6.7   Analysis of absorbance values:

In June 2022, absorbance levels range from 0.7 to 4.5, with a rising trend shown as ablation time rises. This implies that longer ablation times result in greater absorbance values, which point to higher nanoparticle concentrations or bigger particle sizes in the nanofluid. For most of the time of ablation durations, there is a drop in absorbance values in August 2022 compared to June 2022. This could be the result of elements such nanoparticle aggregation, settling, or other alterations in the stability or composition of the nanofluid over time. When compared to August 2022, the absorbance values in October 2022 show a greater decline. This suggests that the characteristics of the nanofluid will continue to change over time because of particle growth, sedimentation, or deterioration.

83

6.7.1 Evaluation and consequences

Three conclusions concerning the stability of the silver water nanofluid may be drawn from the table:

Variation in absorbance: The table shows how absorbance values change noticeably over time and with various ablation times. This implies that the optical characteristics of nanofluids can be significantly influenced by the production settings and ageing.

Changes that are time-dependent: The declining trend in absorbance values from June to October 2022 suggests that the nanofluids are changing with time. For nanofluids to work well in real-world applications, stability of these changes must be understood.

Effect of ablation time: The absorbance values also change with ablation time, demonstrating that the length of laser ablation used to create nanofluids affects the optical characteristics of those fluids. The association between ablation time and nanoparticle properties has to be further examined.

CHAPTER 7 : Ag-H₂O Thermal conductivity

7.1 Introduction

The steady-state cylindrical cell methodology is an effective technique for figuring out a material's thermal conductivity [287]. Researchers can determine the thermal conductivity by applying Fourier's rule of heat conduction to compute the temperature differential across a cylindrical sample under steady-state circumstances [288]. This method is frequently used in fields including materials science, engineering, and thermal management applications because it offers an efficient way to describe the thermal transport characteristics of various materials.

7.2 Thermal Conductivity measurement

Using the steady-state cylindrical cell approach, the thermal conductivity of Ag-water nanofluids was determined,[289]. The schematic diagram of the testing equipment is displayed in Figure 7.1. Two copper cylinders that are coaxial make up the measurement cell. Electricity is used to heat and maintain a high temperature in the inner cylinder (T_h). Changing the electric power delivered to the heater altered the hot temperature. A DC power that enables for current adjustment with stability of 0.1% was used to supply power to the heater resistance. A cooling water flow from a water bath is used to keep the outer cylinder at a chilly temperature (T_c). To prevent heat loss during the characterization, the walls of the test cell are insulated.
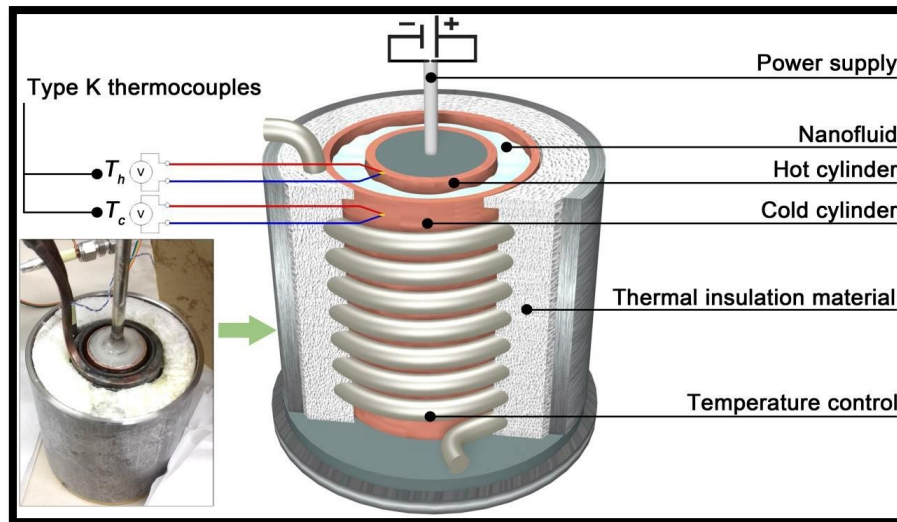
Figure 7.1: Schematic description of a cylindrical cell for steady-state thermal-conductivity measurement of nanofluids.

- ❖ To measure the temperatures in the experiment, T-type (Copper/Constantan) thermocouples were employed. These thermocouples were calibrated and inserted on the outer surfaces of both the internal and external cylinders. The temperature sensors have a maximum error of 0.5 degrees Celsius or 0.4%.

- ❖ A Keithley 3706 data system acquisition is connected to the instrumentation, facilitating the collection, and recording of temperature data.

- ❖ The region between the internal and external cylinders, which is circular in shape, is filled with the nanofluid under investigation. A consistent heat flux is applied in the radial direction by the internal hot cylinder. Consequently, the generated heat flux within the nanofluid propagates unidirectional towards the outer cold cylinder.

- ❖ To determine the thermal conductivity of the nanofluid, the one-dimensional Fourier's equation of thermal conduction can be utilized. This equation enables the calculation of thermal conductivity based on the observed temperature profiles and heat flux within the experimental setup.

7.3   Analyzing how AgNPs-H₂O thermal conductivity is improved by examining the impact of nanoparticle stability.

To determine how stability affected thermal conductivity, experiments on *AgNPs-H₂O* nanofluids' thermal conductivity were carried out in October 2022, five months after the

synthesis of the nanofluid in Table 7-1and Table 7-2 represents the thermal conductivity and thermal enhancement respectively of *AgNPs-H₂O* nanofluid synthesized by PLAL. The corresponding plot are shown Figure 7.2 and Figure 7.3 respectively. This was carried out to examine how stability affected thermal enhancement. When the temperature rises, the thermal conductivity of a nanofluid also rises, although this rise is more pronounced for smaller nanoparticle volume fractions. Due to equipment limitations, the experiment's maximum increase in thermal conductivity corresponds to a temperature of 45 °C.

The thermal conductivity is calculated by Fourier's law:

$$k = \frac{q}{4\pi\Delta T}\ln{(t_2 - t_1)}$$

7-1

Where q is the heat flux per unit of length, T and t_2 & t_1 are the temperature and time of the wire, respectively, and k is the fluid's thermal conductivity. The thermal gradient can be calculated from the platinum wire's electrical resistance's temperature coefficient, which changes with time.

7.4   Thermal conductivity results

The experimental findings for AgNPs- water thermal conductivity is reported in this section. The studies were conducted at temperatures between 25 °C and 45 °C. The observed thermal conductivity of the Ag-water nanofluid is shown in Table 7-1 as a function of temperature and volume fraction of nanoparticles.

Table 7-1: A table showing thermal conductivity Vs Temperature of PLAL synthesized silver –water nanofluid. The measurements were conducted in October 2022.

Temperature (K)	Thermal Conductivity DW	Thermal Conductivity NF1	Thermal Conductivity NF2	Thermal Conductivity NF3	Thermal Conductivity NF4	Thermal Conductivity NF5	Thermal Conductivity NF6
298	0.6153	0.6455	0.7018	0.6215	0.6237	0.6188	0.6291
303	0.6581	0.6923	0.7595	0.6664	0.6685	0.6622	0.6739
308	0.6816	0.7226	0.7967	0.6918	0.6949	0.6866	0.6995
313	0.7078	0.7551	0.8345	0.7194	0.7229	0.7141	0.7277
318	0.7311	0.7864	0.8733	0.7455	0.7492	0.7393	0.7543

It was demonstrated that compared to pure water, AgNPs-H_2O nanofluids have higher thermal conductivities. With an increase in temperature, a nanofluid's thermal conductivity rises, and this rise is more noticeable at smaller nanoparticle volume fractions. For all solid volume fractions, a temperature of 45 °C corresponds to the greatest increase in thermal conductivity. Figure 7.2 It is crystal obvious from the results that only the low concentration *AgNPs-H_2O* nanofluid exhibits high thermal conductivity.
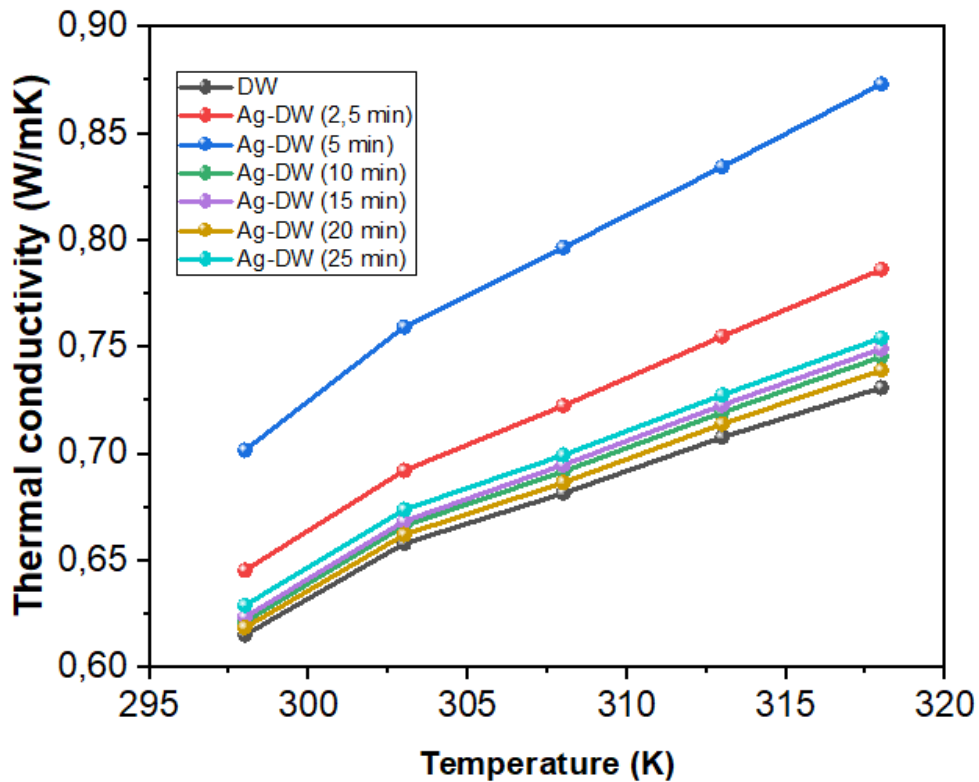
Figure 7.2: Thermal conductivity Vs Temperature of PLAL synthesized silver –water nanofluid (October 2022)

It is clear that nanofluids' thermal conductivity rises in direct proportion to temperature. Nonetheless, it is important to remember that the best thermal conductivity is found in nanofluids with the lowest concentrations (NF2& NF2). NF2 exhibits higher thermal conductivity due to a more uniform dispersion of nanoparticles within the nanofluid, which promotes more efficient phonon transfer. Stability, as seen in Figure 6.9 confirms this while nanofluids at higher concentration are unstable over time as evident in Figure 6.16.

7.5   Relationship between Thermal Conductivity and Stability of *AgNPs-H$_2$O* Nanofluids:

Thermal conductivity and stability in silver water nanofluids have been found to be trade-offs. Specifically, Figure 6.14 and Figure 6.16 show that, the stability of the nanofluid falls as the concentration of silver nanoparticles in the fluid rises, whereas the thermal conductivity of the fluid increases. Due to the nanoparticles' propensity to agglomerate at higher concentrations, which can affect the stability of the nanofluid, there is a trade-off involved [290]. The

aggregation of the nanoparticles can lead to pockets of the nanofluid with low thermal conductivity, which can influence the fluid's thermal conductivity [291, 292]. The concentration and size of the nanoparticles must be carefully balanced to maximize the thermal conductivity and stability of silver water nanofluids [293].

Table 7-2: A table showing thermal conductivity enhancement Vs Temperature of PLAL synthesized silver –water nanofluid The measurements were conducted in October 2022.

Temperature (K)	Thermal Conductivity Enhancement $(\eta)(\%)$ Ag-Dw (2.5 min)	Thermal Conductivity Enhancement $(\eta)(\%)$ Ag-Dw (5 min)	Thermal Conductivity Enhancement $(\eta)(\%)$ Ag-Dw (10 min)	Thermal Conductivity Enhancement $(\eta)(\%)$ Ag-Dw (15 min)	Thermal Conductivity Enhancement $(\eta)(\%)$ Ag-Dw (20 min)	Thermal Conductivity Enhancement $(\eta)(\%)$ Ag-Dw (25 min)
298	4.91	14.06	1.01	1.37	0.57	2.24
303	5.20	15.40	1.27	1.56	0.63	2.41
308	6.06	16.88	1.50	1.95	0.74	2.63
313	6.69	17.90	1.64	2.14	0.89	2.81
318	7.57	19.45	1.97	2.47	1.12	3.17
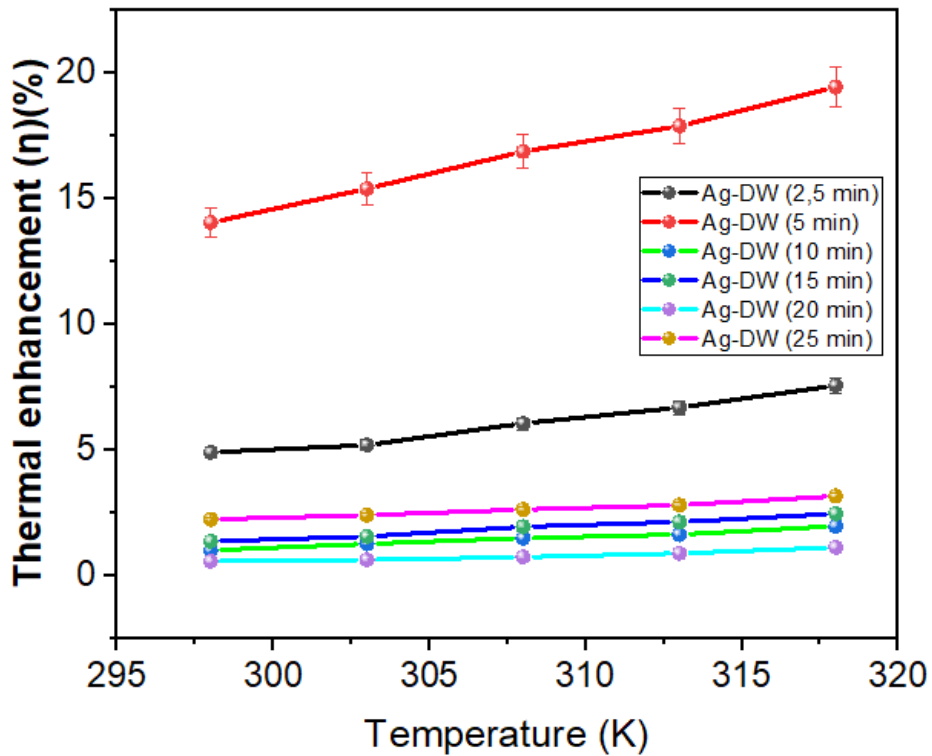
Figure 7.3: A Figure showing thermal conductivity enhancement Vs Temperature of PLAL synthesized silver –water nanofluid (October 2022).

The enhancement $\eta(\%)$ in thermal conductivity is derived by applying the following equation as a percentage difference between the thermal conductivity of the nanofluids (k_{nf}) and the base fluid (k_{bf}).

$$\eta(\%) = \frac{100 \times (k_{nf} - k_{bf})}{k_{bf}} \qquad\qquad 7\text{-}2$$

Where k_{nf} and k_{bf} *are* the Thermal conductivity of nanofluid and the Thermal conductivity of the base fluid, respectively.

The aforementioned equation was used to compute and plot the relative improvement ($\eta(\%)$) in the percentage of thermal conductivity of *AgNPs-H₂O* nanofluids obtained after 2.5, 5, 10, 15, 20, and 25 min of ablation times. The thermal conductivity was enhanced from 0.7311 to 0.8733 W/m.k compared to the base fluid at a volume fraction corresponding to t_a = 5min with

a temperature increase from 25 °C to 45 °C, representing a 19.45% thermal improvement (see Figure 7.3) . This is confirmed by UV-Vis stability results at this time of ablation (see Figure 6.9). This enhancement is followed by 7.5% at 45 °C for ta = 2.5 min. However, at large concentrations, the agglomeration process and decreased area-to-volume proportion (A/V) cause the effective thermal conductivity to drop. Additionally, the ablation time is a crucial parameter since it has a significant impact on the concentration of AgNPs. By adjusting the ablation time, the *AgNPs-H$_2$O* nanofluid may be tuned to match any application that calls for high-performance heat transfer fluids.

CHAPTER 8 : AgNPs-H₂O Contact angle.

8.1 Introduction

The rate of heat transfer and the system's overall efficiency can be affected by the contact angle since it impacts how thoroughly the fluid wets the heat transfer device's surface [294]. Heat transfer performance and efficiency may suffer if the fluid's contact angle is too high and prevents it from adequately wetting the heat transfer device's surface [160, 295, 296]. On the other hand, if the contact angle is too small, the fluid could create a film on the surface of the heat transfer device, which can also lower the effectiveness of heat transmission [160]. To maximize the effectiveness and reliability of thermal transfer systems, heat transfer fluids must have a certain contact angle [160, 297]. Engineers and scientists may develop better systems with higher performance and efficiency by knowing how heat transfer fluids behave on solid surfaces. As a result, there are considerable advantages for a variety of industrial and technical applications. Measuring the contact angle of heat transfer fluids may also help with the creation of new and improved fluids that are optimized for applications and operating circumstances [230].

8.2 AgNPs-H₂O contact angle measurements method.

The contact angle of droplets of nanofluid deposited on smooth copper and rough copper sulphide substrates were measured experimentally, and the results demonstrate that the contact angle is dependent on the concentration of nanoparticles (see Figure 8.1).

Preparation of CuS and pure Cu substrates: For the experiment, we utilised CuS or Cu substrates with a reasonable level of surface polish. We also made sure the substrates were free of contaminants and any surface coatings that would affect wetting behaviour.

Droplet deposition: Using a dropper, a very little amount of the AgNPs-H2O nanofluid was deposited to the CuS or Cu substrate. The droplets were uniform in size and location.

Imaging and analysis: To capture images of the droplet on the substrate, a high-resolution imaging camera designed for contact angle measurement was employed. To enable accurate analysis, it made sure the images were clear and focused. Contact angles for nanofluids

prepared over different times (t_a) of ablation on Cu and CuS substrate were calculated by an online protractor.

To calculate the sessile droplet, contact angle, 10 µl was used. A gradual injection of the nanofluid was made using a syringe onto the solid surfaces of copper and copper sulphide.

Figure 8.1: Contact angle measurement

A contact angle resulted from the equilibrium conditions in which the contact angle measurements were made. The contact angle, contact line radius, and apex position were all measured for each unique concentration of the *AgNPs-H₂O* nanofluid. The same volume (6 µl) and the same procedure were performed for six distinct nanofluid (*AgNPs-H₂O*) synthesized by PLAL over intervals of 2.5, 5, 10, 15, 20, and 25 min. The trials took place in climate-controlled lab settings that were like one another.

8.3   Investigation of the AgNPs-H₂O nanofluid's contact angle with various substrates.

This section examines how the contact angle changes when deionized water droplets with distributed silver nanoparticles (nanofluid) which have varying concentrations and sizes of nanoparticles are involved. The PLAL process was used to create water-silver nanoparticles with an average size of 25 to 37nm. When even a very small concentration of nanoparticles is added, the wetting properties of the surface are drastically altered for a pure water droplet (zero mass concentration case not included in the pictures).

8.3.1 Investigation of the AgNPs-H₂O nanofluid's contact angle with Cu substrates.

The observed contact angle increases and reaches a maximum when the concentration does as well. The observed trends for the droplet shape may also be caused by the interactions between nanoparticles with themselves, with the fluid, or a solid surface (see Figure 8.2).
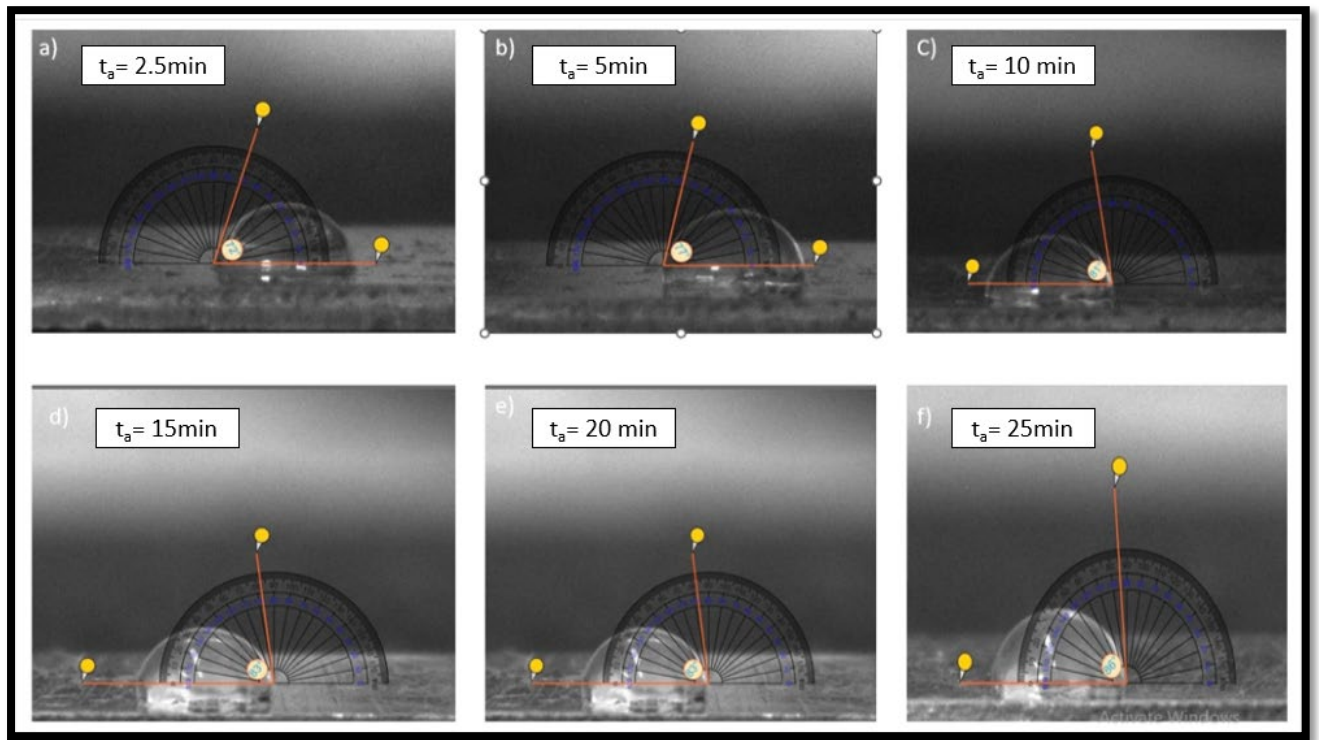
Figure 8.2: Contact angles silver-water nanofluid corresponding to different times of ablation on Cu.
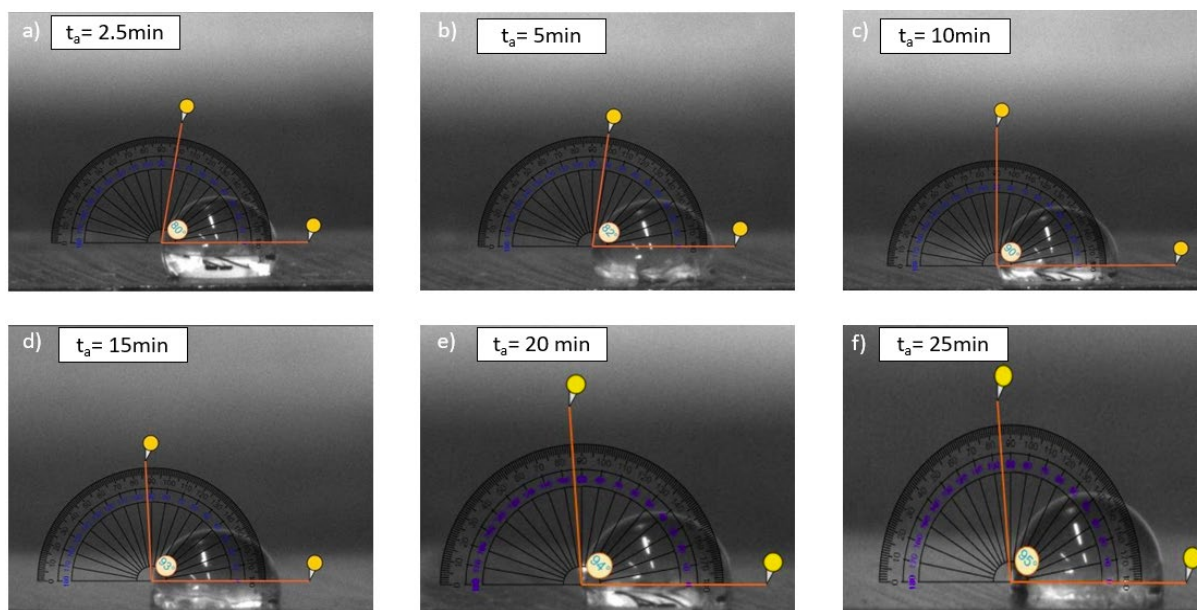
Figure 8.3:Contact angles silver-water nanofluid corresponding to different times of ablation on CuS.

This trend may be attributed to three factors, that is Nanoparticle stability, Aggregation, and Surface oxidation.

Nanoparticle stability: Stability improves wetting behaviour. The stabilising ingredient might deteriorate, or the surface charge could lessen with time, which would enhance particle aggregation and reduce stability. Aggregated nanoparticles frequently form bigger clusters, which alters the wetting behaviour of the nanofluid and increases the contact angle [169].

Aggregation: Van der Waals forces, ionic strength, or pH shifts are just a few of the variables that might cause AgNPs in the nanofluid to aggregate [298]. The nanoparticles cluster together because of accumulation, generating bigger structures that are less likely to efficiently moisten the substrate. The accumulation of nanoparticles, which hinders the nanofluid's wetting behaviour and limits its capacity to spread on the substrate surface, is responsible for the increased contact angle that was noticed after months of shelf life.

Surface oxidation: When exposed to air or other oxidising agents over time, silver nanoparticles may experience surface oxidation. The creation of an oxide layer on the nanoparticle surface because of oxidation changes the surface chemistry and the wetting behaviour. By generating a less hydrophilic surface, the oxide layer can increase the contact angle and make it more challenging for the nanofluid to efficiently wet the substrate.

8.3.2 Investigation of the AgNPs-H₂O nanofluid's contact angle with CuS substrates.

Table 8-1: Contact angles silver-water nanofluid corresponding to different times of ablation on CuS and Cu.

Ablation time (t_a) (min)	The contact angle of Ag-H$_2$O on the CuS substrate(degrees)	The contact angle of Ag-H$_2$O on the pure Cu substrate (degrees)
2.5	80	72
5	82	77
10	90	81
15	93	83
20	94	84
25	95	86

The substrate material affects the contact angle that result from concentration (see Table 8-1). This is explained by the differing surface energies of copper and copper sulphide substrates. Nanofluids have a tendency to spread more readily and have a lower contact angle if their surface energies are higher than those of the substrate. In contrast, if the surface energy of the nanofluid is lower than that of the substrate, it has a tendency to bead up and create a greater contact angle. Silver nanoparticles may have clustered or agglomerated in an unstable *AgNPs-H₂O* nanofluid. These agglomerates might cause inconsistent wetting behaviour when they are placed on various surfaces. Higher nanoparticle concentrations on some parts of the surface may cause less wetting and a greater contact angle. On the other hand, regions with less nanoparticles or greater dispersion can have lower contact angles. Finally, surface roughness might be blamed for this. Surface roughness caused copper sulphide substrate to exhibit greater fluctuations in contact angle than pure copper for the same volume and concentration. The fact that the contact angle is smaller for pure water drops shows that even very small amounts of silver nanoparticles have a significant impact on how well a surface wets. As a result, since the fluid flow depends on the tube's roughness, AgNPs will have an impact on it from the laminar

to the turbulent regime. As a result, it is important to properly build the tube through which the nano fluid must pass.

8.4 Analyzing how contact angle behavior is affected by nanoparticle concentration.

It is noted that the contact angle also rises in the circumstance when the amount of silver nanoparticles in the water increases. Contrary to the overall tendency, a lower contact angle is generally associated with larger nanoparticle concentrations (Figure 8.3.). The nature of the nanoparticles, the substance of the substrate, or the experimental settings can all have an impact on the unique behavior in this scenario. Understanding the underlying mechanisms causing the observed rise in contact angle with increasing nanoparticle concentration in this situation calls for more study and research.
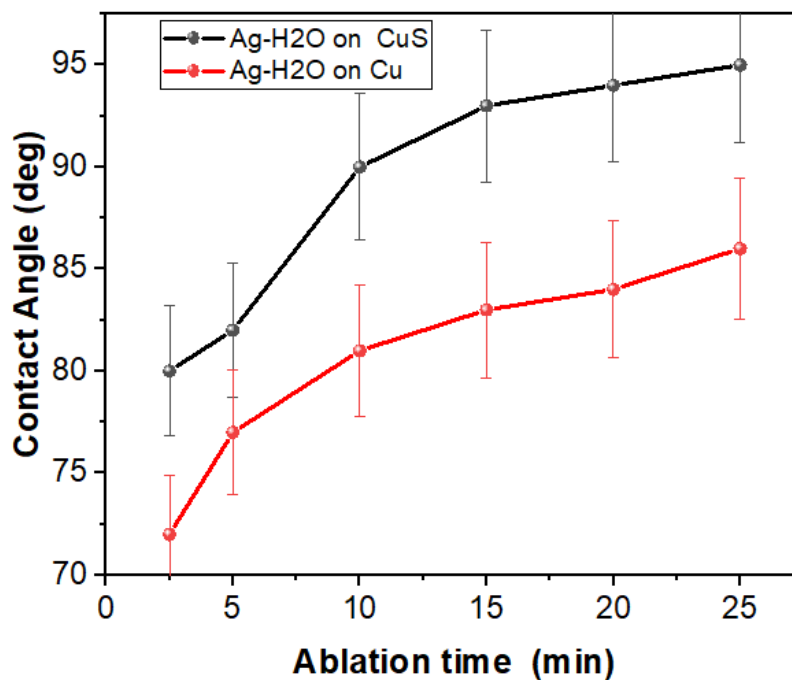
Figure 8.4:Contact angles silver-water nanofluid corresponding to different times of ablation on CuS and Cu.

However, we might speculate that the cause may be related to the clustering or agglomeration of nanoparticles. The silver nanoparticles in the water may have a tendency to cluster or assemble at larger concentrations. The solid surface may become rough or heterogeneous because of these nanoparticle clusters, increasing the contact angle. The presence of surface impurities or pollutants along with the greater concentration of silver nanoparticles may be the

cause of the rise in contact angle. The surface qualities of these impurities may be changed, or they could add surface roughness, increasing the contact angle.

CHAPTER 9 : Discussion, Conclusion And future directions

Introduction

We shall perform a thorough analysis and interpretation of the experimental findings in this chapter. Pulsed laser ablation was used to create a silver-water nanofluid. The objective is to get a greater comprehension of the interaction between nanoparticle formation, optical properties, morphology, stability, thermal conductivity, and contact angle. To uncover major takeaways and patterns, we will compare our results with previously published literature and theoretical frameworks.

9.1 Detailed Evaluation and Interpretation of the Experimental Findings:

A novel coolant for nano electronics may be created by creating nanofluids by pulsed laser ablation (PLAL) thanks to the thorough analysis and interpretation of the experimental data in this work. The main goal of the study was to comprehend the synthesis, stability, thermal conductivity, and contact angle characteristics of Ag-H_2O nanofluids. The study uncovered important details regarding the behaviour of Ag nanoparticles in water and their effect on the overall performance of the nanofluid through a series of experiments and observations.

9.1.1 Morphology and composition Ag-H_2O nanofluids.

One significant observation was the development of an aggregation network in water by Ag nanoparticles. This finding implies that the nanoparticles have a propensity to cluster, which may impact their stability and dispersion in the nanofluid. The study also showed that clean silver nanofluids devoid of outside impurities are produced by the PLAL approach. This is a crucial discovery since contaminants may affect the effectiveness and dependability of nanofluids in real-world settings.

9.1.2 Optical investigation Ag-H_2O nanofluids.

In the study, optical experiments were undertaken to get further understanding of how Ag nanoparticles were distributed in the silver-water nanofluid. Ag nanoparticles were successfully dispersed in the nanofluid as shown by the existence of a plasmonic peak at 400 nm. It was observed that the stability of these nanoparticles over time is not perfect. The loss of plasmonic peaks was caused by the Ag nanoparticles' tendency to gravitationally settle down

at large concentrations. When creating nanofluids for long-term uses, it is essential to take this instability into account.

9.1.3 Stability Ag-H$_2$O nanofluids.

Ag nanoparticles at low concentrations showed sustained plasmon peaks even after five months, indicating that the stability of the nanoparticles was concentration dependent. Higher concentrations, on the other hand, caused nanoparticles to settle and subsequently lost plasmonic peaks. A careful management of the nanoparticle concentration is required to maintain the long-term stability of the nanofluid, according to this result, which implies that nanoparticles are more stable at lower concentrations.

9.1.4 Thermal enhancement Ag-H$_2$O nanofluids.

The study also looked at how Ag-H$_2$O nanofluids improved thermal conductivity when compared to plain water. Ag nanoparticles significantly increased thermal conductivity when added to water, demonstrating their potential as efficient heat transfer agents. With a thermal enhancement percentage (%) of 19.45% at 45 °C, the sample with the highest enhancement was found when the ablation period was 5 minutes. The lowest concentrations of nanoparticles were indicated by the thermal enhancement (%) of 7.5% at 45 °C for a duration of ablation of 2.5 minutes after this enhancement. The potential of Ag-H$_2$O nanofluids as excellent coolants for nanoelectronics, where efficient heat dissipation is crucial, is highlighted by these findings.

9.1.5 Contact angle Ag-H$_2$O nanofluids.

The study also looked at the contact angle's dependence on concentration, which is a crucial factor in fluid flow behaviour. The measurements of the contact angle showed unequivocally that the Ag nanoparticle concentration affects the contact angle of the nanofluid. The presence of nanoparticles might potentially have a considerable impact on fluid flow, switching it from a laminar to a turbulent state, according to this concentration dependency. It implies that to get the best results and prevent undesirable flow interruptions, the roughness of the tube through which the nanofluid passes must be carefully taken into account.

9.2 An examination of the connections between the creation of nanoparticles, their morphology, stability, thermal conductivity, and contact angle

The complex interrelationships between nanoparticle production, shape, stability, thermal conductivity, and contact angle were discussed in this work. Ag nanoparticles' apparent

creation of an aggregate network in water is intimately tied to the production and shape of those particles. Regulating the spreading and stability of nanoparticles in the nanofluid requires an understanding of the mechanisms and variables driving this agglomeration. This study's PLAL approach was discovered to create clean silver nanofluids free of external impurities, which is crucial for retaining the nanofluid's desirable qualities and performance. The clean synthesis method makes sure that the nanoparticles contribute to the required improvement in heat conductivity without adding any extra contaminants or unfavourable side effects.

The optical analyses carried out in the study shed light on the Ag nanoparticle dispersion inside the silver-water nanofluid. The existence of a plasmonic peak at 400 nm demonstrated that Ag nanoparticles were successfully dispersed. The stability of the nanoparticles within the nanofluid is directly correlated with this distribution. The observed gravitational settling of Ag nanoparticles at high concentrations emphasises the significance of stability factors. For nanofluids to maintain the appropriate characteristics and long-term performance, stable dispersions must be maintained.

The increased heat transfer capabilities that the nanoparticles bring are what cause the thermal conductivity improvement that was seen in this study with the addition of Ag nanoparticles to water. A greater efficiency in the transmission of thermal energy results from the creation of new channels for heat conduction caused by the presence of nanoparticles. The fact that the thermal conductivity improvement is concentration-dependent emphasises the need of managing the nanoparticle concentration to maximise heat transfer efficiency. The lowest concentrations produced the greatest thermal increase, indicating an ideal range for getting the greatest thermal conductivity enhancement.

According to this study's observation of the concentration dependence of the contact angle, the inclusion of Ag nanoparticles alters the nanofluid's wetting behaviour. The interactions between the surface of the tube and the nanofluid have an impact on the fluid flow properties, which in turn alter the contact angle. The concentration-dependent contact angle suggests that the roughness of the tube and the existence of nanoparticles can drastically change the fluid flow behaviour, switching from laminar to turbulent regimes. To create effective fluid flow systems that take into consideration the existence of nanofluids and their related properties, it is essential to comprehend these impacts.

9.3 Studying the Results considering Current Theories and Literature.

9.3.1 Morphology and Composition

It is crucial to compare the results of this study with current literature and ideas to validate them and put them in perspective. Similar observations of nanoparticle aggregation and settling at high concentrations have been made before in studies on the fabrication and stability of nanofluids [299-303]. The results of the current investigation are consistent with these conclusions, emphasizing the necessity of meticulous management of nanoparticle concentration to maintain stability and avoid settling.

9.3.2 Optical studies

The optical experiments' 400 nm plasmonic peak agrees with the plasmonic behavior of Ag nanoparticles described in earlier research [304-306]. This result demonstrates that Ag nanoparticles are efficiently dispersed in the nanofluid using the PLAL production technique used in this work, enabling effective heat transfer increase.

9.3.3 Thermal conductivity

This study's observation that the inclusion of Ag nanoparticles increased thermal conductivity is consistent with earlier studies on nanofluids [307-310]. Due to their high surface-to-volume ratio and improved heat conduction capabilities, nanoparticles have been found to have a favorable effect on thermal conductivity in several investigations. The enhanced thermal conductivity's concentration-dependent nature adds credence to preexisting hypotheses about the ideal concentration of nanoparticles to achieve the highest possible heat transfer efficiency.

9.3.4 Contact angle

The contact angle concentration dependency is consistent with existing hypotheses of wetting behaviour in nanofluids [311, 312]. Previous studies have demonstrated that the presence of nanoparticles can change the contact angle, which impacts the properties of fluid flow. The results of this study add to the body of knowledge on fluid flow behaviour in the presence of nanofluids by offering additional proof of the concentration-dependent influence on the contact angle.

9.4   Discovering Significant Insights and Patterns

This study's primary findings and trends are based on the thorough analysis and interpretation of the experimental data. These consist of:

1. **Aggregate network formation**: In water, Ag nanoparticles have a tendency to form an aggregate network, which impacts their stability and dispersion in the nanofluid. For stable nanofluids to be produced, aggregation must be managed.

2. **Clean synthesis procedure:** The PLAL approach used in this work results in clean silver nanofluids, guaranteeing that there are no outside impurities that can affect the performance of nanofluids.

3. **Plasmonic peak and nanoparticle stability**: The existence of a plasmonic peak at around 400 nm signifies that the nanofluid successfully distributed the nanoparticles. At greater concentrations, however, nanoparticle stability declines, causing settling and the disappearance of plasmonic peaks.

4. **Improvement in thermal conductivity**: Ag nanoparticles improve thermal conductivity in water, making nanofluids suitable coolants for nanoelectronics. The lowest concentrations of nanoparticles result in the largest thermal enhancement.

5. **Concentration-dependent contact angle**: The nanofluid's concentration-dependent contact angle indicates that the presence of nanoparticles impacts fluid flow behaviour, especially when laminar to turbulent transitions occur.

9.5   An Overview of the Study's Results

In summary, this work concentrated on the PLAL-based synthesis of Ag-H_2O nanofluids for prospective usage as coolants in nanoelectronics. Important trends and insights about nanoparticle synthesis, shape, stability, thermal conductivity, and contact angle were discovered by the inquiry. Ag nanoparticles in water were seen to form an aggregate network, highlighting the necessity of rigorous control over dispersion and stability. It was discovered that the PLAL approach produced pure silver nanofluids devoid of outside contamination. Ag nanoparticles were successfully distributed, according to optical measurements, albeit at

greater concentrations, their stability was compromised. Ag nanoparticles improved heat conductivity when they were added, with the lowest concentrations showing the greatest improvement. It was discovered that the contact angle was concentration-dependent, demonstrating the impact of nanoparticles on fluid flow characteristics.

9.6   Reiteration of Study Goals and Contributions.

The purpose of this work was to examine the manufacture of Ag-H_2O nanofluids using PLAL and to determine whether they have any application as coolants for nanoelectronics. The goal of the study was to comprehend the production, stability, thermal conductivity, and contact angle characteristics of Ag nanoparticles in the nanofluid. By accomplishing these goals, the study makes a contribution to the area by offering insightful information and expertise that may direct the creation of effective nanofluid coolants for nano electronics.

9.7   Limitations and Ideas for Further Study

This study has some important findings, but it also has several limitations that need to be noted. The concentration on Ag-H_2O nanofluids restricts the applicability of the findings to other types of nanoparticles or base fluids. To better understand the behavior and functionality of nanofluids, future study may investigate various nanoparticle materials and base fluids. Ag nanoparticles' concentration-dependent stability is another drawback that makes long-term use difficult. To make nanoparticles more stable at larger concentrations and make them viable for use in various cooling systems, more research is required to create techniques and additives. Although the contact angle and increased thermal conductivity of the nanofluid were the main topics of this investigation, more significant characteristics might be investigated in further studies. The total effectiveness of nanofluids as coolants is greatly influenced by these factors, which also include viscosity, specific heat capacity, and flow properties.

9.8   The study's findings' implications and potential applications:

The findings of this work have important ramifications and prospective uses in the realm of cooling nanoelectronics. Ag nanoparticles added to water have been shown to improve thermal conductivity, which opens the door to effective heat dissipation in nano electrical devices. Higher power densities and increased reliability of nanoelectronics are made possible by the

development of better cooling systems, which is facilitated by the improved thermal performance of nanofluids.

Additionally, the concentration-dependent behaviour of the nanofluid emphasises the value of careful design considerations for fluid flow systems in nano electronics, notably the contact angle and fluid flow characteristics. For maximising cooling effectiveness and avoiding flow interruptions, it is essential to comprehend and take into account the existence of nanofluids and their effect on flow behaviour.

Overall, the study's findings offer insightful information and uses for creating and using nanofluids as coolants in the field of nano electronics, advancing thermal management and the overall effectiveness of nano electronic devices.

References

[1] C. Buzea, I. Pacheco, and K. Robie, " Biointerphases," no. 2, 2007.

[2] M. C. Roco, C. A. Mirkin, and M. C. Hersam, "Nanotechnology research directions for societal needs in 2020: retrospective and outlook," 2011.

[3] T. Appenzeller, "The man who dared to think small," *Science,* vol. 254, no. 5036, pp. 1300-1301, 1991. [Online]. Available: https://science.sciencemag.org/content/254/5036/1300.long.

[4] S. K. Das, S. U. S. Choi, W. Yu, and T. Pradeep, *Nanofluids Science and Technology.* USA: Wiley, 2007.

[5] K. E. Drexler, "Molecular engineering: An approach to the development of general capabilities for molecular manipulation," *Proceedings of the National Academy of Science of the United States of America,* vol. 78, no. 9, pp. 5275-5278, 1981.

[6] H. Babar and H. Muhamed ali, "Towards hybrid nanofluids: Preparation, thermophysical properties,applications, and challenges," *Journal of Molecular Liquids,* pp. 598-633, 2019.

[7] A. A. Almubarak, "The effects of heat on electronic components," *Int. J. Eng. Res. Appl,* vol. 7, no. 5, pp. 52-57, 2017.

[8] P. M. Kirad and T. Sharma, "Degradation of Electronic Devices Overtime," *Journal homepage: www. ijrpr. com ISSN,* vol. 2582, p. 7421.

[9] R. R. Schaller, "Moore's law: past, present and future," *IEEE spectrum,* vol. 34, no. 6, pp. 52-59, 1997.

[10] T. Balaji, C. Selvam, and D. M. Lal, "A Review on Electronics Cooling using Nanofluids," in *IOP Conference Series: Materials Science and Engineering*, 2021, vol. 1130, no. 1: IOP Publishing, p. 012007.

[11] M. H. SÖKÜCÜ, "MINICHANNEL EVAPORATOR DESIGN FOR HEAT TRANSFER ENHANCEMENT IN COMPUTER COOLING APPLICATIONS."

[12] J. A. Eastman, U. Choi, S. Li, L. Thompson, and S. Lee, "Enhanced thermal conductivity through the development of nanofluids," *MRS Online Proceedings Library (OPL),* vol. 457, 1996.

[13] J. C. Maxwell, ""A treatise on electricity and magnetism"," *Dover Publications,* 1873.

[14] H. Masuda, A. Ebata, K. Teramae, and N. Hishinuma, "Alteration of Thermal Conductivity and Viscosity of Liquid by Dispersing Ultra-Fine Particles (Dispersion of Al2O3, SiO2 and TiO2 Ultra-Fine Particles)," *Netsu Bussei,* vol. 7, no. 4, pp. 227-233, 1993.

[15] B. Wang, L. Zhou , and X. Peng, "A fractal model for predicting the effective thermal conductivity of liquid with suspension of nanoparticles," *Int. J. Heat Mass Transfer,* vol. 46, no. 14, pp. 2665-2672, 2003.

[16] A. S. Ahuja, "Augmentation of heat transport in laminar flow of polystyrene suspensions. II. Analysis of the data," *Journal of Applied Physics,* vol. 46, no. 8, pp. 3417-3425, 1975.

[17] A. S. Ahuja, "Thermal design of a heat exchanger employing laminar flow of particle suspensions," *International Journal of Heat and Mass Transfer,* vol. 25, no. 5, pp. 725-728, 1982.

[18] R. A. Taylor, ""Small particles, big impacts: A review of the diverse applications of nanofluids","" *Journal of Applied Physics,* vol. 113, no. 1, 2013.

[19] S. K. Das, N. Putra, and W. Roetzel, "Pool boiling characteristics of nano-fluids," *International Journal of Heat and Mass Transfer,* vol. 46, no. 5, pp. 851-862, 2003.

[20] S. Choi and J. A. Eastman, "ENHANCING THERMAL CONDUCTIVITY OF FLUIDS WITH NANOPARTICLES," *Energy Technology Division and Materials Science Division Argonne National Laboratory,* 1995.

[21] K. S. Suganthi and K. S. Rajan, "Metal oxide nanofluids: Review of formulation, thermo-physical properties, mechanisms, and heat transfer performance," *Renewable and Sustainable Energy Reviews,* vol. 76, pp. 226-255, 2017.

[22] K. R. Sreelakshmy, S. Aswathy, K. M. Vidhyar, T. R. Saranya, and C. N. Sreeja, "An overview of recent nanofluid research," *International Research Journal of Pharmacy,* vol. 5, no. 4, pp. 239-243, 2014.

[23] X.-Q. Wang and A. S. Mujumdar, "A review on nanofluids-part I: theoretical and numerical investigations," *Brazilian Journal of Chemical Engineering,* vol. 25, no. 4, pp. 613-630, 2008.

[24] E. V. Timofeeva, "Nanofluids for heat transfer-potential and engineering strategies," *Two phase flow, phase change and numerical modeling,* pp. 435-450, 2011.

[25] P. K. Namburu, D. P. Kulkarni, D. Misra, and D. K. Das, "Viscosity of copper oxide nanoparticles dispersed in ethylene glycol and water mixture," *Experimental Thermal and Fluid Science,* vol. 32, no. 2, pp. 397-402, 2007.

[26] M. Jama *et al.,* "Critical review on nanofluids: preparation, characterization, and applications," *Journal of Nanomaterials,* vol. 2016, 2016.

[27] S. K. Das, S. U. Choi, and H. E. Patel, "Heat transfer in nanofluids—a review," *Heat transfer engineering,* vol. 27, no. 10, pp. 3-19, 2006.

[28] J. Contreras, E. Rodriguez, and J. Taha-Tijerina, "Nanotechnology applications for electrical transformers—A review," *Electric Power Systems Research,* vol. 143, pp. 573-584, 2017.

[29] M. Chandrasekar and S. Suresh, "A review on the mechanisms of heat transport in nanofluids," *Heat Transfer Engineering,* vol. 30, no. 14, pp. 1136-1150, 2009.

[30] T. T. Baby and R. Sundara, "Synthesis and transport properties of metal oxide decorated graphene dispersed nanofluids," *The Journal of Physical Chemistry C,* vol. 115, no. 17, pp. 8527-8533, 2011.

[31] D. Cabaleiro, C. Gracia-Fernández, J. Legido, and L. Lugo, "Specific heat of metal oxide nanofluids at high concentrations for heat transfer," *International journal of heat and mass transfer,* vol. 88, pp. 872-879, 2015.

[32] W. Yu, D. M. France, J. L. Routbort, and S. U. Choi, "Review and comparison of nanofluid thermal conductivity and heat transfer enhancements," *Heat transfer engineering,* vol. 29, no. 5, pp. 432-460, 2008.

[33]   L. H. Kumar, S. Kazi, H. Masjuki, and M. Zubir, "A review of recent advances in green nanofluids and their application in thermal systems," *Chemical Engineering Journal,* vol. 429, p. 132321, 2022.

[34]   A. Nasir and A. Kausar, "A review on materials derived from polystyrene and different types of nanoparticles," *Polymer-Plastics Technology and Engineering,* vol. 54, no. 17, pp. 1819-1849, 2015.

[35]   S. K. Das, S. U. Choi, W. Yu, and T. Pradeep, *Nanofluids: science and technology.* John Wiley & Sons, 2007.

[36]   Z. Said *et al.*, "Recent advances on the fundamental physical phenomena behind stability, dynamic motion, thermophysical properties, heat transport, applications, and challenges of nanofluids," *Physics Reports,* vol. 946, pp. 1-94, 2022.

[37]   T. GEBREMESKEL, "ENHANCEMENT OF COOLING PERFORMANCE OF ELECTRONICS PROCESSOR USING GREEN SYNTHESIZED SILVER-WATER NANOFLUID," 2021.

[38]   W. N. Septiadi, I. A. N. T. Trisnadewi, N. Putra, and I. Setyawan, "Synthesis of hybrid nanofluid with two-step method," in *E3S Web of Conferences*, 2018, vol. 67: EDP Sciences, p. 03057.

[39]   G. Paul, J. Philip, B. Raj, P. K. Das, and I. Manna, "Synthesis, characterization, and thermal property measurement of nano-Al95Zn05 dispersed nanofluid prepared by a two-step process," *International Journal of Heat and Mass Transfer,* vol. 54, no. 15-16, pp. 3783-3788, 2011.

[40]   N. A. C. Sidik, H. Mohammed, O. A. Alawi, and S. Samion, "A review on preparation methods and challenges of nanofluids," *International Communications in Heat and Mass Transfer,* vol. 54, pp. 115-125, 2014.

[41]   A. Mota-Babiloni *et al.*, "Ultralow-temperature refrigeration systems: Configurations and refrigerants to reduce the environmental impact," *International Journal of Refrigeration,* vol. 111, pp. 147-158, 2020.

[42]   A. A. Lakew and O. Bolland, "Working fluids for low-temperature heat source," *Applied Thermal Engineering,* vol. 30, no. 10, pp. 1262-1268, 2010.

[43]   A. Heinzel *et al.*, "Liquid metals as efficient high-temperature heat-transport fluids," *Energy Technology,* vol. 5, no. 7, pp. 1026-1036, 2017.

[44]   H. Mao, Y. Yang, H. Zhang, J. Zhang, and Y. Huang, "A critical review of the possible effects of physical and chemical properties of subcritical water on the performance of water-based drilling fluids designed for ultra-high temperature and ultra-high pressure drilling applications," *Journal of Petroleum Science and Engineering,* vol. 187, p. 106795, 2020.

[45]   S. Mokhatab, M. Fresky, and M. Islam, "Application of Nanotechnology in Oil and Gas E&P. JPT," *Society of Petroleum Engineers,* vol. 18, 2006.

[46]   M. S. Hale and J. G. Mitchell, "Motion of submicrometer particles dominated by Brownian motion near cell and microfabricated surfaces," *Nano Letters,* vol. 1, no. 11, pp. 617-623, 2001.

[47]   P. Liu, P. J. Ziemann, D. B. Kittelson, and P. H. McMurry, "Generating particle beams of controlled dimensions and divergence: I. Theory of particle motion in aerodynamic

lenses and nozzle expansions," *Aerosol Science and Technology,* vol. 22, no. 3, pp. 293-313, 1995.

[48]   N. F. Azman and S. Samion, "Dispersion stability and lubrication mechanism of nanolubricants: a review," *International journal of precision engineering and manufacturing-green technology,* vol. 6, no. 2, pp. 393-414, 2019.

[49]   H. Liu, E. Schubert, and D. McNiel, "μAWJ technology for meso-micro machining," in *Proceedings of 2011 WJTA-IMCA conference and exposition*, 2011, pp. 19-21.

[50]   G. Paul and I. Manna, "Nanofluids including ceramic and other nanoparticles: applications and rheological properties," in *Ceramic Nanocomposites*: Elsevier, 2013, pp. 323-345.

[51]   C. N. R. Rao, A. Muller, and A. K. Cheetham, " The Chemistry of Nanomaterials: Synthesis, Properties and Applications," *Wiley-VCH,Weinhein,* 2004.

[52]   S. Choi, Z. G. Zhang, W. Yu, F. Lockwood, and E. Grulke, "Anomalous thermal conductivity enhancement in nanotube suspensions," *Applied physics letters,* vol. 79, no. 14, pp. 2252-2254, 2001.

[53]   S. K. Das, N. Putra, P. Thiesen, and W. Roetzel, "Temperature dependence of thermal conductivity enhancement for nanofluids," *J. Heat Transfer,* vol. 125, no. 4, pp. 567-574, 2003.

[54]   C. H. Chon, K. D. Kihm, S. P. Lee, and S. U. Choi, "Empirical correlation finding the role of temperature and particle size for nanofluid (Al 2 O 3) thermal conductivity enhancement," *Applied Physics Letters,* vol. 87, no. 15, p. 153107, 2005.

[55]   S. K. Das, G. P. Narayan, and A. K. Baby, "Survey on nucleate pool boiling of nanofluids: the effect of particle size relative to roughness," *Journal of Nanoparticle Research,* vol. 10, no. 7, pp. 1099-1108, 2008.

[56]   I. C. Bang and S. H. Chang, "Boiling heat transfer performance and phenomena of Al2O3–water nano-fluids from a plain surface in a pool," *International Journal of Heat and Mass Transfer,* vol. 48, no. 12, pp. 2407-2419, 2005.

[57]   D. Wen and Y. Ding, "Formulation of nanofluids for natural convective heat transfer applications," *International Journal of Heat and Fluid Flow,* vol. 26, no. 6, pp. 855-864, 2005.

[58]   X. Wang, X. Xu, and S. U. Choi, "Thermal conductivity of nanoparticle-fluid mixture," *Journal of thermophysics and heat transfer,* vol. 13, no. 4, pp. 474-480, 1999.

[59]   B. Nowack, H. F. Krug, and M. Height, "120 years of nanosilver history: implications for policy makers," ed: ACS Publications, 2011.

[60]   B. Reidy, A. Haase, A. Luch, K. A. Dawson, and I. Lynch, "Mechanisms of silver nanoparticle release, transformation and toxicity: a critical review of current knowledge and recommendations for future studies and applications," *Materials,* vol. 6, no. 6, pp. 2295-2350, 2013.

[61]   L. Castillo-Henríquez, K. Alfaro-Aguilar, J. Ugalde-Álvarez, L. Vega-Fernández, G. Montes de Oca-Vásquez, and J. R. Vega-Baudrit, "Green synthesis of gold and silver nanoparticles from plant extracts and their possible applications as antimicrobial agents in the agricultural area," *Nanomaterials,* vol. 10, no. 9, p. 1763, 2020.

[62]   K. Kalantari *et al.*, "Wound dressings functionalized with silver nanoparticles: promises and pitfalls," *Nanoscale,* vol. 12, no. 4, pp. 2268-2291, 2020.

[63] Y. Zhu, Y. Deng, P. Yi, L. Peng, X. Lai, and Z. Lin, "Flexible transparent electrodes based on silver nanowires: Material synthesis, fabrication, performance, and applications," *Advanced Materials Technologies,* vol. 4, no. 10, p. 1900413, 2019.

[64] T. Cheng, Y. Zhang, W. Y. Lai, and W. Huang, "Stretchable thin-film electrodes for flexible electronics with high deformability and stretchability," *Advanced Materials,* vol. 27, no. 22, pp. 3349-3376, 2015.

[65] M. Vaseem, G. McKerricher, and A. Shamim, "Robust design of a particle-free silver-organo-complex ink with high conductivity and inkjet stability for flexible electronics," *ACS applied materials & interfaces,* vol. 8, no. 1, pp. 177-186, 2016.

[66] Y. Li, Y. Wu, and B. S. Ong, "Facile synthesis of silver nanoparticles useful for fabrication of high-conductivity elements for printed electronics," *Journal of the American Chemical Society,* vol. 127, no. 10, pp. 3266-3267, 2005.

[67] R. Güzel and G. Erdal, *Synthesis of silver nanoparticles*. IntechOpen, 2018.

[68] S. Iravani, H. Korbekandi, S. V. Mirmohammadi, and B. Zolfaghari, "Synthesis of silver nanoparticles: chemical, physical and biological methods," *Research in pharmaceutical sciences,* vol. 9, no. 6, p. 385, 2014.

[69] S. W. Wijnhoven *et al.*, "Nano-silver–a review of available data and knowledge gaps in human and environmental risk assessment," *Nanotoxicology,* vol. 3, no. 2, pp. 109-138, 2009.

[70] M. A. Maksoud, A. M. Elgarahy, C. Farrell, H. Ala'a, D. W. Rooney, and A. I. Osman, "Insight on water remediation application using magnetic nanomaterials and biosorbents," *Coordination Chemistry Reviews,* vol. 403, p. 213096, 2020.

[71] M. Cvjetko Bubalo, S. Vidović, I. Radojčić Redovniković, and S. Jokić, "Green solvents for green technologies," *Journal of Chemical Technology & Biotechnology,* vol. 90, no. 9, pp. 1631-1639, 2015.

[72] M. Vivar and V. Everett, "A review of optical and thermal transfer fluids used for optical adaptation or beam-splitting in concentrating solar systems," *Progress in Photovoltaics: Research and Applications,* vol. 22, no. 6, pp. 612-633, 2014.

[73] M. Jain, "Ecological approach to reduce carbon footprint of textile industry," *International Journal of Applied Home Science,* vol. 4, no. 7/8, pp. 623-633, 2017.

[74] I. Chakrabartty, K. R. Hakeem, Y. K. Mohanta, and R. S. Varma, "Greener nanomaterials and their diverse applications in the energy sector," *Clean Technologies and Environmental Policy,* vol. 24, no. 10, pp. 3237-3252, 2022.

[75] M. E. Demir and I. Dincer, "Development and analysis of a new integrated solar energy system with thermal storage for fresh water and power production," *International Journal of Energy Research,* vol. 42, no. 9, pp. 2864-2874, 2018.

[76] S. Nukiyama, "The maximum and minimum values of the heat Q transmitted from metal to boiling water under atmospheric pressure," *International Journal of Heat and Mass Transfer,* vol. 9, no. 12, pp. 1419-1433, 1966.

[77] D. Saidina, M. Abdullah, and M. Hussin, "Metal oxide nanofluids in electronic cooling: a review," *Journal of Materials Science: Materials in Electronics,* vol. 31, pp. 4381-4398, 2020.

[78]   L. Yang, W. Ji, M. Mao, and J.-n. Huang, "An updated review on the properties, fabrication and application of hybrid-nanofluids along with their environmental effects," *Journal of Cleaner Production,* vol. 257, p. 120408, 2020.

[79]   W. Duangthongsuk and S. Wongwises, "Measurement of temperature-dependent thermal conductivity and viscosity of TiO2-water nanofluids," *Experimental thermal and fluid science,* vol. 33, no. 4, pp. 706-714, 2009.

[80]   E. Oró, A. De Gracia, A. Castell, M. M. Farid, and L. F. Cabeza, "Review on phase change materials (PCMs) for cold thermal energy storage applications," *Applied Energy,* vol. 99, pp. 513-533, 2012.

[81]   J.-Y. Sha *et al.*, "Corrosion inhibition behaviour of sodium dodecyl benzene sulphonate for brass in an Al2O3 nanofluid and simulated cooling water," *Corrosion Science,* vol. 148, pp. 123-133, 2019.

[82]   N. Czaplicka, A. Grzegórska, J. Wajs, J. Sobczak, and A. Rogala, "Promising nanoparticle-based heat transfer fluids—environmental and techno-economic analysis compared to conventional fluids," *International Journal of Molecular Sciences,* vol. 22, no. 17, p. 9201, 2021.

[83]   E. Fabre and S. S. Murshed, "A review of the thermophysical properties and potential of ionic liquids for thermal applications," *Journal of Materials Chemistry A,* vol. 9, no. 29, pp. 15861-15879, 2021.

[84]   M. Heyhat, M. Abbasi, and A. Rajabpour, "Molecular dynamic simulation on the density of titanium dioxide and silver water-based nanofluids using ternary mixture model," *Journal of Molecular Liquids,* vol. 333, p. 115966, 2021.

[85]   W. H. Azmi, K. V. Sharma, R. Mamat, G. Najafi, and M. S. Mohamad, "The enhancement of effective thermal conductivity and effective dynamic viscosity of nanofluids–A review," *Renewable and Sustainable Energy Reviews,* vol. 53, pp. 1046-1058, 2016.

[86]   Y. Xuan and W. Roetzel, "Conceptions for heat transfer correlation of nanofluids," *International Journal of heat and Mass transfer,* vol. 43, no. 19, pp. 3701-3707, 2000.

[87]   E. M. C. Contreras, G. A. Oliveira, and E. P. Bandarra Filho, "Experimental analysis of the thermohydraulic performance of graphene and silver nanofluids in automotive cooling systems," *International Journal of Heat and Mass Transfer,* vol. 132, pp. 375-387, 2019.

[88]   P. Gunnasegaran, M. Z. Abdullah, M. Z. Yusoff, and S. F. Abdullah, "Case Studies in Thermal Engineering," 2015.

[89]   N. Putra, W. N. Septiadi, and R. Sahmura, "Analysis of CuO-Water Nanofluid Application on Heat Pipe," in *Applied Mechanics and Materials*, 2014, vol. 590: Trans Tech Publ, pp. 234-238.

[90]   N. M. a. Muhammad, N. A. C. Sidik, and D. Adanta, "On the application of nanofluid in minichannel for heat transfer and fluid flow analysis," *Journal of Advanced Research Design,* vol. 59, pp. 11-38.

[91]   S. Peyghambarzadeh, S. Hashemabadi, M. Naraki, and Y. Vermahmoudi, "Experimental study of overall heat transfer coefficient in the application of dilute nanofluids in the car radiator," *Applied Thermal Engineering,* vol. 52, no. 1, pp. 8-16, 2013.

[92] S. Peyghambarzadeh, S. Hashemabadi, S. Hoseini, and M. S. Jamnani, "Experimental study of heat transfer enhancement using water/ethylene glycol based nanofluids as a new coolant for car radiators," *International communications in heat and mass transfer,* vol. 38, no. 9, pp. 1283-1290, 2011.

[93] J. Philip and P. D. Shima, "Thermal properties of nanofluids," *Advances in colloid and interface science,* vol. 183, pp. 30-45, 2012.

[94] C. H. Li and G. Peterson, "The effect of particle size on the effective thermal conductivity of Al 2 O 3-water nanofluids," *Journal of Applied Physics,* vol. 101, no. 4, p. 044312, 2007.

[95] L. Yang, W. Ji, J.-n. Huang, and G. Xu, "An updated review on the influential parameters on thermal conductivity of nano-fluids," *Journal of Molecular Liquids,* vol. 296, p. 111780, 2019.

[96] E. E. Michaelides and E. E. Michaelides, "Thermal Conductivity," *Nanofluidics: Thermodynamic and Transport Properties,* pp. 163-225, 2014.

[97] L. M. Amoo and R. L. Fagbenle, "Advanced fluids–a review of nanofluid transport and its applications," *Applications of Heat, Mass and Fluid Boundary Layers,* pp. 281-382, 2020.

[98] C. H. Li and G. Peterson, "Experimental investigation of temperature and volume fraction variations on the effective thermal conductivity of nanoparticle suspensions (nanofluids)," *journal of applied physics,* vol. 99, no. 8, p. 084314, 2006.

[99] J.-C. Yang, F.-C. Li, W.-W. Zhou, Y.-R. He, and B.-C. Jiang, "Experimental investigation on the thermal conductivity and shear viscosity of viscoelastic-fluid-based nanofluids," *International Journal of Heat and Mass Transfer,* vol. 55, no. 11-12, pp. 3160-3166, 2012.

[100] A. S. Dalkılıç *et al.*, "Experimental study on the thermal conductivity of water-based CNT-SiO2 hybrid nanofluids," *International Communications in Heat and Mass Transfer,* vol. 99, pp. 18-25, 2018.

[101] H. Alias, "Engineered nanofields for heat transfer process intensification," University of Leeds, 2006.

[102] S. U. Ilyas, R. Pendyala, and N. Marneni, "Preparation, sedimentation, and agglomeration of nanofluids," *Chemical Engineering & Technology,* vol. 37, no. 12, pp. 2011-2021, 2014.

[103] S. Angayarkanni and J. Philip, "Review on thermal properties of nanofluids: Recent developments," *Advances in colloid and interface science,* vol. 225, pp. 146-176, 2015.

[104] S. Iyahraja and J. S. Rajadurai, "Study of thermal conductivity enhancement of aqueous suspensions containing silver nanoparticles," *AIP Advances,* vol. 5, no. 5, p. 057103, 2015.

[105] A. M. Kimulu, W. N. Mutuku, and N. M. Mutua, "Car Antifreeze and Coolant: Comparing Water and Ethylene Glycol as Nano Fluid Base Fluid," *Int. J. Adv. Sci. Res. Eng.,* vol. 4, pp. 17-37, 2018.

[106] P. R. Mashaei and S. M. Hosseinalipour, "A numerical study of nanofluid forced convection in a porous channel with discrete heat sources," *Journal of Porous Media,* vol. 17, no. 6, 2014.

[107] P. Rahim Mashaei, S. M. Hosseinalipour, and M. Bahiraei, "Numerical investigation of nanofluid forced convection in channels with discrete heat sources," *Journal of Applied Mathematics,* vol. 2012, 2012.

[108] Y. Feng, "A new thermal conductivity model for nanofluids with convection heat transfer application," 2009.

[109] R. Irwansyah, "On the experimental investigation of the laminar convective heat transfer of Al2O3-water nanofluids in a microchannel," Universitätsbibliothek der Universität der Bundeswehr München, 2018.

[110] M. P. Beck, Y. Yuan, P. Warrier, and A. S. Teja, "The effect of particle size on the thermal conductivity of alumina nanofluids," *Journal of Nanoparticle research,* vol. 11, no. 5, pp. 1129-1136, 2009.

[111] G. Paul, T. Pal, and I. Manna, "Thermo-physical property measurement of nano-gold dispersed water based nanofluids prepared by chemical precipitation technique," *Journal of colloid and interface science,* vol. 349, no. 1, pp. 434-437, 2010.

[112] G. Paul, S. Sarkar, T. Pal, P. Das, and I. Manna, "Concentration and size dependence of nano-silver dispersed water based nanofluids," *Journal of colloid and interface science,* vol. 371, no. 1, pp. 20-27, 2012.

[113] E. V. Timofeeva, J. L. Routbort, and D. Singh, "Particle shape effects on thermophysical properties of alumina nanofluids," *Journal of applied physics,* vol. 106, no. 1, p. 014304, 2009.

[114] F. Liu, Y. Cai, L. Wang, and J. Zhao, "Effects of nanoparticle shapes on laminar forced convective heat transfer in curved ducts using two-phase model," *International Journal of Heat and Mass Transfer,* vol. 116, pp. 292-305, 2018.

[115] S. Mukherjee, P. C. Mishra, S. Parashar, and P. Chaudhuri, "Role of temperature on thermal conductivity of nanofluids: a brief literature review," *Heat and Mass Transfer,* vol. 52, no. 11, pp. 2575-2585, 2016.

[116] A. Omrani, E. Esmaeilzadeh, M. Jafari, and A. Behzadmehr, "Effects of multi walled carbon nanotubes shape and size on thermal conductivity and viscosity of nanofluids," *Diamond and Related Materials,* vol. 93, pp. 96-104, 2019.

[117] P. K. Das, "A review based on the effect and mechanism of thermal conductivity of normal nanofluids and hybrid nanofluids," *Journal of Molecular Liquids,* vol. 240, pp. 420-446, 2017.

[118] B. Gu, B. Hou, Z. Lu, Z. Wang, and S. Chen, "Thermal conductivity of nanofluids containing high aspect ratio fillers," *International Journal of Heat and Mass Transfer,* vol. 64, pp. 108-114, 2013.

[119] M. Pantzali, A. Kanaris, K. Antoniadis, A. Mouza, and S. Paras, "Effect of nanofluids on the performance of a miniature plate heat exchanger with modulated surface," *International Journal of Heat and Fluid Flow,* vol. 30, no. 4, pp. 691-699, 2009.

[120] H. E. Patel, T. Sundararajan, and S. K. Das, "An experimental investigation into the thermal conductivity enhancement in oxide and metallic nanofluids," *Journal of Nanoparticle Research,* vol. 12, pp. 1015-1031, 2010.

[121] H. Mohammed, G. Bhaskaran, N. Shuaib, and R. Saidur, "Heat transfer and fluid flow characteristics in microchannels heat exchanger using nanofluids: a review," *Renewable and Sustainable Energy Reviews,* vol. 15, no. 3, pp. 1502-1512, 2011.

[122] R. A. Dehkordi, M. H. Esfe, and M. Afrand, "Effects of functionalized single walled carbon nanotubes on thermal performance of antifreeze: an experimental study on thermal conductivity," *Applied Thermal Engineering,* vol. 120, pp. 358-366, 2017.

[123] R. R. Riehl and N. dos Santos, "Water-copper nanofluid application in an open loop pulsating heat pipe," *Applied Thermal Engineering,* vol. 42, pp. 6-10, 2012.

[124] S. Mukherjee, P. C. Mishra, S. Parashar, and P. Chaudhuri, "Role of temperature on thermal conductivity of nanofluids: a brief literature review," *Heat and Mass Transfer,* vol. 52, pp. 2575-2585, 2016.

[125] P. Hänggi, F. Marchesoni, and F. Nori, "Brownian motors," *Annalen der Physik,* vol. 517, no. 1-3, pp. 51-70, 2005.

[126] P. E. Gharagozloo, K. E. Goodson, and J. K. Eaton, "Impact of thermodiffusion on temperature fields in stationary nanofluids," in *International Electronic Packaging Technical Conference and Exhibition*, 2007, vol. 42789, pp. 993-998.

[127] S. Mishra, M. Nayak, and A. Misra, "Thermal conductivity of nanofluids-A comprehensive review," *International Journal of Thermofluid Science and Technology,* vol. 7, no. 3, p. 070301, 2020.

[128] D. Shin and D. Banerjee, "Investigation of nanofluids for solar thermal storage applications," in *Energy Sustainability*, 2009, vol. 48890, pp. 819-822.

[129] C. Ho, W.-C. Chen, and W.-M. Yan, "Experiment on thermal performance of water-based suspensions of Al2O3 nanoparticles and MEPCM particles in a minichannel heat sink," *International Journal of Heat and Mass Transfer,* vol. 69, pp. 276-284, 2014.

[130] C. Ho, J. Huang, P. Tsai, and Y. Yang, "Preparation and properties of hybrid water-based suspension of Al2O3 nanoparticles and MEPCM particles as functional forced convection fluid," *International Communications in Heat and Mass Transfer,* vol. 37, no. 5, pp. 490-494, 2010.

[131] C.-Y. Lin, J.-C. Wang, and T.-C. Chen, "Analysis of suspension and heat transfer characteristics of Al2O3 nanofluids prepared through ultrasonic vibration," *Applied Energy,* vol. 88, no. 12, pp. 4527-4533, 2011.

[132] A. Cetina-Quiñones, J. L. López, L. Ricalde-Cab, A. El Mekaoui, L. San-Pedro, and A. Bassam, "Experimental evaluation of an indirect type solar dryer for agricultural use in rural communities: Relative humidity comparative study under winter season in tropical climate with sensible heat storage material," *Solar Energy,* vol. 224, pp. 58-75, 2021.

[133] V. V. Pinto, M. J. Ferreira, R. Silva, H. A. Santos, F. Silva, and C. M. Pereira, "Long time effect on the stability of silver nanoparticles in aqueous medium: effect of the synthesis and storage conditions," *Colloids and Surfaces A: Physicochemical and Engineering Aspects,* vol. 364, no. 1-3, pp. 19-25, 2010.

[134] F. Mafuné, J.-y. Kohno, Y. Takeda, T. Kondow, and H. Sawabe, "Structure and stability of silver nanoparticles in aqueous solution produced by laser ablation," *The Journal of Physical Chemistry B,* vol. 104, no. 35, pp. 8333-8337, 2000.

[135] A. Sarı, "Form-stable paraffin/high density polyethylene composites as solid–liquid phase change material for thermal energy storage: preparation and thermal properties," *Energy Conversion and Management,* vol. 45, no. 13-14, pp. 2033-2042, 2004.

[136] D. M. Addington and D. L. Schodek, *Smart materials and new technologies: for the architecture and design professions*. Routledge, 2005.

[137] W. D. Callister Jr and D. G. Rethwisch, *Fundamentals of materials science and engineering: an integrated approach*. John Wiley & Sons, 2020.

[138] S. U. Choi and J. A. Eastman, "Enhancing thermal conductivity of fluids with nanoparticles," Argonne National Lab.(ANL), Argonne, IL (United States), 1995.

[139] P. Sharma, I.-H. Baek, T. Cho, S. Park, and K. B. Lee, "Enhancement of thermal conductivity of ethylene glycol based silver nanofluids," *Powder technology,* vol. 208, no. 1, pp. 7-19, 2011.

[140] L. A. Austin, M. A. Mackey, E. C. Dreaden, and M. A. El-Sayed, "The optical, photothermal, and facile surface chemical properties of gold and silver nanoparticles in biodiagnostics, therapy, and drug delivery," *Archives of toxicology,* vol. 88, pp. 1391-1417, 2014.

[141] B. Munkhbayar, M. R. Tanshen, J. Jeoun, H. Chung, and H. Jeong, "Surfactant-free dispersion of silver nanoparticles into MWCNT-aqueous nanofluids prepared by one-step technique and their thermal characteristics," *Ceramics International,* vol. 39, no. 6, pp. 6415-6425, 2013.

[142] T. Yang, J. Ma, S. J. Zhen, and C. Z. Huang, "Electrostatic assemblies of well-dispersed AgNPs on the surface of electrospun nanofibers as highly active SERS substrates for wide-range pH sensing," *ACS Applied Materials & Interfaces,* vol. 8, no. 23, pp. 14802-14811, 2016.

[143] A. Hamad, K. S. Khashan, and A. Hadi, "Silver nanoparticles and silver ions as potential antibacterial agents," *Journal of Inorganic and Organometallic Polymers and Materials,* vol. 30, no. 12, pp. 4811-4828, 2020.

[144] J. Koo and C. Kleinstreuer, "A new thermal conductivity model for nanofluids," *Journal of Nanoparticle research,* vol. 6, pp. 577-588, 2004.

[145] S. P. Jang and S. U. Choi, "Role of Brownian motion in the enhanced thermal conductivity of nanofluids," *Applied physics letters,* vol. 84, no. 21, pp. 4316-4318, 2004.

[146] M. Amjad, H. Jin, X. Du, and D. Wen, "Experimental photothermal performance of nanofluids under concentrated solar flux," *Solar Energy Materials and Solar Cells,* vol. 182, pp. 255-262, 2018.

[147] A. Zeiny, H. Jin, L. Bai, G. Lin, and D. Wen, "A comparative study of direct absorption nanofluids for solar thermal applications," *Solar Energy,* vol. 161, pp. 74-82, 2018.

[148] A. Sharma, R. Sharma, R. C. Thakur, and L. Singh, "An overview of deep eutectic solvents: Alternative for organic electrolytes, aqueous systems & ionic liquids for electrochemical energy storage," *Journal of Energy Chemistry,* 2023.

[149] K. Hui *et al.*, "Green synthesis of dimension-controlled silver nanoparticle–graphene oxide with in situ ultrasonication," *Acta Materialia,* vol. 64, pp. 326-332, 2014.

[150] K.-H. Yang, R. D. Boehm, S. A. Skoog, and R. J. Narayan, "Nanostructured Medical Adhesives," *Journal of Biomedical Nanotechnology,* vol. 16, no. 3, pp. 263-282, 2020.

[151] R. C. Popescu, E. Andronescu, and B. S. Vasile, "Recent advances in magnetite nanoparticle functionalization for nanomedicine," *Nanomaterials,* vol. 9, no. 12, p. 1791, 2019.

[152] A. Marmur, C. Della Volpe, S. Siboni, A. Amirfazli, and J. W. Drelich, "Contact angles and wettability: towards common and accurate terminology," *Surface Innovations,* vol. 5, no. 1, pp. 3-8, 2017.

[153] A. Nogalska, A. Trojanowska, B. Tylkowski, and R. Garcia-Valls, "Surface characterization by optical contact anglemeasuring system," *Physical Sciences Reviews,* vol. 5, no. 2, 2020.

[154] K. Wang and H. O. Fatoyinbo, "Digital microfluidics," *Microfuidics in detection science: Lab-on-a-chip technologies,* pp. 84-135, 2014.

[155] T. Chau, W. Bruckard, P. Koh, and A. Nguyen, "A review of factors that affect contact angle and implications for flotation practice," *Advances in colloid and interface science,* vol. 150, no. 2, pp. 106-115, 2009.

[156] Y. Yuan and T. R. Lee, "Contact angle and wetting properties," *Surface science techniques,* pp. 3-34, 2013.

[157] M. Morra, E. Occhiello, and F. Garbassi, "Knowledge about polymer surfaces from contact angle measurements," *Advances in Colloid and Interface Science,* vol. 32, no. 1, pp. 79-116, 1990.

[158] A. Alghunaim, S. Kirdponpattara, and B.-m. Z. Newby, "Techniques for determining contact angle and wettability of powders," *Powder Technology,* vol. 287, pp. 201-215, 2016.

[159] L. Wen, Y. Tian, and L. Jiang, "Bioinspired super-wettability from fundamental research to practical applications," *Angewandte Chemie International Edition,* vol. 54, no. 11, pp. 3387-3399, 2015.

[160] D. Attinger *et al.*, "Surface engineering for phase change heat transfer: A review," *MRS Energy & Sustainability,* vol. 1, p. E4, 2014.

[161] J. W. Drelich *et al.*, "Contact angles: History of over 200 years of open questions," *Surface Innovations,* vol. 8, no. 1–2, pp. 3-27, 2019.

[162] S. Lim, H. Horiuchi, A. D. Nikolov, and D. Wasan, "Nanofluids alter the surface wettability of solids," *Langmuir,* vol. 31, no. 21, pp. 5827-5835, 2015.

[163] K. Kondiparty, A. Nikolov, S. Wu, and D. Wasan, "Wetting and spreading of nanofluids on solid surfaces driven by the structural disjoining pressure: statics analysis and experiments," *Langmuir,* vol. 27, no. 7, pp. 3324-3335, 2011.

[164] Y. Lai *et al.*, "Recent advances in TiO2-based nanostructured surfaces with controllable wettability and adhesion," *Small,* vol. 12, no. 16, pp. 2203-2224, 2016.

[165] E. Gontarek-Castro, R. Castro-Muñoz, and M. Lieder, "New insights of nanomaterials usage toward superhydrophobic membranes for water desalination via membrane distillation: A review," *Critical Reviews in Environmental Science and Technology,* vol. 52, no. 12, pp. 2104-2149, 2022.

[166] M. M. Pereira *et al.*, "Contact angles and wettability of ionic liquids on polar and non-polar surfaces," *Physical Chemistry Chemical Physics,* vol. 17, no. 47, pp. 31653-31661, 2015.

[167] A. Harikrishnan, P. Dhar, S. Gedupudi, and S. K. Das, "Effect of interaction of nanoparticles and surfactants on the spreading dynamics of sessile droplets," *Langmuir,* vol. 33, no. 43, pp. 12180-12192, 2017.

[168] D. Wasan, A. Nikolov, and K. Kondiparty, "The wetting and spreading of nanofluids on solids: Role of the structural disjoining pressure," *Current Opinion in Colloid & Interface Science,* vol. 16, no. 4, pp. 344-349, 2011.

[169] H. Eltoum, Y.-L. Yang, and J.-R. Hou, "The effect of nanoparticles on reservoir wettability alteration: a critical review," *Petroleum Science,* vol. 18, pp. 136-153, 2021.

[170] K. Gopalan, S. Rajabathar, M. Nagaral, and H. R. Thippeswamy, "Evaluation of mechanical behaviour and tensile failure analysis of 8 wt.% of nano B4C particles reinforced Al2214 alloy nano composites," *Manufacturing Review,* vol. 9, p. 31, 2022.

[171] D. T. Wasan and A. D. Nikolov, "Spreading of nanofluids on solids," *Nature,* vol. 423, no. 6936, pp. 156-159, 2003.

[172] S. J. Kim, I. C. Bang, J. Buongiorno, and L. Hu, "Surface wettability change during pool boiling of nanofluids and its effect on critical heat flux," *International Journal of Heat and Mass Transfer,* vol. 50, no. 19-20, pp. 4105-4116, 2007.

[173] L. Forny, A. Marabi, and S. Palzer, "Wetting, disintegration and dissolution of agglomerated water soluble powders," *Powder technology,* vol. 206, no. 1-2, pp. 72-78, 2011.

[174] R. J. Good, "Contact angle, wetting, and adhesion: a critical review," *Journal of adhesion science and technology,* vol. 6, no. 12, pp. 1269-1302, 1992.

[175] M. A. Hubbe, D. J. Gardner, and W. Shen, "Contact angles and wettability of cellulosic surfaces: a review of proposed mechanisms and test strategies," *BioResources,* vol. 10, no. 4, 2015.

[176] D. Hull, *Fractography: observing, measuring and interpreting fracture surface topography*. Cambridge University Press, 1999.

[177] Y. Tamai and K. Aratani, "Experimental study of the relation between contact angle and surface roughness," *The Journal of Physical Chemistry,* vol. 76, no. 22, pp. 3267-3271, 1972.

[178] T. L. Liu and C.-J. C. Kim, "Turning a surface superrepellent even to completely wetting liquids," *Science,* vol. 346, no. 6213, pp. 1096-1100, 2014.

[179] L.-O. Andersson, C.-G. Golander, and S. Persson, "Ice adhesion to rubber materials," *Journal of adhesion science and technology,* vol. 8, no. 2, pp. 117-132, 1994.

[180] H.-J. Butt, I. V. Roisman, M. Brinkmann, P. Papadopoulos, D. Vollmer, and C. Semprebon, "Characterization of super liquid-repellent surfaces," *Current opinion in colloid & interface science,* vol. 19, no. 4, pp. 343-354, 2014.

[181] D. L. Williams and K. L. Mittal, "Wettability techniques to monitor the cleanliness of surfaces," in *Developments in Surface Contamination and Cleaning*: Elsevier, 2016, pp. 445-476.

[182] T. Verho, C. Bower, P. Andrew, S. Franssila, O. Ikkala, and R. H. Ras, "Mechanically durable superhydrophobic surfaces," *Advanced materials,* vol. 23, no. 5, pp. 673-678, 2011.

[183] J. Drelich, "Guidelines to measurements of reproducible contact angles using a sessile-drop technique," *Surface innovations,* vol. 1, no. 4, pp. 248-254, 2013.

[184] Z. Li *et al.*, "Effect of airborne contaminants on the wettability of supported graphene and graphite," *Nature materials,* vol. 12, no. 10, pp. 925-931, 2013.

[185] R. Benedix, F. Dehn, J. Quaas, and M. Orgass, "Application of titanium dioxide photocatalysis to create self-cleaning building materials," *Lacer,* vol. 5, pp. 157-168, 2000.

[186] V. Silverio, P. A. Canane, and S. Cardoso, "Surface wettability and stability of chemically modified silicon, glass and polymeric surfaces via room temperature chemical vapor deposition," *Colloids and Surfaces A: Physicochemical and Engineering Aspects,* vol. 570, pp. 210-217, 2019.

[187] H. Jeong, B. Kim, T. Park, S. Yoo, and S. K. Nam, "Combined molecular dynamics simulations and reaction kinetics study on wettability of trimethylsilyl functionalized silicon surfaces," *Surfaces and Interfaces,* vol. 35, p. 102463, 2022.

[188] A. Fihri, E. Bovero, A. Al-Shahrani, A. Al-Ghamdi, and G. Alabedi, "Recent progress in superhydrophobic coatings used for steel protection: A review," *Colloids and Surfaces A: Physicochemical and Engineering Aspects,* vol. 520, pp. 378-390, 2017.

[189] V. Starov, S. Kosvintsev, V. Sobolev, M. Velarde, and S. Zhdanov, "Spreading of liquid drops over saturated porous layers," *Journal of colloid and interface science,* vol. 246, no. 2, pp. 372-379, 2002.

[190] J. Padday and N. Uffindell, "The calculation of cohesive and adhesive energies from intermolecular forces at a surface," *The Journal of Physical Chemistry,* vol. 72, no. 5, pp. 1407-1414, 1968.

[191] J. Sebilleau, "Equilibrium thickness of large liquid lenses spreading over another liquid surface," *Langmuir,* vol. 29, no. 39, pp. 12118-12128, 2013.

[192] H. Tavana and A. Neumann, "Recent progress in the determination of solid surface tensions from contact angles," *Advances in colloid and interface science,* vol. 132, no. 1, pp. 1-32, 2007.

[193] A. Baldan, "Adhesion phenomena in bonded joints," *International Journal of Adhesion and Adhesives,* vol. 38, pp. 95-116, 2012.

[194] T. Karbowiak, F. Debeaufort, and A. Voilley, "Importance of surface tension characterization for food, pharmaceutical and packaging products: A review," *Critical Reviews in Food Science and Nutrition,* vol. 46, no. 5, pp. 391-407, 2006.

[195] D. Diamond, S. Coyle, S. Scarmagnani, and J. Hayes, "Wireless sensor networks and chemo-/biosensing," *Chemical reviews,* vol. 108, no. 2, pp. 652-679, 2008.

[196] L. Zhang, A. G. Zhou, B. R. Sun, K. S. Chen, and H.-Z. Yu, "Functional and versatile superhydrophobic coatings via stoichiometric silanization," *Nature communications,* vol. 12, no. 1, p. 982, 2021.

[197] S. S. A. Kumar, S. Bashir, K. Ramesh, and S. Ramesh, "A comprehensive review: Super hydrophobic graphene nanocomposite coatings for underwater and wet applications to enhance corrosion resistance," *FlatChem,* vol. 31, p. 100326, 2022.

[198] V. Dutschk, T. Karapantsios, L. Liggieri, N. McMillan, R. Miller, and V. Starov, "Smart and green interfaces: from single bubbles/drops to industrial environmental and biomedical applications," *Advances in colloid and interface science,* vol. 209, pp. 109-126, 2014.

[199] R. A. Swanson and T. J. Chermack, *Theory building in applied disciplines.* Berrett-Koehler Publishers, 2013.

[200] R. Gohar and H. Rahnejat, *Fundamentals of tribology.* World Scientific, 2018.

[201] C. Aydemir, B. N. Altay, and M. Akyol, "Surface analysis of polymer films for wettability and ink adhesion," *Color Research & Application,* vol. 46, no. 2, pp. 489-499, 2021.

[202] J. Kettle, T. Lamminmäki, and P. Gane, "A review of modified surfaces for high speed inkjet coating," *Surface and coatings Technology,* vol. 204, no. 12-13, pp. 2103-2109, 2010.

[203] D. Kannangara, H. Zhang, and W. Shen, "Liquid–paper interactions during liquid drop impact and recoil on paper surfaces," *Colloids and Surfaces A: Physicochemical and Engineering Aspects,* vol. 280, no. 1-3, pp. 203-215, 2006.

[204] M. Andriot *et al.*, "Silicones in industrial applications," *Inorganic polymers,* pp. 61-161, 2007.

[205] P. A. S. PE, *Paint and coatings: applications and corrosion resistance.* CRC press, 2005.

[206] J. R. Davis, *Surface engineering for corrosion and wear resistance.* ASM international, 2001.

[207] G. Cunningham *et al.*, "Solvent exfoliation of transition metal dichalcogenides: dispersibility of exfoliated nanosheets varies only weakly between compounds," *ACS nano,* vol. 6, no. 4, pp. 3468-3480, 2012.

[208] C. Della Volpe, D. Maniglio, M. Brugnara, S. Siboni, and M. Morra, "The solid surface free energy calculation: I. In defense of the multicomponent approach," *Journal of Colloid and Interface Science,* vol. 271, no. 2, pp. 434-453, 2004.

[209] J. Shen *et al.*, "Liquid phase exfoliation of two-dimensional materials by directly probing and matching surface tension components," *Nano letters,* vol. 15, no. 8, pp. 5449-5454, 2015.

[210] K. J. Anusavice, C. Shen, and H. R. Rawls, *Phillips' science of dental materials.* Elsevier Health Sciences, 2012.

[211] P. Sharma and K. H. Rao, "Analysis of different approaches for evaluation of surface energy of microbial cells by contact angle goniometry," *Advances in Colloid and Interface Science,* vol. 98, no. 3, pp. 341-463, 2002.

[212] S. Giljean, M. Bigerelle, K. Anselme, and H. Haidara, "New insights on contact angle/roughness dependence on high surface energy materials," *Applied Surface Science,* vol. 257, no. 22, pp. 9631-9638, 2011.

[213] I. A. Aksay, C. E. Hoge, and J. A. Pask, "Wetting under chemical equilibrium and nonequilibrium conditions," *The Journal of Physical Chemistry,* vol. 78, no. 12, pp. 1178-1183, 1974.

[214] W. Yu, H. Xie, and D. Bao, "Enhanced thermal conductivities of nanofluids containing graphene oxide nanosheets," *Nanotechnology,* vol. 21, no. 5, p. 055705, 2009.

[215] P. Garg, J. L. Alvarado, C. Marsh, T. A. Carlson, D. A. Kessler, and K. Annamalai, "An experimental study on the effect of ultrasonication on viscosity and heat transfer performance of multi-wall carbon nanotube-based aqueous nanofluids," *International Journal of Heat and Mass Transfer,* vol. 52, no. 21-22, pp. 5090-5101, 2009.

[216] S. V. Garimella, L.-T. Yeh, and T. Persoons, "Thermal management challenges in telecommunication systems and data centers," *IEEE Transactions on Components, Packaging and Manufacturing Technology,* vol. 2, no. 8, pp. 1307-1316, 2012.

[217] S. V. Garimella, T. Persoons, J. Weibel, and L.-T. Yeh, "Technological drivers in data centers and telecom systems: Multiscale thermal, electrical, and energy management," *Applied energy,* vol. 107, pp. 66-80, 2013.

[218] Z. Zhang, X. Wang, and Y. Yan, "A review of the state-of-the-art in electronic cooling," *e-Prime-Advances in Electrical Engineering, Electronics and Energy,* vol. 1, p. 100009, 2021.

[219] W. Yu and H. Xie, "A review on nanofluids: preparation, stability mechanisms, and applications," *Journal of nanomaterials,* vol. 2012, pp. 1-17, 2012.

[220] W. Yu and H. Xie, "A review on nanofluids: preparation, stability mechanisms, and applications," *Journal of nanomaterials,* vol. 2012, 2012.

[221] M. Bernardin, F. Comitani, and A. Vailati, "Tunable heat transfer with smart nanofluids," *Physical Review E,* vol. 85, no. 6, p. 066321, 2012.

[222] G. Donzelli, R. Cerbino, and A. Vailati, "Bistable heat transfer in a nanofluid," *Physical review letters,* vol. 102, no. 10, p. 104503, 2009.

[223] J. Buongiorno *et al.*, "A benchmark study on the thermal conductivity of nanofluids," *Journal of Applied Physics,* vol. 106, no. 9, p. 094312, 2009.

[224] J. Buongiorno, L.-W. Hu, S. J. Kim, R. Hannink, B. Truong, and E. Forrest, "Nanofluids for enhanced economics and safety of nuclear reactors: an evaluation of the potential features, issues, and research gaps," *Nuclear Technology,* vol. 162, no. 1, pp. 80-91, 2008.

[225] R. Saidur, K. Leong, and H. A. Mohammed, "A review on applications and challenges of nanofluids," *Renewable and sustainable energy reviews,* vol. 15, no. 3, pp. 1646-1668, 2011.

[226] M. Gumus, "Reducing cold-start emission from internal combustion engines by means of thermal energy storage system," *Applied thermal engineering,* vol. 29, no. 4, pp. 652-660, 2009.

[227] S. N. A. Yusof, N. A. C. Sidik, Y. Asako, W. M. A. A. Japar, S. B. Mohamed, and N. M. a. Muhammad, "A comprehensive review of the influences of nanoparticles as a fuel additive in an internal combustion engine (ICE)," *Nanotechnology Reviews,* vol. 9, no. 1, pp. 1326-1349, 2020.

[228] M. E. M. Soudagar, N.-N. Nik-Ghazali, M. A. Kalam, I. Badruddin, N. Banapurmath, and N. Akram, "The effect of nano-additives in diesel-biodiesel fuel blends: A comprehensive review on stability, engine performance and emission characteristics," *Energy Conversion and Management,* vol. 178, pp. 146-177, 2018.

[229] H. H. Şahin, "Development of a different catalytic oxidation selection of heavy-duty diesel engines with the use of alternative nanoparticles," *Energy Sources, Part A: Recovery, Utilization, and Environmental Effects,* pp. 1-19, 2019.

[230] K. V. Wong and O. De Leon, "Applications of nanofluids: current and future," *Advances in mechanical engineering,* vol. 2, p. 519659, 2010.

[231] H. Gupta, G. Agrawal, and J. Mathur, "An overview of Nanofluids: A new media towards green environment," *International Journal of environmental sciences,* vol. 3, no. 1, pp. 433-440, 2012.

[232] G. Peterson and A. Ortega, "Thermal control of electronic equipment and devices," in *Advances in heat transfer*, vol. 20: Elsevier, 1990, pp. 181-314.

[233]   K. Aglawe, R. Yadav, and S. Thool, "Preparation, applications and challenges of nanofluids in electronic cooling: a systematic review," *Materials Today: Proceedings,* vol. 43, pp. 366-372, 2021.

[234]   H. Ma *et al.*, "Effect of nanofluid on the heat transport capability in an oscillating heat pipe," *Applied Physics Letters,* vol. 88, no. 14, p. 143116, 2006.

[235]   P. Keblinski, J. A. Eastman, and D. G. Cahill, "Nanofluids for thermal transport," *Materials today,* vol. 8, no. 6, pp. 36-44, 2005.

[236]   S. U. Choi, "Nanofluids: from vision to reality through research," *Journal of Heat transfer,* vol. 131, no. 3, 2009.

[237]   A. EINSTEIN, "Zur quantum theorie der strhlung. PhisZ, v. 18," 1917.

[238]   N. Zlatanov, "Lasers and laser applications," *IEEE Computer Society,* 2002.

[239]   A. Tavakoli, M. Sohrabi, and A. Kargari, "A review of methods for synthesis of nanostructured metals with emphasis on iron compounds," *chemical papers,* vol. 61, no. 3, pp. 151-170, 2007.

[240]   A. P. LaGrow, B. Ingham, M. F. Toney, and R. D. Tilley, "Effect of surfactant concentration and aggregation on the growth kinetics of nickel nanoparticles," *The Journal of Physical Chemistry C,* vol. 117, no. 32, pp. 16709-16718, 2013.

[241]   Z. M. Zhang, Z. M. Zhang, and Luby, *Nano/microscale heat transfer*. Springer, 2007.

[242]   J. Theerthagiri *et al.*, "Unraveling the fundamentals of pulsed laser-assisted synthesis of nanomaterials in liquids: Applications in energy and the environment," *Applied Physics Reviews,* vol. 9, no. 4, p. 041314, 2022.

[243]   N. Zamora-Romero, *Synthesis of Molybdenum Oxide Nanostructures by Using the Laser Ablation of Solids in Liquids Technique*. University of California, Riverside, 2019.

[244]   T. E. Itina, "On nanoparticle formation by laser ablation in liquids," *The Journal of Physical Chemistry C,* vol. 115, no. 12, pp. 5044-5048, 2011.

[245]   V. Archana, J. Johny, M. A. Garza-Navarro, S. Shaji, S. Thomas, and M. Anantharaman, "Synthesis of surfactant free stable nanofluids based on barium hexaferrite by pulsed laser ablation in liquid," *RSC advances,* vol. 8, no. 34, pp. 19261-19271, 2018.

[246]   P. G. Jamkhande, N. W. Ghule, A. H. Bamer, and M. G. Kalaskar, "Metal nanoparticles synthesis: An overview on methods of preparation, advantages and disadvantages, and applications," *Journal of drug delivery science and technology,* vol. 53, p. 101174, 2019.

[247]   C. Niu, T. Zhu, and Y. Lv, "Influence of surface morphology on absorptivity of light-absorbing materials," *International Journal of Photoenergy,* vol. 2019, 2019.

[248]   J. Hecht, *Understanding lasers: an entry-level guide*. John Wiley & Sons, 2018.

[249]   J. Chen *et al.*, "Perovskite quantum dot lasers," *InfoMat,* vol. 2, no. 1, pp. 170-183, 2020.

[250]   M. Rao, "A brief introduction to lasers and applications: Scientific approach," *Res. J. Mater. Sci,* vol. 2320, p. 6055, 2013.

[251] A. Goldman, D. Schavelzon, and G. Blugerman, "Laserlipolysis: liposuction using Nd-YAG laser," *Revista Brasiliera de Cirurgia Plástica,* vol. 17, no. 1, pp. 17-26, 2001.

[252] Y. M. Noor, S. Tam, L. Lim, and S. Jana, "A review of the Nd: YAG laser marking of plastic and ceramic IC packages," *Journal of materials processing technology,* vol. 42, no. 1, pp. 95-133, 1994.

[253] F. Bloisi, M. Barra, A. Cassinese, and L. R. M. Vicari, "Matrix-assisted pulsed laser thin film deposition by using Nd: YAG laser," *Journal of Nanomaterials,* vol. 2012, pp. 14-14, 2012.

[254] A. Riahi *et al.*, "Study of thermal conductivity of synthesized Al2O3-water nanofluid by pulsed laser ablation in liquid," *Journal of Molecular Liquids,* vol. 304, p. 112694, 2020.

[255] A. Voevodin, M. Donley, and J. Zabinski, "Pulsed laser deposition of diamond-like carbon wear protective coatings: a review," *Surface and Coatings Technology,* vol. 92, no. 1-2, pp. 42-49, 1997.

[256] P. Willmott and J. Huber, "Pulsed laser vaporization and deposition," *Reviews of Modern Physics,* vol. 72, no. 1, p. 315, 2000.

[257] N. Bulgakova and A. Bulgakov, "Pulsed laser ablation of solids: transition from normal vaporization to phase explosion," *Applied Physics A,* vol. 73, pp. 199-208, 2001.

[258] M. Stafe, C. Negutu, and I. Popescu, "Combined experimental and theoretical investigation of multiple-nanosecond laser ablation of metals," *Journal of optoelectronics and advanced materials,* vol. 8, no. 3, p. 1180, 2006.

[259] W. Sudnik, D. Radaj, and W. Erofeew, "Computerized simulation of laser beam welding, modelling and verification," *Journal of Physics D: Applied Physics,* vol. 29, no. 11, p. 2811, 1996.

[260] G. Yang, "Laser ablation in liquids: Applications in the synthesis of nanocrystals," *Progress in materials Science,* vol. 52, no. 4, pp. 648-698, 2007.

[261] D. Von der Linde and K. Sokolowski-Tinten, "The physical mechanisms of short-pulse laser ablation," *Applied Surface Science,* vol. 154, pp. 1-10, 2000.

[262] M. Maaza *et al.*, "Valency control in MoO $3-\delta$ nanoparticles generated by pulsed laser liquid solid interaction," *Journal of Nanoparticle Research,* vol. 14, pp. 1-9, 2012.

[263] A. Ghadimi, R. Saidur, and H. Metselaar, "A review of nanofluid stability properties and characterization in stationary conditions," *International journal of heat and mass transfer,* vol. 54, no. 17-18, pp. 4051-4068, 2011.

[264] V. Mankad, R. K. Kumar, and P. K. Jha, "Investigation of blue-shifted plasmon resonance: an optical properties study of silver nanoparticles," *Nanoscience and Nanotechnology Letters,* vol. 5, no. 8, pp. 889-894, 2013.

[265] N. Chouhan, *Silver nanoparticles: Synthesis, characterization and applications.* IntechOpen London, UK: , 2018.

[266] K. B. Mogensen and K. Kneipp, "Size-dependent shifts of plasmon resonance in silver nanoparticle films using controlled dissolution: monitoring the onset of surface screening effects," *The Journal of Physical Chemistry C,* vol. 118, no. 48, pp. 28075-28083, 2014.

[267] R. Tripathi, N. Kumar, A. Shrivastav, P. Singh, and B. Shrivastav, "Catalytic activity of biogenic silver nanoparticles synthesized by Ficus panda leaf extract," *Journal of Molecular Catalysis B: Enzymatic,* vol. 96, pp. 75-80, 2013.

[268] B. Ajitha, Y. A. K. Reddy, and P. S. Reddy, "Green synthesis and characterization of silver nanoparticles using Lantana camara leaf extract," *Materials science and engineering: C,* vol. 49, pp. 373-381, 2015.

[269] D. Eli and P. Gyuk, "High efficiency dye sensitized solar cells by excitation of localized surface plasmon resonance of AgNPs," *Science World Journal,* vol. 14, no. 2, pp. 125-130, 2019.

[270] G. P. Lee, "The chemical properties and characterisation of photomorphic silver nanoparticles and their application as an antimicrobial agent," 2010.

[271] I. O. Sosa, C. Noguez, and R. G. Barrera, "Optical properties of metal nanoparticles with arbitrary shapes," *The Journal of Physical Chemistry B,* vol. 107, no. 26, pp. 6269-6275, 2003.

[272] A. Zielińska, E. Skwarek, A. Zaleska, M. Gazda, and J. Hupka, "Preparation of silver nanoparticles with controlled particle size," *Procedia chemistry,* vol. 1, no. 2, pp. 1560-1566, 2009.

[273] O. M. Bakr *et al.*, "Silver nanoparticles with broad multiband linear optical absorption," *Angewandte Chemie,* vol. 121, no. 32, pp. 6035-6040, 2009.

[274] A.-M. Tugulea *et al.*, "Nano-silver in drinking water and drinking water sources: stability and influences on disinfection by-product formation," *Environmental Science and Pollution Research,* vol. 21, pp. 11823-11831, 2014.

[275] M. Chen, Y. He, J. Zhu, Y. Shuai, B. Jiang, and Y. Huang, "An experimental investigation on sunlight absorption characteristics of silver nanofluids," *Solar Energy,* vol. 115, pp. 85-94, 2015.

[276] F. Mafuné, J.-y. Kohno, Y. Takeda, T. Kondow, and H. Sawabe, "Formation and size control of silver nanoparticles by laser ablation in aqueous solution," *The Journal of Physical Chemistry B,* vol. 104, no. 39, pp. 9111-9117, 2000.

[277] I. Fernando and Y. Zhou, "Impact of pH on the stability, dissolution and aggregation kinetics of silver nanoparticles," *Chemosphere,* vol. 216, pp. 297-305, 2019.

[278] G. A. Rance, D. H. Marsh, S. J. Bourne, T. J. Reade, and A. N. Khlobystov, "van der Waals interactions between nanotubes and nanoparticles for controlled assembly of composite nanostructures," *ACS nano,* vol. 4, no. 8, pp. 4920-4928, 2010.

[279] C. A. Silvera Batista, R. G. Larson, and N. A. Kotov, "Nonadditivity of nanoparticle interactions," *Science,* vol. 350, no. 6257, p. 1242477, 2015.

[280] H. Wu, H. Fang, C. Xu, J. Ye, Q. Cai, and J. Shi, "Transport and retention of copper oxide nanoparticles under unfavorable deposition conditions caused by repulsive van der Waals force in saturated porous media," *Environmental Pollution,* vol. 256, p. 113400, 2020.

[281] N. Ali, J. A. Teixeira, and A. Addali, "A review on nanofluids: fabrication, stability, and thermophysical properties," *Journal of Nanomaterials,* vol. 2018, 2018.

[282] E. Ponticorvo, M. Iuliano, C. Cirillo, A. Maiorino, C. Aprea, and M. Sarno, "Fouling Behavior and Dispersion Stability of Nanoparticle-Based Refrigeration Fluid," *Energies,* vol. 15, no. 9, p. 3059, 2022.

[283] D. D. Kumar and A. V. Arasu, "A comprehensive review of preparation, characterization, properties and stability of hybrid nanofluids," *Renewable and Sustainable Energy Reviews,* vol. 81, pp. 1669-1689, 2018.

[284] S. K. Das and U. Stephen, "A review of heat transfer in nanofluids," *Advances in heat transfer,* vol. 41, pp. 81-197, 2009.

[285] M. Mehrabi, "Modelling and optimisation of thermophysical properties and convective heat transfer of nanofluids by using artificial intelligence methods," University of Pretoria, 2015.

[286] J. M. Zook, V. Rastogi, R. I. MacCuspie, A. M. Keene, and J. Fagan, "Measuring agglomerate size distribution and dependence of localized surface plasmon resonance absorbance on gold nanoparticle agglomerate size using analytical ultracentrifugation," *ACS nano,* vol. 5, no. 10, pp. 8070-8079, 2011.

[287] H. Hiroshi and T. Minoru, "Equivalent inclusion method for steady state heat conduction in composites," *International Journal of Engineering Science,* vol. 24, no. 7, pp. 1159-1172, 1986.

[288] D. Kraemer and G. Chen, "A simple differential steady-state method to measure the thermal conductivity of solid bulk materials with high accuracy," *Review of Scientific Instruments,* vol. 85, no. 2, p. 025108, 2014.

[289] T. Khamliche, S. Khamlich, M. Moodley, B. Mothudi, M. Henini, and M. Maaza, "Laser fabrication of Cu nanoparticles based nanofluid with enhanced thermal conductivity: Experimental and molecular dynamics studies," *Journal of Molecular Liquids,* vol. 323, p. 114975, 2021.

[290] P. Nagarajan, "Influence of stability and particle shape effects for an entropy generation based optimized selection of magnesia nanofluid for convective heat flow applications," *Applied Surface Science,* vol. 489, pp. 560-575, 2019.

[291] J. Eapen, R. Rusconi, R. Piazza, and S. Yip, "The classical nature of thermal conduction in nanofluids," 2010.

[292] P. Keblinski, R. Prasher, and J. Eapen, "Thermal conductance of nanofluids: is the controversy over?," *Journal of Nanoparticle research,* vol. 10, pp. 1089-1097, 2008.

[293] K. Elsaid *et al.,* "Thermophysical properties of graphene-based nanofluids," *International Journal of Thermofluids,* vol. 10, p. 100073, 2021.

[294] M. Edalatpour, L. Liu, A. Jacobi, K. Eid, and A. Sommers, "Managing water on heat transfer surfaces: A critical review of techniques to modify surface wettability for applications with condensation or evaporation," *Applied Energy,* vol. 222, pp. 967-992, 2018.

[295] M. Siddique, A.-R. Khaled, N. Abdulhafiz, and A. Boukhary, "Recent advances in heat transfer enhancements: a review report," *International Journal of Chemical Engineering,* vol. 2010, 2010.

[296] D. Dey and D. S. Sahu, "Nanofluid in the multiphase flow field and heat transfer: A review," *Heat Transfer,* vol. 50, no. 4, pp. 3722-3775, 2021.

[297] A. Lenert, Y. Nam, and E. N. Wang, "Heat transfer fluids," *Annual Review of Heat Transfer,* vol. 15, 2012.

[298]   W. Zhang, J. Crittenden, K. Li, and Y. Chen, "Attachment efficiency of nanoparticle aggregation in aqueous dispersions: modeling and experimental validation," *Environmental science & technology,* vol. 46, no. 13, pp. 7054-7062, 2012.

[299]   S. Witharana, C. Hodges, D. Xu, X. Lai, and Y. Ding, "Aggregation and settling in aqueous polydisperse alumina nanoparticle suspensions," *Journal of Nanoparticle Research,* vol. 14, pp. 1-11, 2012.

[300]   J. M. Pettibone, D. M. Cwiertny, M. Scherer, and V. H. Grassian, "Adsorption of organic acids on TiO2 nanoparticles: effects of pH, nanoparticle size, and nanoparticle aggregation," *Langmuir,* vol. 24, no. 13, pp. 6659-6667, 2008.

[301]   J. T. Quik, D. van De Meent, and A. A. Koelmans, "Simplifying modeling of nanoparticle aggregation–sedimentation behavior in environmental systems: A theoretical analysis," *Water research,* vol. 62, pp. 193-201, 2014.

[302]   L. V. Stebounova, E. Guio, and V. H. Grassian, "Silver nanoparticles in simulated biological media: a study of aggregation, sedimentation, and dissolution," *Journal of Nanoparticle Research,* vol. 13, pp. 233-244, 2011.

[303]   A. Albanese and W. C. Chan, "Effect of gold nanoparticle aggregation on cell uptake and toxicity," *ACS nano,* vol. 5, no. 7, pp. 5478-5489, 2011.

[304]   E. Akman, B. G. Oztoprak, M. Gunes, E. Kacar, and A. Demir, "Effect of femtosecond Ti: Sapphire laser wavelengths on plasmonic behaviour and size evolution of silver nanoparticles," *Photonics and nanostructures-fundamentals and applications,* vol. 9, no. 3, pp. 276-286, 2011.

[305]   M. D. Malinsky, K. L. Kelly, G. C. Schatz, and R. P. Van Duyne, "Chain length dependence and sensing capabilities of the localized surface plasmon resonance of silver nanoparticles chemically modified with alkanethiol self-assembled monolayers," *Journal of the American Chemical Society,* vol. 123, no. 7, pp. 1471-1482, 2001.

[306]   A. Ravindran, A. Singh, A. M. Raichur, N. Chandrasekaran, and A. Mukherjee, "Studies on interaction of colloidal Ag nanoparticles with bovine serum albumin (BSA)," *Colloids and Surfaces B: Biointerfaces,* vol. 76, no. 1, pp. 32-37, 2010.

[307]   X. Zhou *et al.*, "Enhanced thermoelectric properties of Ba-filled skutterudites by grain size reduction and Ag nanoparticle inclusion," *Journal of Materials Chemistry,* vol. 22, no. 7, pp. 2958-2964, 2012.

[308]   L. Ren *et al.*, "Silver nanoparticle-modified alumina microsphere hybrid composites for enhanced energy density and thermal conductivity," *Composites Part A: Applied Science and Manufacturing,* vol. 119, pp. 299-309, 2019.

[309]   D. W. Chae, S. S. Hwang, S. M. Hong, S. P. Hong, B. G. Cho, and B. C. Kim, "Influence of high contents of silver nanoparticles on the physical properties of poly (vinylidene fluoride)," *Molecular Crystals and Liquid Crystals,* vol. 464, no. 1, pp. 233/[815]-241/[823], 2007.

[310]   K. Peng *et al.*, "Optimization of Ag nanoparticles on thermoelectric performance of Ba-filled skutterudite," *Science of Advanced Materials,* vol. 9, no. 3-4, pp. 682-687, 2017.

[311]   R.-H. Chen, T. X. Phuoc, and D. Martello, "Surface tension of evaporating nanofluid droplets," *International Journal of Heat and Mass Transfer,* vol. 54, no. 11-12, pp. 2459-2466, 2011.

[312] S. Vafaei, C. Tuck, R. Wildman, and I. Ashcroft, "Spreading of the nanofluid triple line in ink jet printed electronics tracks," *Additive Manufacturing,* vol. 11, pp. 77-84, 2016.